NANYANG TECHNOLOGICAL UNIVERSITY
SINGAPORE

THE MICROENVIRONMENT:

HOW IT IMPACTS ENTEROCOCCUS FAECALIS

WOUND PATHOGENESIS

TAN AI ZHU CASANDRA

INTERDISCIPLINARY GRADUATE PROGRAM

SINGAPORE CENTRE FOR ENVIRONMENTAL LIFE SCIENCES

ENGINEERING

2022

THE MICROENVIRONMENT: HOW IT IMPACTS ENTEROCOCCUS FAECALIS WOUND PATHOGENESIS

TAN AI ZHU CASANDRA

Interdisciplinary Graduate Program

Singapore Centre for Environmental Life Sciences Engineering

A thesis submitted to the Nanyang Technological University in partial fulfilment of the requirement for the degree of

Doctor of Philosophy

2022

Statement of Originality

I hereby certify that the work embodied in this thesis is the result of original research, is free of plagiarized materials, and has not been submitted for a higher degree to any other University or Institution.

04 August 2022

. . . . . .
Date

. . . . . .
Tan Ai Zhu Casandra

Supervisor Declaration Statement

I have reviewed the content and presentation style of this thesis and declare it is free of plagiarism and of sufficient grammatical clarity to be examined. To the best of my knowledge, the research and writing are those of the candidate except as acknowledged in the Author Attribution Statement. I confirm that the investigations were conducted in accord with the ethics policies and integrity standards of Nanyang Technological University and that the research data are presented honestly and without prejudice.

04 August 2022

. . . . . .
Date

. . . . . .
Kevin Pethe

Authorship Attribution Statement

This thesis contains material from 1 paper published in the following peer-reviewed journal(s) / from papers accepted at conferences in which I am listed as an author.

Chapter 2 is published as **Tan, C. A. Z.**, Lam, L. N., Biukovic, G., Soh, E. Y. C., Toh, X. W., Lemos, J. A., & Kline, K. A. (2022). *Enterococcus faecalis* antagonizes *Pseudomonas aeruginosa* growth in mixed-species interactions. *Journal of Bacteriology*, e00615-21. DOI: https://doi.org/10.1128/jb.00615-21.

The contributions of the co-authors are as follows:

- Prof. Kline, Dr. Biukovic, Dr. Soh and I provided the initial project direction.
- I prepared the manuscript drafts. The manuscript was revised by Dr. Lam, Dr. Biukovic, A/Prof. Lemos and Prof. Kline.
- Except for Figures 1A – E and 3C – D (see below), I designed the study and performed all the laboratory work at the Singapore Centre for Environmental Life Sciences Engineering. I also analyzed the data.
- Dr. Lam performed and analyzed the results from all static biofilm assays at the University of Florida College of Dentistry (Figure 1A – E of the manuscript). For the sake of completion, these data provided by our collaborator are included in Figure 2.1A – E of this thesis.
- Dr. Lam performed and analyzed the results from all macrocolony assays involving PAO1 BAA-47 strain at the University of Florida College of Dentistry (Supplementary Figure 3C – D and Supplementary Figure 6 of

the manuscript). For the sake of completion, these data are included in Figure 2.2C – D and Appendix Figure 2.5 of this thesis.

- Dr. Biukovic generated the PADP6 and PADP6-mCherry strains used in this study and performed the *E. faecalis* transposon library screening at the Singapore Centre for Environmental Life Sciences Engineering.
- Ms. Toh assisted in performing and analyzing the results from planktonic and macrocolony biofilm assays in Figure 2A – B, Figure 2E – F, Figure 3A and Supplementary Figure 5 of the manuscript at the Singapore Centre for Environmental Life Sciences Engineering.
- I performed the transcriptomic analysis and generated the OG1RF Δ*ldh1* and OG1RF Δ*ldh1::ldh1* strains used in this study.

04 August 2022

. . . . . .
Date

. . . . . .
Tan Ai Zhu Casandra

Acknowledgements

This dissertation would not be completed without the help and support from my supervisors, mentors, colleagues, students, and friends. Many often say that PhD journey is never smooth sailing and is full of ups and downs, I couldn't agree more to it. I would like to express my utmost gratitude to my first supervisor, Professor Kimberly Kline, for taking a chance on me and giving me this fantastic opportunity to work on this project. I thank you for the continuous support, patience, and guidance throughout my candidature. I am also grateful that you taught me how to be a good science communicator and writer.

I am thankful for my second supervisor, Associate Professor Kevin Pethe. Although you joined my PhD journey at a later stage, you have been terrific and provided many interesting viewpoints/perspectives to the project. I also would like to thank my co-supervisors Professor David Becker and Professor Staffan Kjelleberg, and mentor Associate Professor Scott Rice for the many thought-provoking discussions we had during our TAC meetings. I am grateful that you all have been always around and providing me with your support.

I am extremely thankful for Dr. Goran Biukovic and Dr. Chong Kian Long Kelvin who started the project on the mixed-species interactions between *Enterococcus faecalis* and *Pseudomonas aeruginosa* as well as *E. faecalis* wound genetic determinants, respectively. Your findings had laid the groundwork for this dissertation, and I am honored to continue from your work.

To Dr. Chong Kian Long Kelvin, I am also thankful that you “forced” me to learn bioinformatics, trained me in animal work and being patient with me.

This journey would not be possible without the Kline Lab (current and present members). You guys have provided me with an amazing learning environment and there is always something to learn from each and every one of you. I would like to thank Choo Pei Yi, Dr. Zeus Nair, Dr. Patrick Kao Hsien-Neng, Dr. Haris Antypas, Dr. Ronni da Silva, Dr. Claudia Stocks, Bala Davient, Ho Foo Kiong, Dr. Adeline Yong Mei Hui, Dr. Lam Ling Ning, Dr. Ch’ng Jun Hong, Dr. Irina Afonina, Dr. Artur Matysik, Dr. Thomas Watts, and Dr. Chen Qingyan for always keeping me on my toes. The rest of the Kline Lab members, Dr. Tay Wei Hong, Dr. Mark Veleba, Dr. Aaron Tan Ming Zhi, Zhichao Chen, Cheryl Neo Jia Yi, Chua Yong Jie Jerome, Navin S/O Jeyabalan, Frederick Reinhart Tanoto for always being there and supportive. Special thanks to these poor fellows who had to wake up in the wee hours to assist me with my animal work: Dr. Chong Kian Long Kelvin, Dr. Wong Jun Jie, Dr. Brenda Tien Yin Qi, Thong Chor Ming, Alicia Tan Qian Ler, and Daryl Yeong Yu Xuan.

I am also thankful to my other friends who are or used to be in SCELSE: Renee Nicole Ng Yun Wen, Dr. Teh Wooi Keong, Dr. Ding Yichen, Dr. Chen Yingying, Dr. Li Yingying, Dr. July Fong, Dr. Yam Kuok Hoong Joey, Joyce Seow Fong Chin, Seng Zi Jing, May Margarette Salido, Wong Lan Li, and Teng Min Ren Aloysius. Special thanks to the SCELSE Lab Management team as well for their tremendous help in the upkeeping of the lab.

I am also immensely grateful to all the students who had confidence in me and decided to join me in this journey: Toh Xiao Wei (mixed-species interactions between *E. faecalis* and *P. aeruginosa*), Daryl Yeong Yu Xuan and Ng Hui Min Celine (*E. faecalis* wound genetic determinants).

I would also like to thank my friends that are “outside” of science for providing me my work-life balance during this journey and a place to switch off: Pakhrin Tan, Gladys Lim, Germin Tan, Eugene Wong, Shawn Tan, Hong Xiang Kang, Nathan Liang, Daryl Tay, Lee Yuncui, Joey Aw, Jesslyn Kwang, Velda Teh, Seow Wan Xuan, Joan Tan, Natalie Sim, Joanne Wong, Cordelia Quak, Emily Chai, Sieng Huishan, Leow Liru, and Natalie Chua.

A special mention to my fiancé, Dr. Muhammad Hafiz Bin Ismail, who have similarly “forced” me to learn bioinformatics, reading through all my manuscripts/thesis, and encouraging me throughout this journey. Also, not forgetting my family, who are still clueless about what I am working on. Thank you for the unwavering support, encouragements and understanding throughout my journey. Love you all!

I hope that I did not miss out anyone. If I do, please do not take it to heart because you definitely have a special place in my heart, and I am grateful for your support and friendship.

Table of Contents

List of Tables

List of Figures

List of Abbreviations

22D	2,2’ Bipyridyl
AS	Aggregation substances
CAUTI	Catheter-associated urinary tract infection
CFU	Colony forming unit
CI	Competitive index
CylA	Cytolysin
DNA	Deoxyribonucleic acid
Dpi	Days post-infection
E. coli	*Escherichia coli*
E. faecalis	*Enterococcus faecalis*
Ebp	Endocarditis and biofilm-associated pili
Esp	Enterococcal surface protein
FDR	False discovery rate
$FeCl_3$	Ferric chloride
GelE	Gelatinase
GI	Gastrointestinal
H^+	Hydrogen ions
HEPES	4-(2-hydroxyethyl)-1-piperazineethanesulfonic acid
Hpi	H post-infection
KEGG	Kyoto Encyclopedia of Genes and Geomes
LDH	Lactate dehydrogenase
MIC	Minimum inhibitory concentration

MOPS	4-Morpholinepropanesulfonic acid, 3-(N-Morpholino)propanesulfonic acid
MRSA	Methicillin-resistance *S. aureus*
N	Biological replicate
n	Technical replicate
OD	Optical density
P-value	Probability value
P. aeruginosa	*Pseudomonas aeruginosa*
PBS	Phosphate buffered saline
PIPES	1,4-Piperazinediethanesulfonic acid disodium salt
PTS	Phosphotransferase system
RNA	Ribonucleic acid
RNA-seq	RNA sequencing
S. aureus	*Staphylococcus aureus*
SprE	Serine proteases
Tn-seq	Transposon sequencing
TSB	Tryptone Soya Broth
TSBG	Tryptone Soya Broth supplemented with 10 mM glucose
UTI	Urinary tract infection

Summary

Enterococcus faecalis is commonly isolated from single- and mixed-species biofilm-associated wound infections. As a defense strategy, the host innately restricts iron availability at infection sites. Despite *E. faecalis* prevalence in wounds, the mechanism of *E. faecalis* wound pathogenesis during single- and mixed-species wound infection are poorly understood. The overall aim of this dissertation is to understand the mixed-species interactions of *E. faecalis* with commonly co-isolated *Pseudomonas aeruginosa* in biofilms under iron-restricted conditions, as well as to determine and explore the genetic determinants that contributes to *E. faecalis* wound pathogenesis. To achieve the first aim, the mixed-species interactions were explored in biofilm conditions, and I found that *E. faecalis* inhibits *P. aeruginosa* growth within biofilms when iron is restricted. *E. faecalis* lactate dehydrogenase (encoded by *ldh1*) gives rise to L-lactate during fermentative growth and I found that an *E. faecalis ldh1* mutant fails to inhibit *P. aeruginosa* growth. Additionally, *ldh1* expression was induced under iron-restricted conditions, resulting in increased lactic acid exported and consequently, a reduction in the local environmental pH which contributes to *P. aeruginosa* growth inhibition. To achieve the second aim, *in vivo E. faecalis* transposon and RNA sequencing were performed to identify genetic determinants that are crucial for acute replication and persistence of *E. faecalis* during wound infection. I found that *E. faecalis* purine biosynthesis genes were important for bacterial replication during the early stages of wound infection, a time when purine metabolites are also low within wounds as quantified by liquid chromatography-mass spectrometry. I also identified the *E.*

faecalis MptABCD phosphotransferase system, involved in the import of galactose and mannose, is crucial for *E. faecalis* persistence within wounds where carbohydrate availability also changes during the course of infection. During *in vitro* growth with mannose as the sole carbohydrate source, shikimate and purine biosynthesis genes were downregulated in the *E. faecalis* OG1RF Δ*mptD* mutant compared to the isogenic wild-type strain, indicating that mannose transport, shikimate and purine biosynthesis are linked. Overall, these findings emphasize the importance of the wound microenvironment during single- and mixed-species wound infection, and how manipulation of the microenvironment can affect the pathogenesis of an infection.

Chapter 1 – Literature Review

1.1 *Enterococcus faecalis* during infections

1.1.1 Epidemiology of enterococci

Enterococci are Gram-positive, diplococci, and commensal bacteria of the human gastrointestinal (GI) tract. Enterococci are also opportunistic pathogens that are implicated in several types of infections (Arias & Murray, 2012). Enterococci are resilient to environmental stressors encountered in their natural and opportunistic infection environments, such as bile salts and high salt conditions (Arias & Murray, 2012; Flahaut et al., 1996). Moreover, enterococci are inherently resistant to certain antibiotics such as aminoglycosides, cephalosporins, and lincosamides (Hollenbeck & Rice, 2012). The two main *Enterococcus* spp. that account for most enterococcal infections in humans are *E. faecalis* and *E. faecium* (Higuita & Huycke, 2014; Kristich et al., 2014).

Among hospital-acquired infections, *E. faecalis* is the top three most common pathogen (Hidron et al., 2008) responsible for approximately 15% of catheter-associated urinary tract infection (CAUTI), 5 – 15% of infective endocarditis, and is often co-isolated from mixed-species chronic wounds (Gjødsbøl et al., 2006; Higuita & Huycke, 2014; Peng et al., 2018). Each of these infection types is biofilm-associated, which confers additional antibiotic tolerance to the bacteria (Ch'ng et al., 2019; Donlan & Costerton, 2002). Due to *E. faecalis* intrinsic and acquired resistance against a range of antibiotics, infections are also harder to treat (Hollenbeck & Rice, 2012).

1.1.2 *E. faecalis* wound infection

Wound infections affect approximately 11 million people worldwide (Demidova-Rice et al., 2012) and about 20 billion USD is spent yearly on treatment (Sen et al., 2009), which impose a substantial economic burden to both patients and the healthcare system. Wounds are broadly classified as acute or chronic. Although acute wounds heal in an expected time course while chronic wounds are perturbed during the wound healing process(es), both are prone to colonization by a diversity of microorganisms such as enterococci (Bowler et al., 2001). *E. faecalis* can colonize a range of wound types including diabetic wounds, chronic ulcers (pressure and venous) and surgical sites (Dowd et al., 2008; Dworniczek et al., 2012; Fisher & Phillips, 2009; Giacometti et al., 2000; Shettigar et al., 2018), and form antibiotic tolerance-associated biofilm microcolonies on the wound bed (Chong et al., 2017; James et al., 2008), rendering *E. faecalis* wound infections difficult to treat.

1.1.2.1 *E. faecalis* wound infection dynamics

Based on a mouse excisional wound infection model, Chong et al. (2017) demonstrated that *E. faecalis* undergoes an acute replication within wounds during the first 8 h post-infection (hpi), followed by a continuous tapering of bacterial colony-forming unit (CFU) until 3 days post-infection (dpi), after which the bacterial load was maintained at 10^5 CFU until 7 dpi (Chong et al., 2017). In the same study, *E. faecalis* multiple peptide resistance factor (MprF) was identified as a genetic determinant involved in *E. faecalis* persistence in wounds, in which OG1RF *mprF* deletion mutant was significantly less fit compared to

parental wild-type OG1RF in a competitive infection at 3 dpi (Chong et al., 2017). To date, besides MprF, no other genetic determinants have been reported that contribute to *E. faecalis* replication (8 hpi) and/or persistence (3 dpi) during wound infection.

1.1.2.2 *E. faecalis* and its "partners-in-crime" during wound infection

In addition to *E. faecalis*, wounds also often contain other pathogens such as *Pseudomonas aeruginosa, Staphylococcus aureus, Corynebacterium spp*, and *Enterobacteriaceae spp* (Bowler et al., 2001; Citron et al., 2007; Giacometti et al., 2000; Gjødsbøl et al., 2006). Therefore, wound infections are typically polymicrobial in nature (Bowler et al., 2001; Frank, D. N. et al., 2009; Mertz, 2003; Pastar et al., 2013), and exist mainly as biofilms (Black, C. E. & Costerton, 2010; Ebright, 2005; Serralta et al., 2001). Such polymicrobial biofilms can escape the host immune responses, thus enabling the survival and persistence of infecting microbes in wounds, and ultimately hindering wound healing (Hall-Stoodley & Stoodley, 2009). An example is the delay of wound closure and higher levels of gentamicin tolerance in *P. aeruginosa* observed following *E. faecalis* co-infection with *S. aureus*, *P. aeruginosa*, and *Finegoldia magna* compared to single-species infection (Dalton et al., 2011). Moreover, wounds which consist of four or more bacterial species correlate positively with non-healing phenotypes (Davies et al., 2007; Trengove et al., 1996).

Although infected wounds often contain a polymicrobial community, most studies have been limited to single-species wound infection models (Chhibber et al., 2020; Harrison-Balestra et al., 2003; Hoffmann et al., 2020), and only few

have explored the mixed-species interactions between the most commonly co-isolated wound bacteria: *S. aureus* and *P. aeruginosa* (DeLeon et al., 2014; Pastar et al., 2013) as well as *E. faecalis* and *Escherichia coli* (Keogh et al., 2016). Mixed-species interactions between methicillin-resistant *S. aureus* USA300 and *P. aeruginosa* result in delayed wound re-epithelization in a porcine wound model through downregulation of keratinocyte growth factor 1 (KGF1) and induced expression of USA300 virulence factors α-hemolysin and Panton-Valentine leucocidin (Pastar et al., 2013). In another example, *E. faecalis* augments *E. coli* growth during wound infection through the export of *E. faecalis* L-ornithine which signals *E. coli* enterobactin biosynthesis under iron-restricting conditions, promoting mixed-species wound infection pathogenesis (Keogh et al., 2016). Understanding how pathogens interact during wound infections may provide more informed and effective treatment strategies, as well as identifying novel therapeutic targets for combating complex infections.

1.1.3 *E. faecalis in vivo* biofilm

Most bacteria can adopt two lifestyles: planktonic or sessile (biofilm) (Flemming et al., 2016). Bacteria biofilms are defined as an assembly of surface-associated communities of single or multiple bacterial species that are frequently embedded in a self-produced extracellular polymeric substances matrix (Vert et al., 2012). In humans, most infections are often biofilm-associated, and when bacteria adopt the biofilm lifestyle within the host, the infection usually becomes harder to treat (Jamal et al., 2018).

Enterococcal biofilms are implicated in several infections such as infective endocarditis, CAUTI, GI tract colonization, and wound infection. In a rabbit model of infective endocarditis, *E. faecalis* microcolonies are firmly attached onto the cardiac endothelia throughout the rabbit aorta and heart (Barnes et al., 2021). Moreover, *E. faecalis* endocarditis clinical isolates formed significantly more *in vitro* biofilm compared to non-endocarditis clinical isolates (Mohamed et al., 2004). CAUTI is the most prevalent complication resulting from indwelling urinary catheters, and these catheters are ideal for *E. faecalis* attachment and biofilm formation. In a mouse model of CAUTI, *E. faecalis* is seen forming *in vivo* biofilm on both the outer surface and entire lumen of the catheters implanted in mice bladders (Guiton et al., 2010), and the biofilm formation is mediated by *E. faecalis* interacting with fibrinogen deposited on the catheters (Flores-Mireles et al., 2014). The formation of *E. faecalis in vivo* biofilm microcolonies is also evident during colonization of the GI tract in a mouse model throughout the lower GI tract, and these microcolonies appeared distinctly and directly attaching to the gut epithelium (Barnes et al., 2017). Likewise, in a mouse wound excisional model, *E. faecalis* forms *in vivo* microcolonies on the wound surface during acute wound infection as well as along the wound edge and in the wound bed during persistence in wounds (Chong et al., 2017). Taken together, these examples reveal that *E. faecalis* adopts the biofilm lifestyle during infections.

1.1.4 *E. faecalis* virulence factors involved in infections

E. faecalis possess a broad array of virulence factors that allow it to colonize many niches and cause a variety of biofilm-associated infections. In

this section, virulence factors that are implicated in *E. faecalis* biofilm-associated infections or biofilm formation will be discussed. The majority of the best studied virulence factors can be broadly categorized into secreted proteases and surface-exposed cell-wall anchored proteins **(Figure 1.1)**. Some *E. faecalis* secreted proteases, that will be elaborated here include gelatinase (GelE), serine proteases (SprE), and cytolysin (CylA).

1.1.4.1 *E. faecalis* secreted proteases

GelE is a matrix metalloprotease which possesses hydrolytic activity that hydrolyzes insulin B-chain and collagen (Mäkinen et al., 1989). GelE activity correlates with disease severity in a rabbit endocarditis model (Gutschik et al., 1979; Thurlow et al., 2010) as well as in mouse and rat peritonitis models (Dupont et al., 1998; Singh et al., 1998). Secreted GelE also facilitates complement resistance mechanism by cleaving complement components C3 (Park et al., 2007; Park et al., 2008) and C5a (Thurlow et al., 2010), thus decreasing opsonization and neutrophil recruitment. GelE enzymatic activity is also required for *E. faecalis in vitro* biofilm formation, in which *gelE* mutants resulted in impaired biofilm formation (Hancock & Perego, 2004; Thomas et al., 2008). Together, these data suggest that disease severity could be attributed in part to the hydrolytic activity and complement resistance of GelE.

The serine protease SprE is co-transcribed with *gelE*, and the expression of both *gelE* and *sprE* is regulated by *E. faecalis* Fsr quorum sensing system (Qin et al., 2000). Thomas et al. (2008) showed that deletion of *sprE* increased *in vitro* biofilm formation on polystyrene and glass substrates as well as

produced more extracellular DNA, a component of the biofilm matrix, compared to isogenic wild-type strain. Mutants of *sprE* display attenuated virulence in mouse peritonitis (Qin et al., 2000), *Caenorhabditis elegans* (Garsin et al., 2001; Sifri et al., 2002), and rabbit endophthalmitis models (Engelbert et al., 2004; Suzuki et al., 2008). Despite the studies performed on SprE, the mechanism(s) by which it contributes to *E. faecalis* pathogenesis remains unknown.

E. faecalis CylA cytolysin is a toxin belonging to type-A lantibiotics which targets neutrophils and macrophages (Miyazaki et al., 1993), and it contributes to the severity of *E. faecalis* infections in rabbit endocarditis (Chow et al., 1993) and endophthalmitis models (Jett et al., 1992). Furthermore, *in vitro* biofilm formation was more commonly detected in *E. faecalis* CylA-positive clinical isolates derived from urinary tract infection (UTI) compared to CylA-negative isolates (Zheng et al., 2018). CylA may exert its effects synergistically with other virulence factors. When both CylA and aggregation substances (AS), a cell-wall anchored protein, are expressed together, the mortality rate of rabbits increased by 40% compared to rabbits infected with *E. faecalis* expressing only AS (Chow et al., 1993). Most likely, AS-expressing *E. faecalis* cells promotes adherence at the infection site which in turn allows CylA to exert its toxic effects.

1.1.4.2 *E. faecalis* surface-exposed cell-wall anchored proteins

E. faecalis encode a number of well-described cell-wall anchored proteins including AS, enterococcal surface protein (Esp), endocarditis and biofilm-associated pili (Ebp). These proteins are important for binding to substrata. For example, AS binds to extracellular matrix proteins such as

collagen type I, thrombospondin, fibronectin, and vitronectin, but not laminin and collagen type IV (Rozdzinski et al., 2001). AS can mediate opsonin-independent phagocytosis by human polymorphonuclear leukocytes (PMNs) but the internalized bacteria are not readily killed by PMNs possibly due to inhibition of phagosomal acidification (Rakita et al., 1999). *E. faecalis* AS also confers resistance to killing by macrophages by inhibiting the respiratory burst (Süßmuth et al., 2000). Although AS is important in endocarditis (Chow et al., 1993; Schlievert et al., 2010), it is dispensable for urinary tract colonization where AS mutants do not impair colonization in the upper or lower urinary tract (Johnson et al., 2004). Moreover, the expression of AS promotes biofilm formation in an *ex vivo* porcine heart valve model, in which AS-expressing *E. faecalis* cells colonizes the heart valve better (by approximately 41%) and has denser exopolymeric matrix around the biofilm compared to AS mutants at 4 hpi (Chuang-Smith et al., 2010).

Another enterococcal surface protein, Esp, seems to have different effects depending on substrate material. While the ability to form biofilm on polystyrene correlates with the presence of Esp (Toledo-Arana et al., 2001), Esp does not promote adhesion to medically relevant substrates like silicone rubber and polyethylene (Waar et al., 2002). However, *E. faecalis* Esp is important in an animal model where it contributed to mouse ascending UTI, possibly due to enhanced bacterial adhesion to bladder epithelium (Shankar et al., 2001).

Lastly, the *E. faecalis* pilus which is made up of EbpA, EbpB and EbpC subunits, is important for adherence to fibrinogen (Flores-Mireles et al., 2014;

Nallapareddy, Singh, et al., 2011), collagen (Nallapareddy, Singh, et al., 2011), and platelets (Nallapareddy, Sillanpää, et al., 2011). *E. faecalis ebp* mutants cannot form biofilms on plastic surfaces and are attenuated in a rat endocarditis model (Nallapareddy et al., 2006) and mouse ascending UTI model (Singh et al., 2007). Ebp pili also contributes to *E. faecalis* pathogenesis during CAUTI (Nielsen et al., 2012) and gastrointestinal tract colonization (Banla et al., 2019), in which a non-piliated pilus mutant was significantly attenuated compared to its isogenic wild-type strain in both models. In addition, Flores-Mireles et al. (2014) demonstrated that EbpA contributes to the formation of *E. faecalis* catheter-associated biofilm, and immunizing mice with an EbpA-based vaccine prevented EbpA from binding to fibrinogen and formation of catheter-associated biofilm, which in turn protected the mice against CAUTI. An *E. faecalis* biofilm and pilus-associated sortase (*bps*) mutant, which cannot polymerize Ebp pilins, was also attenuated in mouse UTI model and had lowered biofilm forming capability (Kemp et al., 2007). These studies suggest that the biofilm forming capability of *E. faecalis* attributed by Ebp pili plays a critical role in contributing to the pathogenesis of infections.

Taken together, *E. faecalis* expresses a repertoire of biofilm-associated virulence factors to colonize and cause infections in difference niches (summarized in **Table 1.1**). The examples mentioned above also revealed how virulence factors have multifunctional roles in host-pathogen interactions in different infection settings. While many studies have been done to investigate how *E. faecalis* virulence factors affects the pathogenesis of endocarditis, UTI,

CAUTI, endophthalmitis and peritonitis, little has been done on *E. faecalis* wound infection.

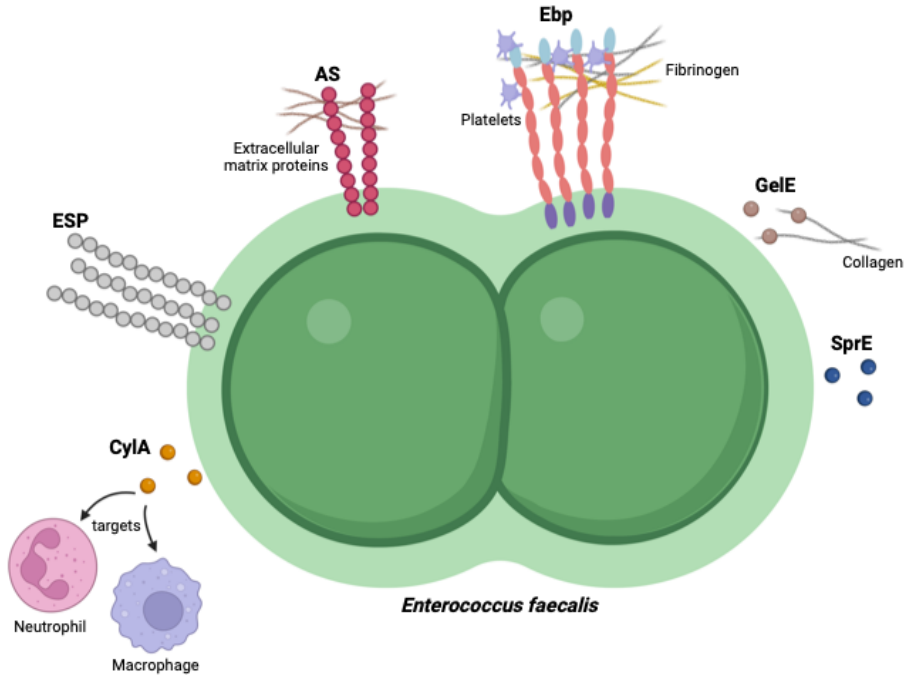

Figure 1.1 *E. faecalis* virulence factors involved in infections.
E. faecalis possesses numerous virulence factors that can be classified into secreted proteases (GelE, SprE and CylA) and surface-exposed cell-wall anchored proteins (AS, Esp and Ebp). GelE has hydrolytic activity that hydrolyzes collagen, and CylA targets neutrophils and macrophages to exert its toxic effects. AS is important for adherence to extracellular matrix proteins like collagen type I, thrombospondin, fibronectin, and vitronectin, while the Ebp pilus adheres to fibrinogen, collagen and platelets. Cells and molecules depicted in this figure is not drawn to scale.

1.1.5 Transposon and RNA sequencing, a step forward to understand *E. faecalis* wound infection

Different approaches can be adopted to elucidate genetic determinants that are involved in infections. Transposon sequencing (Tn-seq), which examines the relative fitness of transposon mutants within a large pool, is useful for investigating the contribution of individuals genes required for growth or

persistence during an infection at a genome-wide level. In particular, Tn-seq has been used to identify genetic determinants that are important for *S. aureus* and *P. aeruginosa* wound infection (Turner et al., 2014; Valentino et al., 2014). Alternatively, or complementarily, transcriptomic approaches such as RNA sequencing (RNA-seq) enable the genome wide evaluation of bacterial genes that are induced during an infection. RNA-seq has been proven successful in profiling pathogenic bacteria transcriptomes from various animal infection models and provided genome-scale insights into differential gene expression during infections (Frank, K. L. et al., 2014; Jorth et al., 2013; Lindenstrauß et al., 2014; Mandlik et al., 2011; Skvortsov et al., 2013; Turner et al., 2014). However, to date, no *in vivo* Tn-seq or RNA-seq studies of *E. faecalis* during wound infection have been reported.

Table 1.1 *E. faecalis* virulence factors and their contribution to infection.

***E. faecalis* virulence factors**	**Implication(s) during *E. faecalis* infections**	**Reference**
Secreted proteases		
Gelatinase (GelE)	Hydrolyzes insulin B-chain and collagen	Mäkinen et al. (1989)
	Increases severity of disease in rabbit endocarditis model	Gutschik et al. (1979); Thurlow et al. (2010)
	Increases severity of disease in mouse peritonitis model	Singh et al. (1998)
	Increases severity of disease in rat peritonitis model	Dupont et al. (1998)
	Decreases opsonization and neutrophil recruitment	Park et al. (2008); Thurlow et al. (2010)
	Affects biofilm formation	Hancock and Perego (2004); Thomas et al. (2008)
Serine proteases (SprE)	Affects biofilm formation	Thomas et al. (2008)
	Increases severity of disease in mouse peritonitis model	Qin et al. (2000)
	Increases severity of disease in rabbit endophthalmitis model	Engelbert et al. (2004); Suzuki et al. (2008)
Cytolysin (CylA)	Targets neutrophils and macrophages	Miyazaki et al. (1993)
	Increases severity of disease in rabbit endocarditis model	Chow et al. (1993)
	Increases severity of disease in rabbit endophthalmitis model	Jett et al. (1992)
Surface-exposed cell-wall anchored proteins		
Aggregation substances (AS)	Binds to extracellular matrix proteins	Rozdzinski et al. (2001)
	Mediates opsonin-independent phagocytosis by PMNs	Rakita et al. (1999)
	Resists killing in macrophages by inhibiting respiratory burst	Süßmuth et al. (2000)
	Increases severity of disease in rabbit endocarditis model	Chow et al. (1993); Schlievert et al. (2010)

	Affects biofilm formation	Chuang-Smith et al. (2010)
Enterococcal surface protein (Esp)	Affects biofilm formation	Toledo-Arana et al. (2001)
	Increases severity of disease in mouse ascending UTI model	Shankar et al. (2001)
Endocarditis and biofilm-associated pili (Ebp)	Adheres to fibrinogen, collagen, and platelets	Nallapareddy, Sillanpää, et al. (2011); Flores-Mireles et al. (2014); Nallapareddy, Singh, et al. (2011)
	Increases severity of disease in rat endocarditis model	Nallapareddy et al. (2006)
	Increases severity of disease in mouse ascending UTI model	Singh et al. (2007); Kemp et al. (2007)
	Increases severity of disease in mouse CAUTI model	Flores-Mireles et al. (2014); Nielsen et al. (2012)
	Increases severity of disease in mouse gastrointestinal tract colonization	Banla et al. (2019)
	Affects biofilm formation	Nallapareddy et al. (2006); Flores-Mireles et al. (2014); Kemp et al. (2007)

1.2 Microenvironment of the infection site

To colonize and persist during an infection, pathogens must overcome both the host innate immune response, as well as numerous environmental aspects of the infection site meant to prevent infection including nutrient limitation and pH changes.

1.2.1 Impact of iron availability on the pathogenesis of infections

Iron is a necessary nutrient for almost all microbial species. In humans, restriction of iron availability functions as a host innate immune mechanism against invading pathogens (Cassat & Skaar, 2013). Human iron metabolism ensures that iron is scarcely available for pathogens by sequestering the majority of iron intracellularly such that only a small amount of free iron (approximately 10^{-24} M) is accessible in the absence of an infection (Raymond et al., 2003). During an infection, there are additional iron-withholding mechanisms to further restrict iron to pathogens (Cassat & Skaar, 2013).

Immune cells such as macrophages and neutrophils synthesize hepcidin to modulate iron availability at the infection foci (Peyssonnaux et al., 2006). Additionally, neutrophils sequester iron locally at infection site through the production of lactoferrin (LF) and siderocalin/lipocalin-2 (Lcn-2) (Baker & Baker, 2012; Masson et al., 1969). Pathogens are typically phagocytosed into phagocytes as part of the host innate immune clearance response. However, some intracellular pathogens like *Mycobacterium tuberculosis* are able to adopt strategies to acquire iron intracellularly (Cassat & Skaar, 2013).

Bacteria also possess mechanisms such as siderophore production, heme uptake systems, and transferrin or lactoferrin receptors to uptake iron from the extracellular environment for successful colonization in the host. Under iron-restricted conditions, many Gram-positive and Gram-negative bacteria produce and secrete siderophores into the extracellular environment, in which the siderophores typically bind to ferric iron with high-affinity and the iron-siderophore complexes are subsequently imported into the microbial cells (Boukhalfa & Crumbliss, 2002; Braun & Killmann, 1999). For example, *P. aeruginosa* produces pyoverdine (Ravel & Cornelis, 2003; Visca et al., 2007) and pyochelin (Brandel et al., 2012; Dumas et al., 2013) when grown under iron-restricted conditions. Most iron in host is contained in hemoglobin, and pathogens like *S. aureus* possesses an iron-responsive surface determinant system for direct heme-iron uptake (Grigg et al., 2010; Hammer & Skaar, 2011). *P. aeruginosa* can also uptake heme from hemoproteins through the Has and Phu systems (Ochsner et al., 2000). Iron in host plasma is mostly bound to host glycoproteins, transferrin and lactoferrin. However, some pathogens like *Neisseria meningitidis*, have evolved mechanisms to acquire iron via transferrin- and lactoferrin-bound iron. *N. meningitidis* expresses both transferrin (Black, J. R. et al., 1986; Legrain et al., 1993; Schryvers, A. B. & Morris, L., 1988; Schryvers, A. B. & Morris, L. J., 1988) and lactoferrin receptors (Quinn et al., 1994; Schryvers, A. B. & Morris, L. J., 1988) under iron-restricted conditions. Although there are no study that characterizes enterococcal iron acquisition systems, *E. faecalis* encodes four putative iron-associated uptake systems that share homology to iron transporters in *E. coli* and *Bacillus subtilis* (Kammler et al., 1993; Ollinger et al., 2006; Sprencel et al., 2000; Zawadzka et al., 2009): (1)

OG1RF_10136 to OG1RF_10139, (2) OG1RF_10359 (*feoA*) and OG1RF_10360 (*feoB*), (3) OG1RF_11352 to OG1RF_11354, and (4) OG1RF_12351 to OG1RF_12354. Therefore, *E. faecalis* is also equipped with iron acquisition systems to uptake iron from the extracellular environment.

In another round of the arms race for iron, to counteract these bacterial iron acquisition strategies, the host secretes proinflammatory cytokines which can decrease expression of transferrin receptors on surface of macrophages to restrict iron uptake such that it limits iron to intracellular pathogens (Cassat & Skaar, 2013). Increased expression of Nramp1, found on phagosomes within the macrophage, also actively remove iron from phagosomes, limiting its availability to some intracellular pathogens (Jabado et al., 2000; Vidal et al., 1995). Moreover, proinflammatory cytokines can modulate iron metabolism by increasing ferritin synthesis to store iron in ferritin to restrict available iron in host cells (Cassat & Skaar, 2013). Hence, the microenvironment, particularly in the context of iron availability, is highly regulated and limited as part of the host defense mechanism during infections.

Multiple studies have demonstrated the importance of iron for pathogenesis. Transport of iron-siderophore complexes depends on TonB-dependent transporters and Runci et al. (2019) showed that *tonB3* of *Acinetobacter baumannii* is essential for its growth under iron-restricted conditions and virulence in *Galleria mellonella* and mouse models of infection. The deletion of *tonB3* resulted in increased survivability of larvae and mice compared to wild-type, indicating the significance of iron acquisition for *A.*

baumannii pathogenesis (Runci et al., 2019). Pyoverdine produced by *P. aeruginosa* is also essential for pathogenesis in *C. elegans* (Kang et al., 2018; Kirienko et al., 2015), mouse burned (Meyer et al., 1996) and lung infection (Minandri et al., 2016) models. More importantly, compounds that inhibit *P. aeruginosa* pyoverdine biosynthesis is effective in suppressing *P. aeruginosa* virulence in *C. elegans* (Kang & Kirienko, 2017) and mouse lung infection model (Imperi et al., 2013). Together, these studies emphasize the importance of bacterial iron acquisition from the microenvironment during various infections.

1.2.2 Impact of pH changes on the pathogenesis of infections

Changes in environmental pH can impact bacterial growth. Decreases in pH can be detrimental to bacteria due to (but not limited to) lowered enzyme activity, cell membrane perturbation, and DNA damage (Lund, P. et al., 2014). Some examples of low pH environments in humans are in the stomach (~pH 1 – 2) where gastric cells produce hydrochloric acid (Fallingborg, 1999) and the vaginal epithelium (~pH 4) where commensals such as *Lactobacillus* spp. produce weak acids as metabolic byproducts (O'Hanlon et al., 2019). Hence, to colonize and infect these acidic niches, bacteria usually adopt one of the following strategies in response to acid stress: (1) promote reactions that produces basic products to neutralize the decrease pH, (2) promote enzyme-catalyzed reactions that uses hydrogen ions, and (3) remove hydrogen ions at the expanse of ATP consumption (Lund, P. A. et al., 2020).

An acidic pH environment can also negatively impact the efficiency of immune functions. For example, secretion of tumor necrosis factor alpha (TNF-

α) by lipopolysaccharide-induced alveolar macrophages is decreased at low pH (Heming et al., 2001). A decrease in pH can also result in lowered lymphocyte-mediated cytotoxicity and chemotaxis of polymorphonuclear leukocytes (Lardner, 2001; Nakagawa et al., 2015; Severin et al., 1994). Although an acidic pH can enhance the ability of neutrophils for endocytosis through PI3K and ERK pathways (Martínez et al., 2006), the intracellular bacteria killing ability is simultaneously decreased by approximately 50% compared to normal conditions at pH 7.4 (Cao, S. et al., 2015). By contrast, a low pH environment can have a positive effect on complement activation, in which human C-reactive protein are found to activate the complement system at acidic pH 6.5 (Miyazawa & Inoue, 1990). In summary, the effect of acidic pH environment on immunological responses in human host is complex, and a low pH can exert a variety of effects depending on the different aspects of the host immune defense system.

The pH of healthy skin is usually slightly acidic, with a pH range of pH 4.2 – 5.6 (Hampton, 2008). During wound infection, the pH of wounds inclines towards a more alkaline pH due to the diffusion of interstitial fluids and plasma extravasation from injured capillaries (Scalise et al., 2015). Simultaneously, acute inflammation as a result of wound infection stimulates acidification of the wound microenvironment. Consequently, the final pH of the wound microenvironment depends on the pathophysiology of the wound and this pH can in turn affect the wound healing process. Generally, wound healing correlates with a pH transition from alkaline to neutral and then to acidic (Gethin, 2007). However, chronic wounds tend to be more alkaline, exhibit lower healing

rate and more conducive for bacterial growth (Gethin, 2007; Hoffman et al., 1999; Leveen et al., 1973; Schneider et al., 2007; Shukla et al., 2007). An increase in bacterial growth can further increase alkalinity of the wound microenvironment which in turn can further promote bacterial growth and simultaneously impede wound healing (Shukla et al., 2007). As such, modulating the pH of the wound microenvironment towards an acidic pH can promote wound healing (Bennison et al., 2017; Milne & Connolly, 2014; Schmid-Wendtner & Korting, 2006; Sharpe et al., 2009). Another characteristic of chronic wounds is tissue hypoxia which is one of the most important factors that hinder wound healing (Castilla et al., 2012). A factor that affects oxygen availability is the changes in pH, whereby decreasing the pH by 0.6 units causes the release of approximately 50% more oxygen and in turn, promotes wound healing (Hunt & Beckert, 2005; Leveen et al., 1973). Altogether, pH changes to the wound microenvironment can impact the wound healing process and bacterial growth.

1.2.3 Impact of purines availability on the pathogenesis of infections

Purine metabolites are obligatory in all living organisms for their critical role in the synthesis of DNA and RNA, as well as serving as main energy donors for cellular processes such cell signaling and energy metabolism (Kilstrup et al., 2005). In *E. faecalis*, the purine biosynthesis genes are organized in the *pur* operon. The first and last genes of the *pur* operon are *purE* and *purD*, respectively **(Figure 1.2A)**. The first step of *E. faecalis* purine biosynthesis begins with the formation of 5-phosphoribosylamine from L-glutamine and phosphoribosyl diphosphate (PRPP), catalyzed by an enzyme encoded by *purF* (Ramsey et al., 2014). Subsequently, 5-phosphoribosylamine undergoes ten

additional reactions catalyzed by genes products of the *pur* operon until inosine monophosphate (IMP) is formed (Ramsey et al., 2014). Purine biosynthesis then branches into specific pathways to produce either adenosine monophosphate which is catalyzed by enzymes encoded by *purA* and *purB* or guanosine monophosphate by enzymes encoded by *guaB* and *guaA* (Ramsey et al., 2014) **(Figure 1.2B)**.

The Pur enzymes are only required when there is sufficient supply of PRPP to kickstart the purine biosynthesis. Therefore, PRPP functions as a feed-forward inducer for the *pur* operon (Kilstrup et al., 2005). In other Gram-positive bacteria like *B. subtilis* and *Lactococcus lactis*, the PurR repressor regulates the expression of purine biosynthesis genes (Gitton et al., 2005; Jendresen et al., 2012; Kilstrup & Martinussen, 1998). Likewise, *E. faecalis* also encodes PurR which has high sequence similarity to PurR of these two species (Gitton et al., 2005; Jendresen et al., 2012; Kilstrup & Martinussen, 1998). As such, it is believed that the *pur* operon in *E. faecalis* is regulated by PurR in a similar fashion. In the absence of PRPP, PurR binds to the promoter of the *pur* operon. As a result, it prevents RNA polymerase from binding to the promoter and consequently, transcription of the *pur* operon is inhibited (Weng et al., 1995).

Multiple studies have hinted that purine metabolite availability is likely limited during infections. For example, Samant et al. (2008) showed that *de novo* purine and pyrimidine biosynthesis pathways are crucial for *E. coli* and *Salmonella typhimurium* growth in human serum. In the same study, the virulence of *B. anthracis* Δ*purE* mutant was significantly attenuated in a

bacteremia mouse model (Samant et al., 2008). Similarly, *S. aureus* purine biosynthesis is also essential for its replication and pathogenesis during bacteremia (Goncheva et al., 2020). In another example, a methicillin-resistance *S. aureus* Δ*purF* mutant colonized more poorly than its isogenic wild-type strain and was hypersusceptible to vancomycin treatment in an infective endocarditis rabbit model. More importantly, Turner et al. (2014) showed that the virulence of *P. aeruginosa* Δ*purF* mutant was completely attenuated during wound infection. Together, these studies reveal the limited availability of purine metabolites in the microenvironment of the infection site, and the importance of *de novo* purine biosynthesis across various bacteria during different infections.

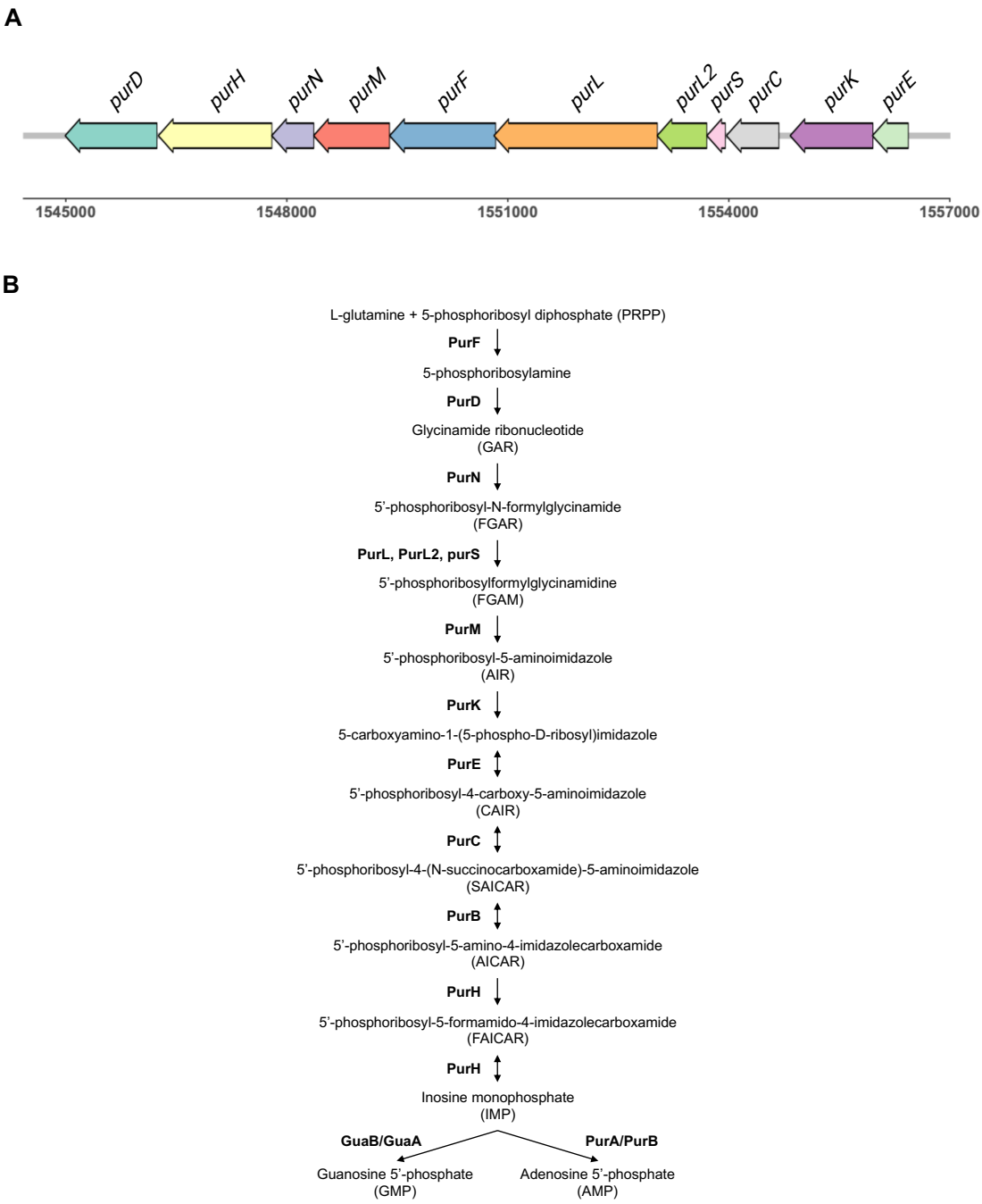

Figure 1.2 The *de novo* purine biosynthesis in *E. faecalis*.
(A) *pur* operon arrangement in *E. faecalis*. **(B)** Purine biosynthesis begins with L-glutamine and PRPP until IMP is formed, and then branches into specific pathways to synthesize GMP or AMP. Adapted from KEGG pathways efi00230.

1.2.4 Impact of carbohydrate availability on the pathogenesis of infections

Carbohydrates are usually large uncharged polar molecules and thus cannot cross the bacterial plasma membrane freely (Cooper, G. & Hausman, R.,

2000). Consequently, phosphotransferase systems (PTS) are used by bacteria for the import of carbohydrates from the environment for use in metabolic pathways as well as in signal transduction (Deutscher et al., 2006). A PTS is made up of several subunits: (1) two cytosolic subunits (EI and HPr) which is common to all PTS, (2) two hydrophilic subunits (EIIA and EIIB), and (3) at least one or two integral membrane subunit(s) (EIIC and/or EIID) (Deutscher et al., 2006). The carbohydrate specificity of each PTS is contributed by the EII subunits (Deutscher et al., 2006), and thus, there are many PTS found in each bacterial species to enable the transport of different carbohydrates into the cells.

The carbohydrate import process is a multi-step phosphorelay system, which begins with the transfer of a phosphoryl group from phosphoenolpyruvate (PEP) to EI subunit of the PTS (**Figure 1.3**, step 1), followed by EI to HPr (step 2), HPr to EIIA (step 3), and the phosphoryl group continues to transfer through the PTS subunits (step 4 and 5) until it reaches the carbohydrate it is designed to import, where the phosphoryl group is then transferred to the intended carbohydrate as it translocate across the membrane into the cytosol (step 6) (Deutscher et al., 2006). Depending on the phosphorylation state of HPr, it will have different regulatory functions. Phosphorylation of HPr at His-15 promotes carbohydrate import from the environment while phosphorylation at Ser-46 greatly reduces phosphorylation at His-15 and thus inhibits carbohydrate import (Deutscher et al., 2006). The phosphorylation of HPr at Ser-46 (and not His-15) also promotes association of HPr with the transcriptional regulator, catabolite control protein A (CcpA), to regulate gene expression involved in catabolite

repression (Deutscher et al., 2006). Hence, the HPr protein is the master regulator in Gram-positive bacteria for carbohydrate metabolism.

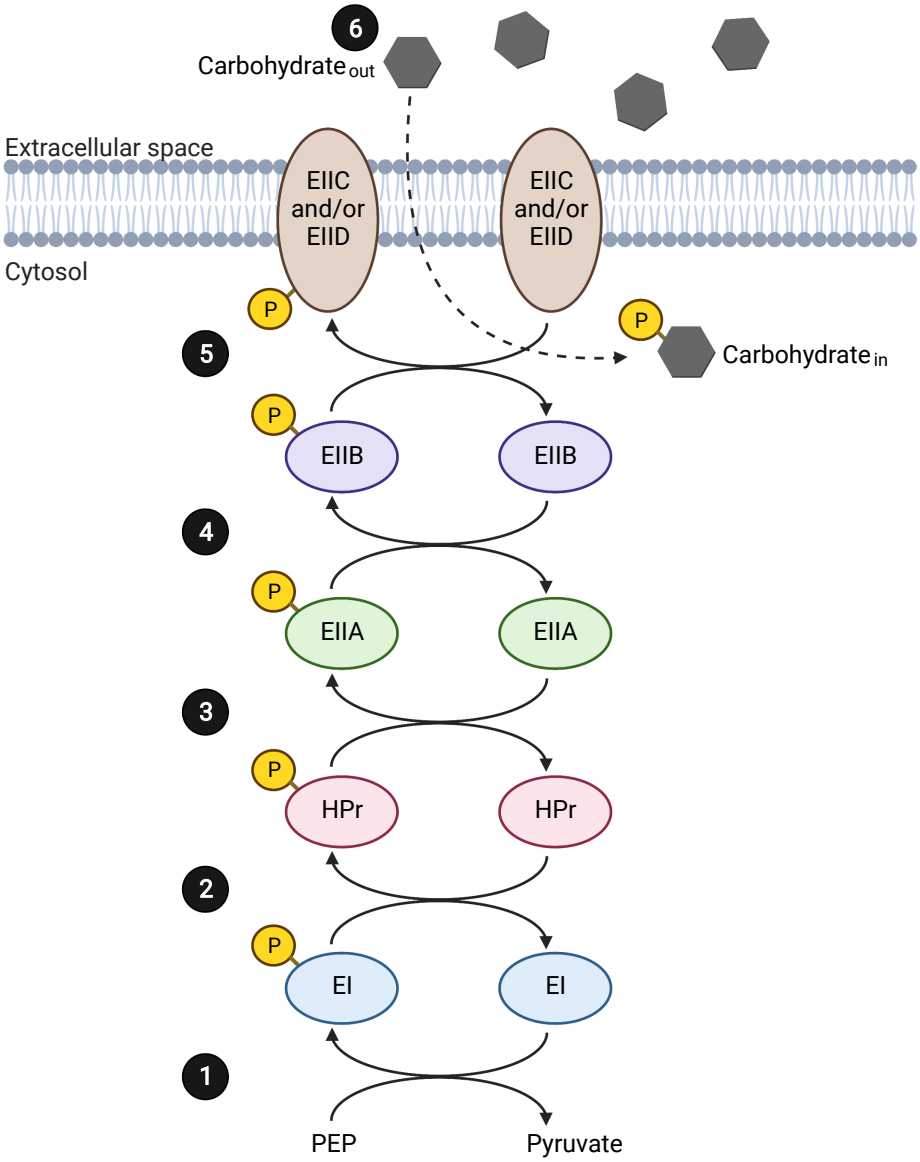

Figure 1.3 Phosphorylation of carbohydrate by phosphotransferase system during import.
A PTS consists of the following subunits: EI, HPr, EIIA, EIIB, EIIC and/or EIID. Transport of carbohydrate from the extracellular space into the bacteria by PTS starts with the transfer of a phosphoryl group from phosphoenolpyruvate (PEP) to E1 (step 1), followed by EI to HPr (step 2), HPr to EIIA (step 3), EIIA to EIIB (step 4), EIIB to EIIC and/or EIID (step 5), and finally the phosphoryl group is transferred to the intended carbohydrate for import as the carbohydrate translocate across the bacteria cell membrane into the cytosol (step 6).

Different studies have showed how carbohydrate availability and utilization in some Gram-positive bacteria can affect the progress of infections. In one study, the expression of *Streptococcus suis* virulence genes was influenced by carbohydrate availability (Ferrando et al., 2014). The expression of *S. suis* virulence genes, involved in adhesion and invasion of mucosal epithelial cells, were significantly increased when grown in starch/pullulan compared to glucose (Ferrando et al., 2014). In another study, Paixão et al. (2015) demonstrated the importance of carbohydrate utilization and disease progression in *Streptococcus pneumoniae*. Although free carbohydrates are limited during nasopharyngeal colonization of the human upper respiratory tract, *S. pneumoniae* encodes for galactosidases which can depolymerize glycoconjugates composed of monosaccharides for potential use as nutrients. Galactose (derived from glycoconjugates) is an important carbohydrate in nasopharynx and the deletion of *S. pneumoniae* galactose catabolic genes resulted in a decreased ability of these mutants to colonize the nasopharynx (Paixão et al., 2015). Additionally, based on a *S. pneumoniae* signature-tagged mutagenesis screen, genes involved in the import and metabolism of carbohydrates such as mannose, cellobiose, mannitol, lactose, and fructose were identified as essential for lung infection (Hava & Camilli, 2002). These studies suggest a possible link between carbohydrate metabolism as a result of carbohydrate availability at the infection site and pathogenesis of infections.

Altogether, the different examples in section **1.2** suggest that the environmental conditions of the infection site can affect the pathogenesis of

infections, and that these conditions could be playing a role in *E. faecalis* wound pathogenesis as well.

1.3 Thesis outline and aims

1.3.1 Research motivation

E. faecalis is usually co-isolated with *P. aeruginosa* during wound infection (Citron et al., 2007; Giacometti et al., 2000; Gjødsbøl et al., 2006) and it is clinically significant that wound infections are usually polymicrobial and biofilm-associated in nature (Bowler et al., 2001; Frank, D. N. et al., 2009; Mertz, 2003; Pastar et al., 2013). As a host defense response against invading pathogens, the host may change the microenvironment, in particular iron availability, to limit these pathogens. Further, Keogh et al. (2016) is the only study that investigated the mechanistic basis for mixed-species wound interactions of *E. faecalis* in low iron condition. Despite the prevalence of *E. faecalis* and *P. aeruginosa* during wound infections, and that the site of infection is likely to be low in iron availability, no studies have been undertaken to explore the interactions between these two pathogens in an infection-relevant, low iron condition. As such, understanding the mixed-species interactions between *E. faecalis* and *P. aeruginosa* is of interest and clinical relevance, and is explored in this dissertation in **Chapter 2**.

E. faecalis is an opportunistic pathogen implicated in several infections, and many studies have endeavored to understand the pathogenic mechanisms of *E. faecalis* in infection settings such as endocarditis, urinary tract infection, endophthalmitis and peritonitis. However, given the widespread and clinical

importance of *E. faecalis* during wound infection (Dowd et al., 2008; Dworniczek et al., 2012; Fisher & Phillips, 2009; Giacometti et al., 2000; Shettigar et al., 2018), the contributions of how this pathogen contributes to wound infection remains poorly understood. Hence, identifying and understanding the genetic determinants that contributes to *E. faecalis* wound pathogenesis is of great interest, and is explored in this dissertation in **Chapter 3**.

1.3.2 Thesis aims

The specific aims of this dissertation are:

Aim 1: To explore the mixed-species interactions between *E. faecalis* and *P. aeruginosa* under iron-restricted conditions. We characterized the nature of the mixed-species interactions under *in vitro* iron-restricted conditions using static biofilm and macrocolony biofilm assays and *in vivo* mouse wound excisional model. To understand the mechanism(s) underlying *E. faecalis* and *P. aeruginosa* mixed-species interactions, we performed an *E. faecalis* mariner transposon library screen. This work is described in **Chapter 2**.

Aim 2: To determine *E. faecalis* genetic determinants that contributes to wound infection. We identified genetic determinant(s) that is/are important for acute replication and persistence of *E. faecalis* during wound infection using *in vivo* Tn- and RNA-seq approaches in a mouse wound excisional model. To understand how the genetic determinant(s) discovered contributes to wound pathogenesis, we examined the nutrients availability of the wound microenvironment using the same mouse model. This work is described in **Chapter 3**.

The research undertaken in this dissertation contributes to our understanding of the mechanistic basis and pathogenic requirements of *E. faecalis* wound infection in a single- and mixed-species settings. A summary of the findings in this dissertation, the future applications, and future directions are discussed in **Chapter 4**. Overall, the studies conducted here advance our knowledge of *E. faecalis* wound pathogenesis and may help to better design current treatment options for improved management of *E. faecalis* wound infection.

Chapter 2 – *Enterococcus faecalis* antagonizes *Pseudomonas aeruginosa* growth in mixed-species interactions

---

This chapter contains material that has been published as ***Tan, C. A. Z.****, Lam, L. N., Biukovic, G., Soh, E. Y. C., Toh, X. W., Lemos, J. A., & Kline, K. A. (2022). Enterococcus faecalis antagonizes Pseudomonas aeruginosa growth in mixed-species interactions. Journal of Bacteriology, e00615-21. DOI: https://doi.org/10.1128/jb.00615-21. Permission has been granted by the licensed content publisher "American Society for Microbiology" to use the published content as a chapter in this thesis.*

2.1 Introduction

Many infections are often polymicrobial in nature (Bakaletz, 2004; Brogden et al., 2005; Nelson et al., 2012) and include wound infections (Bowler et al., 2001; Frank, D. N. et al., 2009; Mertz, 2003; Pastar et al., 2013), periodontitis (Darveau, 2010; Roberts, F. A. & Darveau, 2015), otitis media (Bakaletz, 2010; Marom et al., 2012), urinary tract infections (UTI) (Croxall et al., 2011; Mobley & Warren, 1987; Siegman-Igra et al., 1994; Warren et al., 1982) and cystic fibrosis (Coburn et al., 2015; Filkins et al., 2012; Lyczak et al., 2002; Shinzato & Saito, 1995; Sibley et al., 2008). Biofilms are also implicated in all these infections (Bakaletz, 2007; Bakar et al., 2018; Black, C. E. & Costerton, 2010; Colombo, A. & Tanner, 2019; Colombo, A. P. V. et al., 2016; Delcaru et al., 2016; Ebright, 2005; Hatt & Rather, 2008; Høiby, 2002; Høiby et al., 2010;

Kovach et al., 2017; Kriebel et al., 2018; Lasserre et al., 2018; Naginyte et al., 2019; Serralta et al., 2001; Soto, 2014; Thornton et al., 2011). Polymicrobial biofilms can better tolerate antibiotic treatment and escape from host immune responses, enabling the survival and persistence of the infecting bacteria (Hall-Stoodley & Stoodley, 2009; Radlinski et al., 2017). Hence, understanding how pathogens interact in biofilms may inform improved treatment strategies.

Iron is an essential nutrient for almost all microbial species. In humans, iron regulation functions as a host innate immune mechanism against invading pathogens (Cassat & Skaar, 2013). In the human body, iron is scarcely available to pathogens due to the sequestration of most iron intracellularly such that only a small amount of free iron (approximately 10^{-24} M) is accessible in the absence of infection (Raymond et al., 2003). During an infection, additional iron-withholding mechanisms further restrict iron availability to pathogens (Cassat & Skaar, 2013). For example, immune cells producing hepcidin (Peyssonnaux et al., 2006) or lactoferrin (Baker & Baker, 2012), and siderocalin/lipocalin-2 (Baker & Baker, 2012; Masson et al., 1969) to modulate iron availability at the infection site. As a result, when developing *in vitro* polymicrobial biofilm interaction models, it is critical to take into account the iron availability in the environment.

Enterococci are opportunistic pathogens implicated in several types of infections (Arias & Murray, 2012), and enterococcal infections in humans are mostly caused by *Enterococcus faecalis* and *Enterococcus faecium* (Higuita & Huycke, 2014; Kristich et al., 2014). *E. faecalis* is often co-isolated with *Pseudomonas aeruginosa* in biofilm-associated infections such as wound

infections, urinary tract infections, and periodontitis (Bowler et al., 2001; Citron et al., 2007; Colombo, A. V. et al., 2013; Dalton et al., 2011; Giacometti et al., 2000; Gjødsbøl et al., 2006; Tsuchimori et al., 1994). As such, understanding the polymicrobial interactions between these two species is of interest. The biofilm forming potential of *E. faecalis* and *P. aeruginosa* is well-studied individually (Ch' ng et al., 2019; del Mar Cendra & Torrents, 2021; Tolker-Nielsen, 2014). However, despite their co-occurrence as well as increasing efforts made to understand the polymicrobial interactions between bacterial species, there have been no reports examining *E. faecalis* and *P. aeruginosa* polymicrobial interactions in both biofilms and under iron-restricted conditions.

In this work, we show that *E. faecalis* inhibited *P. aeruginosa* growth within biofilms when iron is restricted. The growth inhibition is a consequence of increased L-lactate produced by *E. faecalis*, catalyzed by lactate dehydrogenase (*ldh1*) from pyruvate. We also show that *ldh1* expression is upregulated when iron is restricted. L-lactate produced by *E. faecalis* is exported from the cell as lactic acid (Harold & Levin, 1974), whereupon it is deprotonated to L-lactate releasing a hydrogen ion (H^+) and in turn lowering the pH in the surrounding environment. We demonstrate that this lowered environmental pH and L-lactate-mediated chelation of iron ultimately contributes to *P. aeruginosa* growth inhibition by *E. faecalis* under iron-restricted conditions. Together, our work highlights the possibility of manipulating the microenvironment to antagonize specific bacterial species within biofilms.

2.2 Materials and methods

2.2.1 Bacterial strains and growth conditions

Bacterial strains used in this study are listed in **Table 2.1**. Unless stated, all *P. aeruginosa* and *E. faecalis* bacterial strains were grown at 37 °C in shaking or static conditions for 16 – 18 h, respectively. Cells were harvested by centrifugation at 12,000 *g* for 5 min and cell pellets were washed twice with 1 mL of 1X sterile phosphate buffered saline (PBS). The final pellet was resuspended in 3 mL of 1X sterile PBS prior to optical density (OD) measurement at 600 nm. Cell suspensions were then normalized to the required cell number for different experimental assays. For *Pseudomonas* selection, bacteria were spotted onto *Pseudomonas* Isolation agar (PIA) (Difco™ BD, USA) supplemented with 100 µg/mL ampicillin (Sigma-Aldrich, USA). For *E. faecalis* OG1RF selection, bacteria were spotted onto Tryptone Soya Broth (TSB) (Oxoid, Canada) solidified with 1.5% agar (Oxiod Technical No. 3) and supplemented with 10 mM glucose (TSBG), 10 µg/mL colistin (Sigma-Aldrich, USA) and 10 µg/mL nalidixic acid (Sigma-Aldrich, USA).

Table 2.1 Bacterial strains used in Chapter 2.

Strain	Description	Reference
	P. aeruginosa	
PAO1 WT	Wild-type	Hentzer et al. (2002)
PADP6	PAO1 WT with a single nucleotide polymorphism in the *nalC* repressor gene (4166561G>T, R15L)	This study
PADP6-mCherry	PADP6 tagged with mCherry chromosomally	This study
PAO1 BAA-47	Wild-type	Pirnay et al. (2009)
PR1	Clinical isolate	Pirnay et al. (2009)
PR2	Clinical isolate	Pirnay et al. (2009)
PR30	Clinical isolate	Pirnay et al. (2009)
PR80	Clinical isolate	Pirnay et al. (2009)
PR82PR101	Clinical isolate	Pirnay et al. (2009)
PR305	Clinical isolate	Pirnay et al. (2009)
PR325	Clinical isolate	Pirnay et al. (2009)
	E. faecalis	
OG1RF	Wild-type, rif^r	Dunny et al. (1978)
OG1RF Δ*ldh1*	OG1RF with *ldh1* deletion	This study
OG1RF Δ*ldh1::ldh1*	Δ*ldh1* with *ldh1* complemented chromosomally	This study
DS16 MG1505 ST40	Clinical isolate	McBride et al. (2007)
Merz 192 MG1519 ST40	Clinical isolate	McBride et al. (2007)
WH257 MG1422 ST9	Clinical isolate	McBride et al. (2007)
WH571 MH1424 ST9	Clinical isolate	McBride et al. (2007)
SF26630 MG1556 ST6	Clinical isolate	McBride et al. (2007)
V583MG899 ST6	Clinical isolate	McBride et al. (2007)
T13 MG1344 ST21	Clinical isolate	McBride et al. (2007)

SF24396 MG1544 ST21	Clinical isolate	McBride et al. (2007)
UAA1014 MG2962 ST23	Clinical isolate	PRJNA88811
B84847 MG3030 ST23	Clinical isolate	Guardabassi et al. (2010)
SF21521 MG1542 ST28	Clinical isolate	McBride et al. (2007)
B56765 MG3031 ST28	Clinical isolate	Guardabassi et al. (2010)
	E. coli	
E. coli pTNS1	Helper plasmid for Tn7 transposase, amp^r	Choi et al. (2005)
E. coli pUC18-miniTn7-P_{tac}-mCherry	Mini-Tn7 vector containing mCherry under the control of *tac* promoter, gm^r	Lagendijk et al. (2010)

Rif^r, amp^r and gm^r represents rifampicin, ampicillin and gentamycin resistance, respectively.

2.2.2 Planktonic, static biofilms and macrocolony biofilm assays

Bacterial cultures were normalized to 1 – 2 × 10^8 CFU/mL in 1X sterile PBS. Macrocolonies were produced by inoculating 5 µL of the respective bacterial cultures onto the surface of TSB or TSBG solidified with 1.5% agar and incubated at 37 °C for either 24 h or 48 h. For mixed-species macrocolonies, bacterial species were mixed at a 1:1 ratio. When appropriate, the TSB or TSBG agar was further supplemented with or without 2,2' Bipyridyl (22D) (Sigma-Aldrich, USA), iron (III) chloride hexahydrate (Merck, USA), citric acid (Merck, USA), lactic acid, iron (II) sulfate heptahydrate, copper (II) chloride anhydrous, manganese (II) sulfate, magnesium (II) chloride, zinc chloride anhydrous, 1,4-Piperazinediethanesulfonic acid disodium salt (PIPES), 4-Morpholinepropanesulfonic acid, 3-(N-Morpholino)propanesulfonic acid (MOPS) or 4-(2-hydroxyethyl)-1-piperazineethanesulfonic acid (HEPES) buffer (all purchased from Sigma-Aldrich, USA). Macrocolonies were excised and resuspended in 2 mL of 1X sterile PBS, followed by bacteria enumeration on respective selection agar. For supernatant transfer and static biofilm assays, single- and mixed-species inocula were prepared as described above and inoculated in TSBG media for 24 h at 37 °C unless stated otherwise. For static biofilm assays, CFU enumeration were performed first by scraping the wells of 6-well microtiter plates, then pipetting to mix homogenously and serially diluted for plating on selective agar plates. For preparation of supernatant media, 24 h biofilms were first scraped, suspended in conical tubes (cells and spent media together) and centrifuged at 4,000 rpm for 20 min to pellet the cells. Spent media is transferred to a new tube and filter-sterilized to obtain cell-free supernatant. The cell-free supernatant was then mixed with fresh TSBG media or water, and

then supplemented with 1 mM 22D, prior to inoculating for subsequent growth at 37 °C in static conditions for 24 h. For planktonic assay, 5 µL of the respective bacterial cultures were inoculated into TSBG media and incubated at 37 °C in shaking conditions for 24 h.

2.2.3 Construction of PADP6 and PADP6-mCherry strains

Overnight cultures of PAO1-WT were diluted to 10^9, 10^8, 10^7 and 10^6 CFU/mL in 1X sterile PBS, and 300 µL of each cell suspension were plated onto LB Lennox agar (Difco™ BD, USA) supplemented with 1.5, 2, 2.5, 3 and 4 mM 22D. Plates were incubated at 37 °C for 24 to 36 h. PAO1-WT and few colonies that grew in 3 mM 22D-chelated condition were isolated and gDNA extracted using Wizard® Genomic DNA Purification Kit (Promega, USA) for use in whole genome sequencing. PADP6 was chromosomally tagged with mCherry through triparental conjugation using PADP6 as a recipient with delivery plasmid pUC18-miniTn7-P_{tac}-mCherry (*E. coli*) and helper plasmid pTNS1 (*E. coli*) resulting in PADP6-mCherry (Choi et al., 2005; Choi & Schweizer, 2006; Sambrook et al., 1989).

2.2.4 Genome sequencing and analysis

Raw reads were imported into CLC Genomics Workbench 8.0 (Qiagen, Germany), followed by quality trimming to remove bad quality reads. The trimmed reads were then mapped to the reference genome before the Basic Variant Detection module was used to detect for mutations using the default parameters. The mutations detected in the isolate was then filtered against

PAO1-WT control to determine the mutations acquired for survival under iron-restricted conditions.

2.2.5 Planktonic growth assay

Bacterial cultures were normalized to OD_{600} of 0.01 in the respective media and inoculated into 24-well microtiter plates. All microtiter plates were incubated at 37 °C in shaking conditions. Planktonic growth was measured by recording the OD_{595} at intervals of 30 min to 1 h using a Tecan Infinite© M200 Pro spectrophotometer (Tecan Group Ltd., Switzerland) until early stationary growth phase was reached.

2.2.6 RNA extraction from planktonic cultures and absolute quantification by RT-qPCR

P. aeruginosa cultures were normalized to OD_{600} of 0.01 in the respective media and inoculated into 24-well microtiter plates. All microtiter plates were incubated at 37 °C in shaking conditions. Planktonic growth was measured at OD_{600} at regular intervals using a Tecan Infinite© M200 Pro spectrophotometer (Tecan Group Ltd., Switzerland) until approximately OD_{600} of 0.5 was reached. Bacteria were then harvested in RNAprotect™ Bacteria Reagent (Qiagen, Germany) and incubated at room temperature for 5 mins before centrifuging at 10,000 *g* for 10 mins. The supernatant was decanted, and bacteria pellets collected were subjected to total RNA extraction using RNeasy® mini kit (Qiagen, Germany) according to manufacturer's protocol. Extracted RNA samples were subsequently treated with DNase (TURBO DNA-free™ kit, Invitrogen, USA) for removal of contaminating genomic DNA before the RNA was purified with

Monarch® RNA cleanup kit (New England Biolabs, USA). The concentration of RNA and potential DNA contamination were quantified using Qubit™ RNA BR and Qubit™ dsDNA HS assay kits, respectively (Invitrogen, USA). The extracted RNA was also quality checked using a TapeStation instrument (RNA ScreenTape, Aligent Technologies, USA). RNA samples with a maximum of 10% DNA contamination and a RINe value ≥ 7.5 were used for RT-qPCR. Equivalent amounts of RNA across all samples were converted to cDNA using SuperScript™ III First-Strand Synthesis SuperMix (Invitrogen, USA). Following cDNA synthesis, absolute quantification of *mexA*, *mexB* and *oprM* were performed using KAPA SYBR® FAST qPCR Master Mix (2X) kit (Kapa Biosystems, USA). The primers used for amplification of *mexA*, *mexB* and *oprM* are listed in **Table 2.2**.

Table 2.2 Primers used in Chapter 2.

Primer name	Sequence (5' to 3')	Reference
qPCR_*mexA*_F	GCCTCGAATTCTCCGAGGTT	This study
qPCR_*mexA*_R	CTTCTGCTTGACGCCTTCCT	This study
qPCR_*mexB*_F	GTGTTCGGCTCGCAGTACTC	(Pourakbari et al., 2016)
qPCR_*mexB*_R	AACCGTCGGGATTGACCTTG	(Pourakbari et al., 2016)
qPCR_*oprM*_F	CCATGAGCCGCCAACTGTC	(Savli et al., 2003)
qPCR_*oprM*_R	CCTGGAACGCCGTCTGGAT	(Savli et al., 2003)
1-*ldh1*_UpF	TGTGTGATGGATATCTGCACGGA CCAACAGAGCGACCTGATTC	This study
2-*ldh1*_UpR	GTGTACCATTCCTTCCTCTACATT CTTTTTCGTG	This study
3-*ldh1*_DownF	TAGAGGAAGGAATGGTACACAAC TCCTTCTATAATAGTCGAAAATTA AAAACAACCA	This study

4-*ldh1*_DownR	AGTGTGCTGGAATTCTGCATAGC GAATGGTACGAATACAATGTGTG TG	This study
COM_*ldh1*_F	CTGAGCGGCCGCTTTGTAAAGC GCCTGCCATC	This study
COM_*ldh1*_R	ACTGGGATCCGTGAACGTTGGTT TCCCGTG	This study

2.2.7 Pyoverdine quantification

P. aeruginosa cultures were normalized to OD_{600} of 0.01 in the respective media and inoculated into 24-well microtiter plates. All microtiter plates were incubated at 37 °C in shaking conditions. Planktonic growth was measured at OD_{600} at regular intervals using a Tecan Infinite© M200 Pro spectrophotometer (Tecan Group Ltd., Switzerland) until approximately OD_{600} of 0.5 was reached. Cell-free supernatant was then obtained from these samples. Pyoverdine secretion was quantified by measuring the fluorescence intensity of the supernatants (excitation at 400 nm and emission at 450 nm) and normalizing it to the respective OD_{600} of each sample.

2.2.8 *E. faecalis* transposon library screen

An *E. faecalis* OG1RF mariner transposon library consisting of 14,978 mutants was cryogenically stocked in 96-well microtiter plates (Kristich et al., 2008). These OG1RF transposon mutants were cultured in 180 µL BHI broth at 37 °C in static conditions for 16 – 18 h in 96-well microtiter plates using a cryo-replicator (Adolf Kühner AG, Switzerland) and spotted onto BHI agar plates for incubation at 37 °C for 24 h. Following that, OG1RF transposon mutants from the BHI agar plates were cultured for primary screening in 180 µL BHI broth as described above. PADP6-mCherry cultures were grown and washed as

described above. Both the OG1RF transposon mutant cultures and PADP6-mCherry were normalized to OD_{600} of 0.01 in TSBG media supplemented with 1.2 mM 22D. A primary screen of the *E. faecalis* transposon library was done by mixing the normalized OG1RF transposon mutant cultures and PADP6-mCherry at a 1:1 ratio in 96-well microtiter plates (total volume of 200 µL). The microtiter plates were then incubated at 37 °C in static conditions for 22 h. The growth of PADP6-mCherry was quantified by measuring mCherry fluorescence intensity (excitation = 480 nm, emission = 615 nm) using a Tecan Infinite© M200 Pro spectrophotometer. Secondary validation of the OG1RF transposon mutants was performed by mixed-species macrocolony biofilm assays as described above to quantify the growth of PADP6 and each transposon mutant (CFU/mL) in 1 mM 22D iron-restricted conditions at 37 °C for 24 h.

2.2.9 Molecular cloning

The primers used in this study are listed in **Table 2.2**. Transformants were screened using respective selection agar as follows: (A) *E. coli* strains, LB with 500 µg/mL erythromycin (pGCP213); and (B) *E. faecalis* strains, BHI with 25 µg/mL erythromycin (pGCP213). Generation of *E. faecalis* knock-out mutants were done by allelic replacement using a temperature-sensitive shuttle vector described previously (Nielsen et al., 2012). Vector pGCP213 was linearized using restriction enzymes (New England Biolabs, USA) for the construction of OG1RF ∆*ldh1* and OG1RF ∆*ldh1::ldh1*. Linearized vector and inserts were ligated using In-Fusion® HD Cloning Kit (Clontech, Takara, Japan) and transformed into Stellar™ competent cells. Successful plasmid constructs were verified by Sanger sequencing and subsequently extracted and transformed into

OG1RF. Transformants were selected with erythromycin at 30 °C, then passaged at non-permissive temperature at 42 °C with erythromycin to select for bacteria with successful plasmid integration into the chromosome. For plasmid excision, bacteria were serially passaged at 37 °C without erythromycin for erythromycin-sensitive colonies. These colonies were then subjected to PCR screening for detection of deletion mutant (OG1RF Δ*ldh1*) or chromosomal complementation of *ldh1* (OG1RF Δ*ldh1::ldh1*).

2.2.10 Lactate-Glo™ assay

L-lactate quantification was done using the Lactate-Glo™ assay kit (Promega, USA). A 3 cm by 3 cm section of agar surrounding the macrocolonies were excised, resuspended in 5 mL of 1X sterile PBS and homogenized using a homogenizer (PRO Scientific, USA) to measure secreted L-lactate in the agar surrounding the macrocolonies. Supernatant were then collected by centrifuging homogenate at 5,000 *g* for 10 min and used for L-lactate quantification. Briefly, an equal volume of Lactate Detection Reagent was added to the supernatant and incubated for 60 min at room temperature before luminescence was read using a Tecan Infinite© M200 Pro spectrophotometer.

2.2.11 Total iron quantification

Iron quantification was done using the Iron Assay Kit (Colorimetric) (Abcam, UK) as per manufacturer's instruction. Prior to quantification, samples were prepared by supplementing different concentrations of 22D or sodium L-lactate (Sigma-Aldrich, USA) to 200 μM iron (II) sulfate heptahydrate ($FeSO_4 \cdot 7H_2O$) and iron (III) chloride hexahydrate ($FeCl_3 \cdot 6H_2O$). The output was

measured immediately at OD_{593} using a Tecan Infinite© M200 Pro spectrophotometer. The iron concentration in each sample was computed based on the standard curve generated using the iron standards.

2.2.12 RNA extraction from macrocolonies

Matured single- and mixed-species macrocolonies grown for 48 h on TSBG agar supplemented with and without 2,2' bipyridyl, in biological triplicates, were first scraped into RNAprotect™ Bacteria Reagent (Qiagen, Germany) and incubated at room temperature for 5 mins before centrifuging at 10,000 *g* for 10 mins. The supernatant was decanted, and bacteria pellets collected were then subjected to total RNA extraction using RNeasy® mini kit (Qiagen, Germany) with slight modifications. Briefly, cell pellets were resuspended in TE buffer containing 20 mg/mL lysozyme (Sigma-Aldrich, USA) and each sample was further supplemented with 20 µL proteinase K (Qiagen, Germany). This was followed by incubation at 37 °C for 1 h, and subsequent extraction steps was performed according to manufacturer's protocol. Extracted RNA samples were treated with DNase (TURBO DNA-free™ kit, Invitrogen, USA) for removal of contaminating genomic DNA before the RNA was purified with Monarch® RNA cleanup kit (New England Biolabs, USA). The concentration of RNA and potential DNA contamination were quantified using Qubit™ RNA BR and Qubit™ dsDNA HS assay kits, respectively (Invitrogen, USA). The extracted RNA was quality checked using a TapeStation instrument (RNA ScreenTape, Aligent Technologies, USA) before it was sent for sequencing. Every sample had to have a minimum RNA concentration of 40 – 80 ng/µL, a maximum of 10% DNA contamination and a RINe value ≥ 8.0, before being used for library

preparation and subsequent sequencing as 100 bp paired end reads on an Illumina HiSeq2500 at Singapore Centre for Environmental Life Sciences Engineering (SCELSE) sequencing facility.

2.2.13 Transcriptomic analysis

The raw reads obtained were checked using FastQC (Version 0.11.9) and adaptor trimmed using bbduk from BBMap tools (Version 39.79) (Bushnell, 2015). Trimmed reads were then mapped using bwa-mem of BWA (Version 0.7.17-r1188) with options "-T 20 -k 13" against *E. faecalis* OG1RF (NCBI accession: CP002621) or *P. aeruginosa* PAO1 (NCBI accession: NC_002516) reference genomes. Reads mapped to open reading frames were quantified using htseq-count of HTSeq (Version 0.12.4) with option "-m intersection-strict" (Anders et al., 2015). Ribosomal sequences were filtered out from all data sets. Differential gene expression analysis was performed in R using *edgeR* (Version 3.28.1) (Robinson et al., 2010). The log2 fold change values extracted were based on the false discovery rate (FDR) < 0.05.

2.2.14 Mouse wound excisional model

Mouse wound infections were performed similarly to a previous study (Chong et al., 2017). Bacterial cultures were normalized to 2 – 4 × 10^8 CFU/mL in 1X sterile PBS. Male C57BL/6 mice (7 – 8 weeks old, InVivos, Singapore) were anesthetized by inhalation of 3% isoflurane. The dorsal hair was shaved, and a depilatory cream (Nair™ cream, Church and Dwight Co, USA) was applied to remove fine hair through shaving with a scalpel. The skin was next disinfected with 70% ethanol and a wound was created using a 6 mm biopsy

punch (Integra Miltex, USA). This was followed by inoculation with 10 µL of respective bacterial cultures per wound before the wound site was covered with a transparent dressing (Tegaderm™ 3M, USA). At 24 h post-infection (hpi), the mice were euthanized. Subsequently, a 1 × 1 cm piece of skin encompassing the wound site was excised and transferred into 1 mL of 1X sterile PBS. The excised wounds were homogenized and spotted onto respective selection agars for enumeration of *P. aeruginosa* and *E. faecalis*. Animals without the wound dressing at the point of sacrifice were excluded from data analysis.

2.2.15 Statistical analysis

Statistical analyses were performed with GraphPad Prism software (Version 9.0.0, California, USA) and are described in the respective figure legends.

2.2.16 Data availability

All RNA-seq sequences were deposited in the National Center for Biotechnology Information Gene Expression Omnibus database under accession number GSE190090 (https://www.ncbi.nlm.nih.gov/geo/query/acc.cgi?acc=GSE190090).

2.3 Results

2.3.1 *E. faecalis* inhibits *P. aeruginosa* growth under iron-restricted conditions.

The compound 2,2'-dipyridyl (22D) is widely used as a neutral ligand for the chelation of metal ions and is a high affinity chelator of iron (Kaes et al., 2000). Therefore, 22D was supplemented into TSBG growth media to restrict iron availability. We first investigated the interactions between 12 different *E. faecalis* clinical isolates and *P. aeruginosa* PAO1 BAA-47 using static biofilm assays. In iron-restricted media (TSBG supplemented with 1 mM 22D), PAO1 BAA-47 growth was inhibited in all of the mixed-species biofilms compared to PAO1 BAA-47 single-species biofilm **(Figure 2.1A)**. By contrast, *E. faecalis* growth was similar in the single- and mixed-species biofilms **(Figure 2.1B)**. These data indicate that *E. faecalis* inhibition of *P. aeruginosa* is not strain specific. We next performed the biofilm assay, now with *E. faecalis* OG1RF and eight different *P. aeruginosa* clinical isolates, to examine whether *P. aeruginosa* susceptibility to *E. faecalis*-mediated inhibition was strain specific. We observed that the growth of all *P. aeruginosa* isolates was inhibited in the mixed-species biofilms compared to their respective single-species counterpart **(Figure 2.1C)**, while *E. faecalis* growth in the single- and mixed-species biofilms remained unaffected **(Figure 2.1D)**. These data demonstrate that all tested *E. faecalis* and *P. aeruginosa* clinical isolates engage in mixed-species antagonism under iron-restricted conditions.

We next performed supernatant transfer assays in which either *E. faecalis* or *P. aeruginosa* single- or mixed-species biofilms were grown in iron-

restricted media, and their cell-free biofilm supernatants were collected and supplied to *P. aeruginosa* at a 1:1 ratio with fresh media for subsequent growth assays. There were minimal differences in PAO1 BAA-47 growth when supplemented with biofilm supernatant obtained from single-species PAO1 BAA-47 biofilm compared to supplemented with water **(Figure 2.1E)**. However, when PAO1 BAA-47 was grown with supernatant obtained from single-species OG1RF or mixed PAO1 BAA-47 and OG1RF biofilms, we observed a significant inhibition of PAO1 BAA-47 growth compared to control supplementation **(Figure 2.1E)**, suggesting that *P. aeruginosa* inhibition is mediated by the presence of *E. faecalis*.

Next, to validate the above findings and to determine the mechanistic basis of polymicrobial interactions between *E. faecalis* and *P. aeruginosa* under iron-restricted conditions, we performed mixed-species macrocolony biofilm assays (Keogh et al., 2016; Lam et al., 2020), initially using *E. faecalis* OG1RF and *P. aeruginosa* PAO1 for our experiments. However, PAO1-WT was sensitive to iron restriction at 22D concentrations greater than 1 mM **(Appendix Figure 2.1A and B)** and had a minimum inhibitory concentration (MIC) of 0.8 mM to 22D (data not shown), while there was minimal effect on OG1RF up to 3 mM 22D **(Appendix Figure 2.1C)**. As such, a *P. aeruginosa* PAO1 spontaneous mutant that was resistant to 22D chelation was generated and named PADP6. Whole genome sequencing of this mutant revealed a single nucleotide polymorphism in the *nalC* repressor gene (4166561G>T, R15L). This mutation in PADP6 restored growth in 2 mM 22D to similar levels as PAO1-WT macrocolonies grown in unchelated media **(Appendix Figure 2.1A)**, and

PADP6 was less sensitive to 22D iron restriction compared to PAO1-WT **(Appendix Figure 2.1B and D)**. Mutation in *nalC* causes an overexpression of the iron-regulated *mexAB-oprM* operon encoding the MexAB-OprM efflux pump upon severe iron restriction (Cao, L. et al., 2004; Poole, Heinrichs, et al., 1993). Additionally, the MexAB-OprM efflux pump is implicated in pyoverdine siderophore secretion (Poole, Heinrichs, et al., 1993; Poole, Krebes, et al., 1993). Hence, to understand how the single nucleotide polymorphism in *nalC* enhances 22D resistance in PADP6, we quantified the expression of *mexA*, *mexB* and *oprM* as well as pyoverdine production in PAO1-WT and PADP6 when grown in iron-restricted media. As expected, we observed higher expression of *mexA*, *mexB* and *oprM* in PADP6 compared to PAO1-WT in both unchelated and 0.5 mM 22D-chelated media **(Appendix Figure 2.2A, B and C)**. Pyoverdine secretion was also higher in PADP6 than PAO1-WT when grown in 0.5 mM 22D-chelated media **(Appendix Figure 2.2D)**, suggesting that PADP6 confers tolerance to iron starvation by increasing pyoverdine secretion. Moving forward, *E. faecalis* OG1RF and *P. aeruginosa* PADP6 were used for all subsequent experiments.

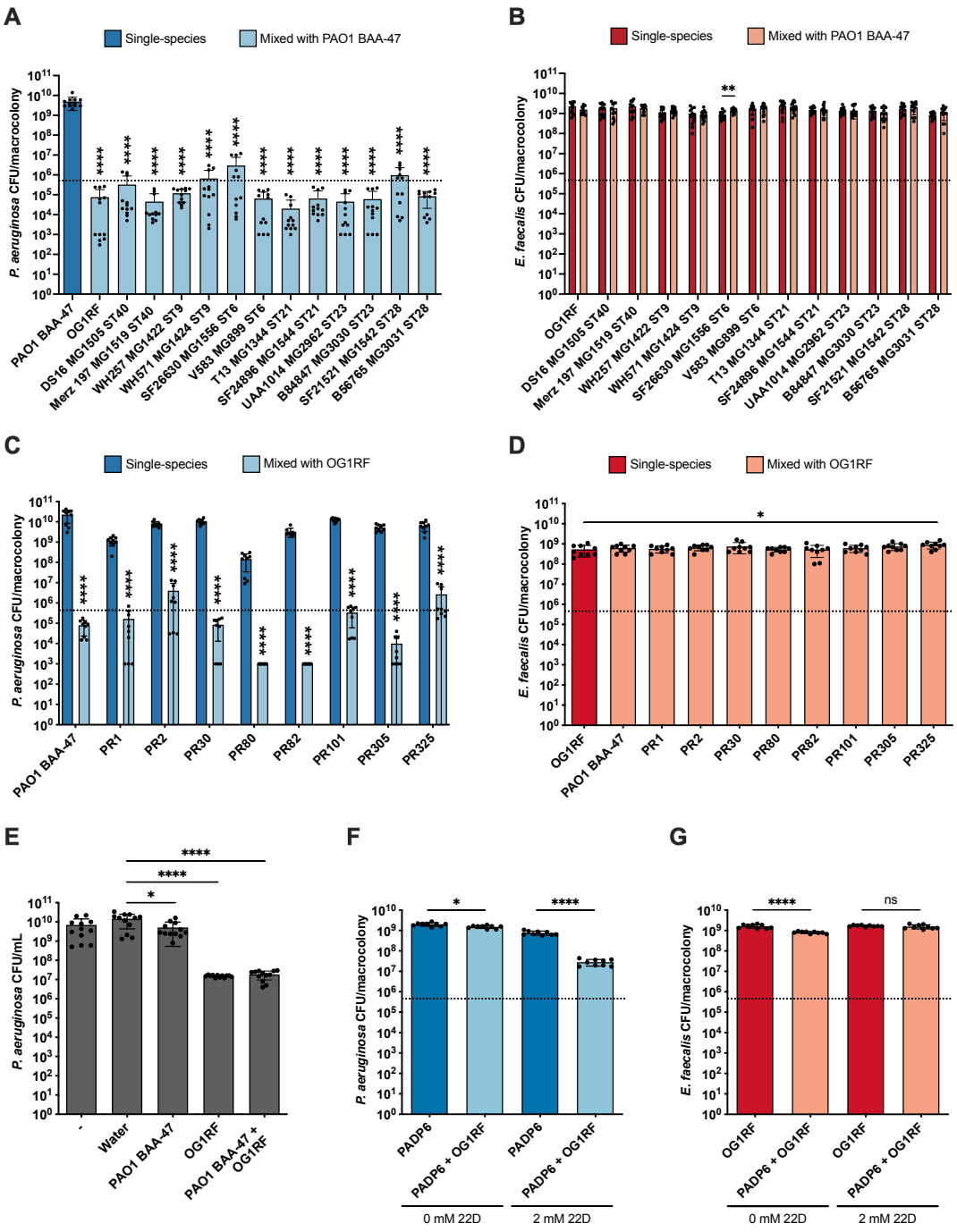

Figure 2.1 *E. faecalis* inhibits *P. aeruginosa* growth under iron-restricted conditions.

Enumeration of **(A)** PAO1 BAA-47, **(B)** *E. faecalis* clinical isolates, **(C)** *P. aeruginosa* clinical isolates and **(D)** OG1RF from 24 h biofilms with single or mixed inoculums grown in TSBG media supplemented with 1 mM 22D. Dotted lines represent inoculum of bacteria spotted. N ≥ 3 with 3 technical replicates; error bars represent SD from the mean. Statistical analysis was performed using Mann-Whitney U test, *p < 0.05, **p < 0.01, ***p < 0.001, ****p < 0.0001. For **(A)**, statistical significance is for all strains when compared to PAO1 BAA-47. Enumeration of **(E)** PAO1 BAA-47 from 24 h cultures grown with fresh TSBG

media, water, or cell-free supernatant obtained from 24 h biofilms of PAO1 BAA-47, OG1RF and PAO1 BAA-47 mixed with OG1RF. The water and respective supernatants were mixed at a 1:1 ratio with fresh TSBG media supplemented with 1 mM 22D for PAO1 BAA-47 growth. N = 4 with 3 technical replicates; error bars represent SD from the mean. Statistical analysis was performed using Mann-Whitney U test, *p < 0.05, **p < 0.01, ***p < 0.001, ****p < 0.0001. Enumeration of **(F)** PADP6 and **(G)** OG1RF from 24 h macrocolonies with single or mixed inoculums grown in TSBG media supplemented without and with 2 mM 22D. Bacterial species were mixed at a 1:1 ratio for mixed-species macrocolonies. Dotted lines represent inoculum of bacteria spotted. N = 3 with 3 technical replicates; error bars represent SD from the mean. Statistical analysis was performed using Mann-Whitney U test, *p < 0.05, **p < 0.01, ***p < 0.001, ****p < 0.0001.

To validate that PADP6 was also susceptible to *E. faecalis*-mediated growth inhibition when iron was restricted (supplemented with 2 mM 22D), we performed the macrocolony biofilm assay and observed that PADP6 growth was inhibited in mixed-species macrocolonies compared to PADP6 single-species macrocolonies **(Figure 2.1F)**, whereas OG1RF growth in the single- and mixed-species macrocolonies was unaffected **(Figure 2.1G)**. Further, the addition of ferric chloride ($FeCl_3$) to 22D-chelated media restored PADP6 growth in the mixed-species macrocolonies to levels similar to PADP6 single-species growth in chelated media without $FeCl_3$ supplementation **(Figure 2.2A and B)**, indicating that PADP6 growth inhibition in mixed-species macrocolonies is specific to the presence of *E. faecalis* and iron restriction. The supplementation of other trace metals to 22D-chelated media were unable to rescue growth inhibition of *P. aeruginosa* **(Figure 2.2C and D)**. We also explored the polymicrobial interactions between *E. faecalis* and *P. aeruginosa* in 2 mM 22D-chelated TSB growth media (lacking the supplemental glucose of TSBG). However, we did not observe an antagonistic relationship between these two bacteria **(Appendix Figure 2.3A and B)**, suggesting that nutritional differences

contribute to the antagonistic relationship between *E. faecalis* and *P. aeruginosa*. Subsequently, TSBG media was used for all experiments as we wanted to understand and exploit the mechanistic basis of the antagonism between *E. faecalis* and *P. aeruginosa* for future possibilities in treatment applications. Hence, based on the mixed-species antagonism observed in TSBG media, we hypothesized that *E. faecalis* OG1RF produces a factor, or modulates the local environment, such that it is unfavorable for the growth of PADP6 under iron-restricted conditions.

Planktonic growth was also examined to determine whether PADP6 growth inhibition in the presence of OG1RF was specific to biofilms. In unchelated media, we observed PADP6 growth inhibition by approximately 1 log in co-culture with *E. faecalis* OG1RF compared to PADP6 alone, while OG1RF growth in co-culture remained unaffected **(Figure 2.3)**. However, PADP6 was further inhibited by more than 2 logs in the presence of 22D. Therefore, *E. faecalis* OG1RF inhibition of *P. aeruginosa* PADP6 growth is not a biofilm-specific phenotype.

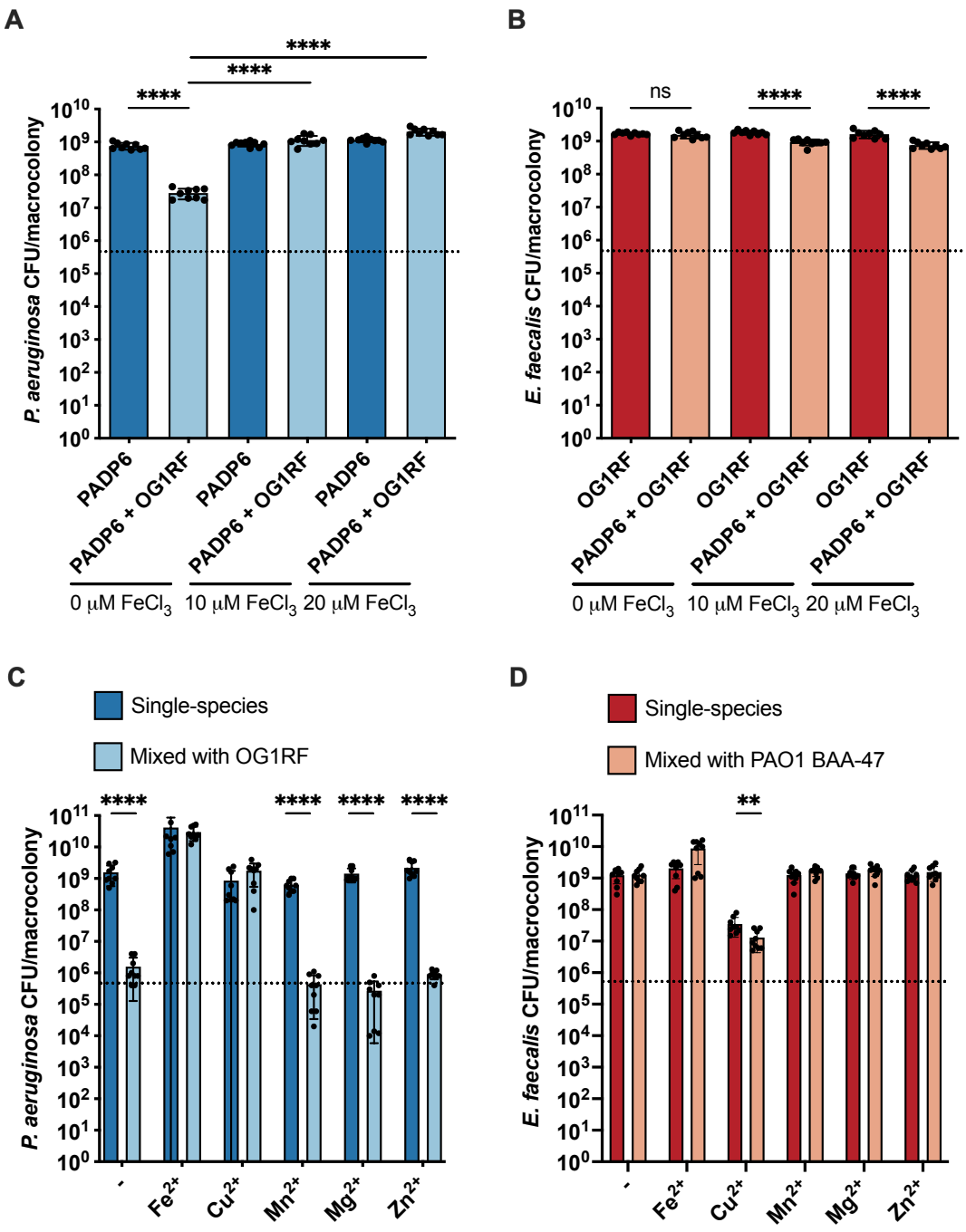

Figure 2.2 Growth inhibition of *P. aeruginosa* by *E. faecalis* is iron-specific. Enumeration of **(A)** PADP6 and **(B)** OG1RF from 24 h macrocolonies with single or mixed inoculums grown in 2 mM 22D-chelated TSBG media without and with $FeCl_3$ (10 and 20 μM). Bacterial species were mixed at a 1:1 ratio for mixed-species macrocolonies. Dotted lines represent inoculum of bacteria spotted. N = 3 with 3 technical replicates; error bars represent SD from the mean. Statistical analysis was performed using Mann-Whitney U test, *p < 0.05, **p < 0.01, ***p < 0.001, ****p < 0.0001. Enumeration of **(C)** PAO1 BAA-47 and **(D)** OG1RF from 24 h single- and mixed-species macrocolonies grown in 1 mM 22D-chelated TSBG media without and with 100 μM of varying trace metals. Bacterial species

were mixed at a 1:1 ratio for mixed-species macrocolonies. Dotted lines represent inoculum of bacteria spotted. N = 3 with 3 technical replicates; error bars represent SD from the mean. Statistical analysis was performed using Mann-Whitney U test, *p < 0.05, **p < 0.01, ***p < 0.001, ****p < 0.0001.

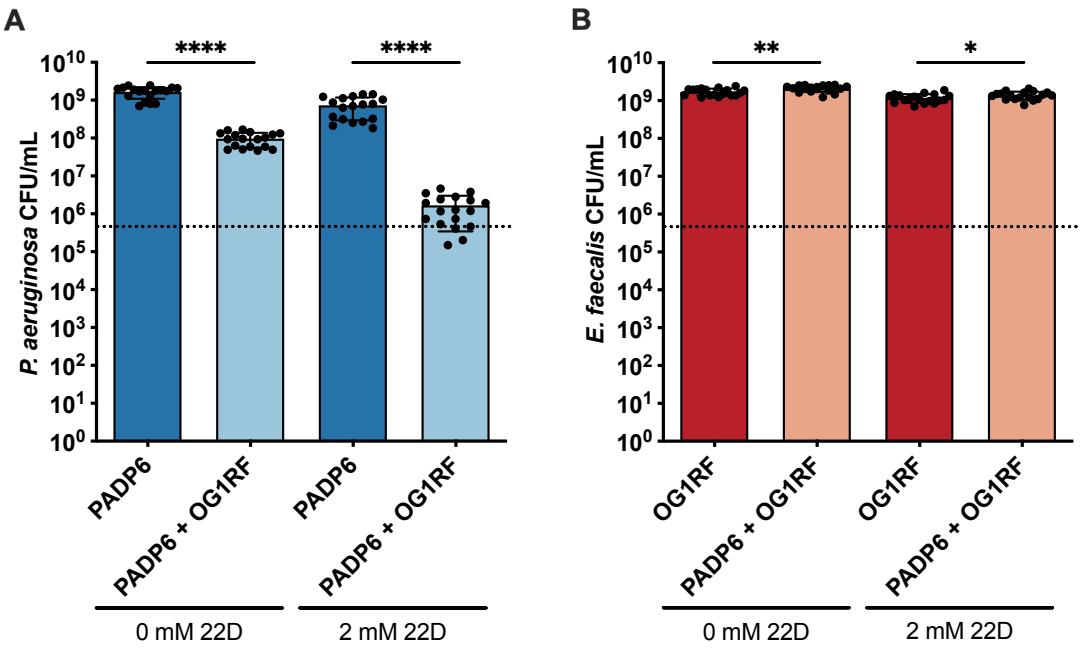

Figure 2.3 *E. faecalis* inhibits *P. aeruginosa* growth in planktonic conditions regardless of iron levels.
Enumeration of **(A)** PADP6 and **(B)** OG1RF from single or mixed inoculums grown for 24 h in TSBG media supplemented without and with 2 mM 22D. Bacterial species were mixed at a 1:1 ratio for mixed-species macrocolonies. Dotted lines represent inoculum of bacteria spotted. N ≥ 3 with 3 technical replicates; error bars represent SD from the mean. Statistical analysis was performed using Mann-Whitney U test, *p < 0.05, **p < 0.01, ***p < 0.001, ****p < 0.0001.

2.3.2 *E. faecalis ldh1* is responsible for *P. aeruginosa* growth inhibition under iron-restricted conditions.

An *E. faecalis* mariner transposon library screen was performed to identify *E. faecalis* mutants that did not inhibit PADP6 planktonic growth under iron-restricted conditions. We identified six *E. faecalis* mutants that did not inhibit PADP6 growth when co-cultured; however, upon validation of these six mutants

in the macrocolony assay, three of which were validated for failure to inhibit PADP6 growth: *ldh1*, *gloA3* and *guaB* **(Appendix Table 2.1)**. There was a bimodal pattern for PADP6 growth in the mixed PADP6 and OG1RF *guaB*::Tn macrocolonies, in which among 5 independent experiments, only ~30% of the replicates did not result in PADP6 growth inhibition **(Appendix Figure 2.4A)**. As such, *guaB* was not followed up on due to this bimodality. On the other hand, PADP6 growth was not inhibited in the mixed PADP6 and OG1RF *gloA3*::Tn macrocolonies across all 3 independent experiments performed **(Appendix Figure 2.4B)**. *E. faecalis gloA3* encodes for glyoxalase and is involved in detoxifying methylglyoxal to D-lactate (Chakraborty et al., 2014). Among *gloA3* and *ldh1*, we were more interested in *ldh1* and therefore, decided to focus on the transposon insertion in *ldh1* (*ldh1::Tn*). In *E. faecalis*, there are two copies of *ldh* (*ldh1* and *ldh2*) that encode L-lactate dehydrogenase (LDH) to catalyze the reduction of pyruvate to L-lactate (Ramsey et al., 2014). Of the two copies, *ldh1* accounts for the majority of L-lactate produced in *E. faecalis* in laboratory settings (Jönsson et al., 2009; Ramsey et al., 2014)

We then created a *ldh1* deletion mutant (OG1RF Δ*ldh1*) and validated the transposon screening results in a macrocolony biofilm assay with PADP6 and OG1RF Δ*ldh1*. Specifically, PADP6 growth was not inhibited in the mixed PADP6 and OG1RF Δ*ldh1* macrocolonies compared to mixed PADP6 and OG1RF macrocolonies **(Figure 2.4A)**. Importantly, OG1RF Δ*ldh1* growth in single- and mixed-species macrocolonies was unaffected **(Figure 2.4B)**. Upon *ldh1* chromosomal complementation in OG1RF Δ*ldh1*, PADP6 growth was

inhibited to levels as when grown with OG1RF **(Figure 2.4A)**, suggesting that *ldh1* plays a role in inhibiting PADP6 growth under iron-restricted conditions.

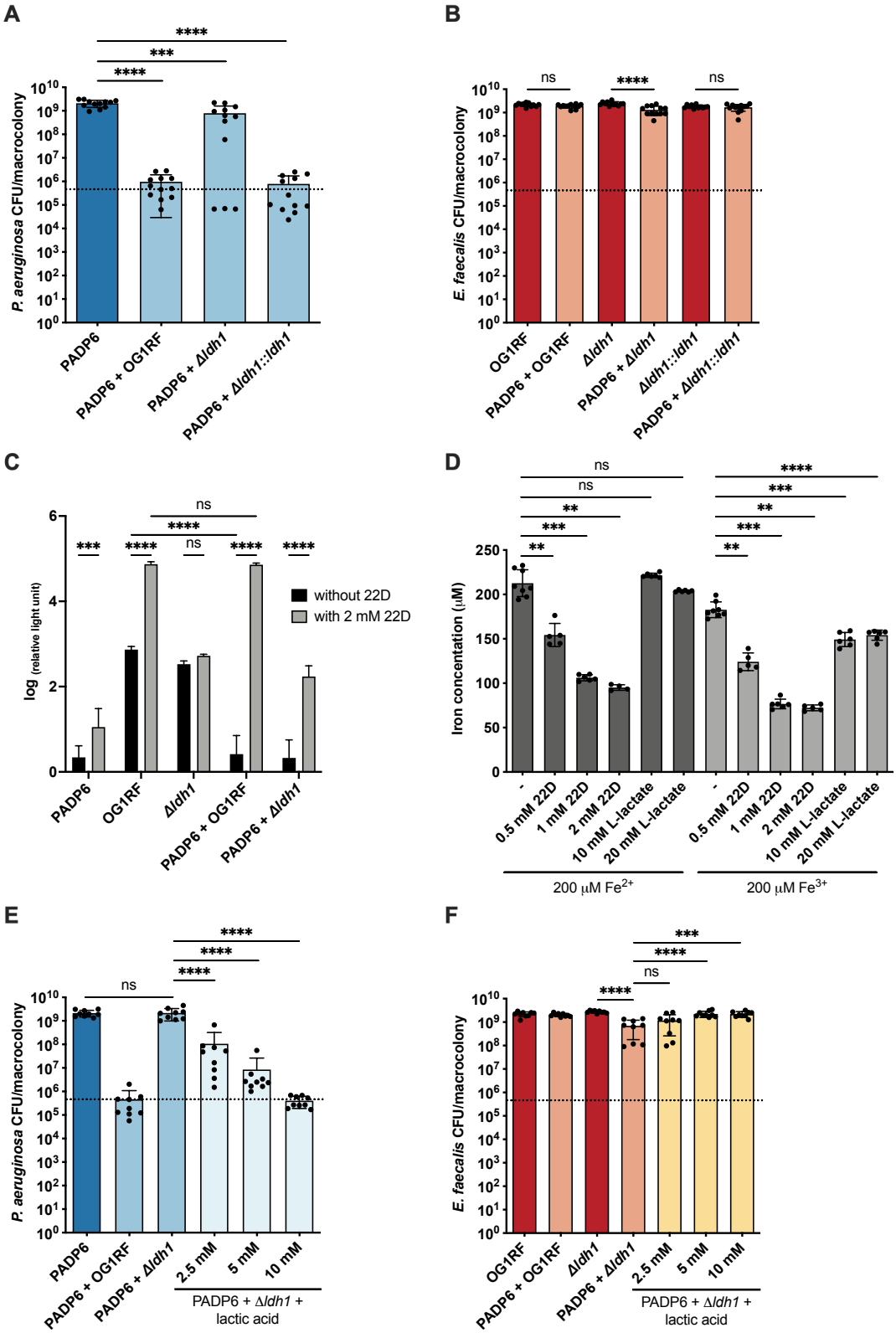

Figure 2.4 L-lactate produced by *E. faecalis* inhibits *P. aeruginosa* growth in iron-restricted media.
Enumeration of **(A)** PADP6 and **(B)** OG1RF, Δ*ldh1*, Δ*ldh1::ldh1* from 48 h macrocolonies with single or mixed inoculums grown in 2 mM 22D-chelated TSBG media. Bacterial species were mixed at a 1:1 ratio for mixed-species macrocolonies. Dotted lines represent inoculum of bacteria spotted. N = 4 with 3 technical replicates; error bars represent SD from the mean. Statistical analysis was performed using Mann-Whitney U test, *p < 0.05, **p < 0.01, ***p < 0.001, ****p < 0.0001. **(C)** Quantification of L-lactate exported from 48 h single- and mixed-species macrocolonies grown in TSBG media supplemented without and with 2 mM 22D. N = 3 with 2 technical replicates; error bars represent SD from the mean. Statistical analysis was performed using two-way ANOVA with Tukey's test for multiple comparisons, *p < 0.05, **p < 0.01, ***p < 0.001, ****p < 0.0001. **(D)** Quantification of iron when 200 μM of iron (II) sulfate heptahydrate (Fe^{2+}) and iron (III) chloride hexahydrate (Fe^{3+}) were supplemented without and with varying concentrations of 22D (0.5, 1 and 2 mM) or L-lactate (10 and 20 mM). N ≥ 3 with 2 technical replicates; error bars represent SD from the mean. Statistical analysis was performed using Mann-Whitney U test, *p < 0.05, **p < 0.01, ***p < 0.001, ****p < 0.0001. Enumeration of **(E)** PADP6 and **(F)** OG1RF, Δ*ldh1* from 48 h macrocolonies with single or mixed inoculums grown in 2 mM 22D-chelated TSBG media without and with increasing lactic acid concentrations (2.5, 5, and 10 mM). Bacterial species were mixed at a 1:1 ratio for mixed-species macrocolonies. Dotted lines represent inoculum of bacteria spotted. N = 3 with 3 technical replicates; error bars represent SD from the mean. Statistical analysis was performed using Mann-Whitney U test, *p < 0.05, **p < 0.01, ***p < 0.001, ****p < 0.0001.

2.3.3 *E. faecalis*-derived L-lactate is responsible for *P. aeruginosa* growth inhibition in mixed-species macrocolonies when iron is restricted.

In a previous study, the amount of lactate exported in the supernatant of *E. faecalis* V583 Δ*ldh1* was lower than *E. faecalis* V583 (Jönsson et al., 2009). Thus, to investigate the possible role of L-lactate in inhibiting PADP6 growth in mixed-species macrocolonies grown under iron-restriction conditions, we quantified the extracellular L-lactate. We detected significantly more L-lactate from OG1RF single-species macrocolonies grown under iron-restricted compared to unchelated conditions **(Figure 2.4C)**, indicating that OG1RF

increased L-lactate production in iron-restricted media is independent of PADP6 presence. Increased L-lactate production was further supported by transcriptomic data, in which we observed upregulation of *ldh1* (log2FC = 0.57) in OG1RF single-species macrocolonies grown in iron-restricted media compared to those grown in unchelated media **(Table 2.3)**. Next, we detected a significant reduction of L-lactate in mixed PADP6 and OG1RF macrocolonies compared to OG1RF single-species macrocolonies in unchelated media, whereas L-lactate levels were comparable between single- and mixed-species macrocolonies under iron-restricted conditions **(Figure 2.4C)**. Based on transcriptomic data, we observed an upregulation of *ldh1* (log2FC = 3.27) in mixed PADP6 and OG1RF macrocolonies grown in iron-restricted media compared to those grown in unchelated media **(Table 2.3)**. Together, these data indicate that *ldh1* is upregulated when iron is restricted, leading to increase production and export of L-lactate. In previous studies, lactate was found to chelate iron (Bergqvist et al., 2005; Ghio et al., 2021; Gorman & Clydesdale, 1984), which we confirmed in our assay conditions for ferric iron **(Figure 2.4D)**. Consequently, even mild iron chelating effects of *E. faecalis*-derived L-lactate could further restrict iron availability in the environment.

To confirm this, we compared PADP6 and OG1RF transcriptomes of mixed PADP6 and OG1RF macrocolonies to mixed PADP6 and OG1RF Δ*ldh1* macrocolonies grown in iron-restricted media. Unfortunately, due to the low PADP6 cell numbers in the mixed PADP6 and OG1RF macrocolonies and therefore, lesser number of PADP6 raw counts, we were unable to draw conclusions regarding iron availability based on the gene expression profile of

PADP6 **(Table 2.4)**. However, OG1RF iron acquisition genes, such as ABC transporters (Latorre et al., 2018), were upregulated in the mixed PADP6 and OG1RF macrocolonies, suggesting that iron availability was restricted when L-lactate levels was high **(Table 2.5)**. Consistent with this, increased L-lactate levels in the environment was inversely correlated with PADP6 growth in the mixed PADP6 and OG1RF macrocolonies under iron-restricted conditions **(Figure 2.4A and C)**.

Due to the anionic nature of L-lactate at all metabolic pH, it cannot pass through the *E. faecalis* cell membrane freely (Ramsey et al., 2014). As a result, L-lactate is exported out of *E. faecalis* as lactic acid (Harold & Levin, 1974) with a pKa of 3.86 (Eyal & Canari, 1995; Featherstone & Rodgers, 1981; Gonzalez et al., 2008), which is lower than the surrounding environmental pH. Therefore, upon export, lactic acid is deprotonated to L-lactate and releases H^+ into the environment resulting in a lowered environmental pH. To further investigate the role of L-lactate, we supplemented increasing amounts of lactic acid to mixed PADP6 and OG1RF Δ*ldh1* macrocolonies in 22D-chelated media. We observed a dose-dependent inhibition of PADP6 growth in the mixed-species macrocolonies with increasing lactic acid concentrations from 2.5 mM to 10 mM **(Figure 2.4E)**, while OG1RF Δ*ldh1* growth in the mixed-species macrocolonies remained relatively unchanged **(Figure 2.4F)**.

Table 2.3 *E. faecalis* L-lactate dehydrogenase differentially regulated under iron-restricted conditions.

Comparison conditions	Locus tag	Name	Description	log2FC	p-value	FDR
OG1RF single-species macrocolonies grown in iron restriction relative to OG1RF single-species macrocolonies grown under unchelated conditions	OG1RF_10199	*ldh1*	L-lactate dehydrogenase	0.57	8.75E-05	1.68E-03
Mixed OG1RF and PADP6 macrocolonies grown in iron restriction relative to mixed OG1RF and PADP6 macrocolonies grown under unchelated conditions	OG1RF_10199	*ldh1*	L-lactate dehydrogenase	3.27	9.02E-25	8.91E-24

*Complete table can be found in **Supplementary File 1** at https://bit.ly/3tOvqhy.*

Table 2.4 Selected *P. aeruginosa* raw counts of iron acquisition genes from mixed PADP6 + OG1RF macrocolonies and mixed PADP6 + OG1RF ∆*ldh1* macrcolonies under iron-restricted conditions.

Locus tag	Name	PADP6 + OG1RF			PADP6 + OG1RF ∆*ldh1*		
PA2386	*pvdA*	0	3	0	102	68	46
PA4228	*pchD*	0	2	0	79	42	33
PA2399	*pvdD*	0	2	0	146	95	54
PA2424	*pvdL*	0	1	0	56	68	64
PA4221	*fptA*	1	0	0	134	72	62
Total *P. aeruginosa* raw counts		1005	191602	1362	217172	192025	172212
Total *E. faecalis* raw counts		258404	243639	260881	881980	733793	764946
Percentage of *P. aeruginosa* raw counts (%)		0.39	44.02	0.52	19.76	20.74	18.38

Table 2.5 *E. faecalis* iron acquisition genes upregulated in PADP6 + OG1RF macrocolonies relative to PADP6 + OG1RF Δ*ldh1* macrocolonies grown under iron-restricted conditions.

Upregulated in PADP6 + OG1RF macrocolonies grown under iron-restricted conditions					
Locus tag	**Name**	**Description**	**log2FC**	**p-value**	**FDR**
OG1RF_11917	*metI*	ABC transporter permease	4.39	1.07E-06	7.70E-06
OG1RF_11762		ABC transporter permease	3.33	1.04E-10	1.55E-09
OG1RF_10136		Ferrichrome ABC transporter substrate-binding protein	2.03	1.74E-05	9.86E-05
OG1RF_12352		Iron ABC transporter ATP-binding protein	1.86	9.35E-05	4.60E-04
OG1RF_12351		Iron ABC transporter substrate-binding protein	1.75	2.11E-04	9.47E-04
OG1RF_12353		Iron ABC transporter permease	1.73	3.16E-04	1.37E-03
OG1RF_10360	*feoB*	Ferrous iron transport protein B	1.64	1.47E-04	6.97E-04
OG1RF_10128		ABC transporter permease	1.51	1.77E-03	5.99E-03
OG1RF_12354		Iron ABC transporter permease	1.50	9.31E-04	3.48E-03

*Complete table can be found in **Supplementary File 1** at https://bit.ly/3tOvqhy.*

2.3.4 L-lactate is necessary, but not sufficient, for inhibiting *P. aeruginosa* growth under iron-restricted conditions.

To investigate whether L-lactate alone was sufficient for inhibiting PADP6 growth in iron-restricted media, we grew PADP6 single-species macrocolonies supplemented with increasing 22D and lactic acid concentrations. When supplemented with 10 mM or 20 mM lactic acid in unchelated media, PADP6 growth remained relatively unchanged compared to unchelated media without lactic acid supplementation **(Figure 2.5A)**. Based on the lactic acid supplementation results obtained in **Figure 2.4E and F**, we expected that PADP6 growth would be inhibited when supplemented with 10 mM lactic acid under iron-restricted conditions. However, upon supplementation of 10 mM lactic acid, we only observed a significant inhibition of PADP6 growth when it was grown in 4 mM 22D-chelated media, but not in 2 mM and 3 mM 22D-chelated media compared to unchelated media **(Figure 2.5A)**. Whereas, when supplemented with 20 mM lactic acid, we observed significant PADP6 growth inhibition at all tested 22D concentrations, compared to unchelated media **(Figure 2.5A)**. A possible explanation for why more lactic acid was needed to inhibit single-species PADP6 growth in 2 mM 22D could be that *E. faecalis ldh2* is also contributing to L-lactate production in OG1RF Δ*ldh1*, hence a lower amount of lactic acid was sufficient to inhibit PADP6 growth in the mixed-species macrocolonies. Taken together, these data demonstrate that L-lactate is necessary, but not sufficient, for PADP6 growth inhibition in iron-restricted media.

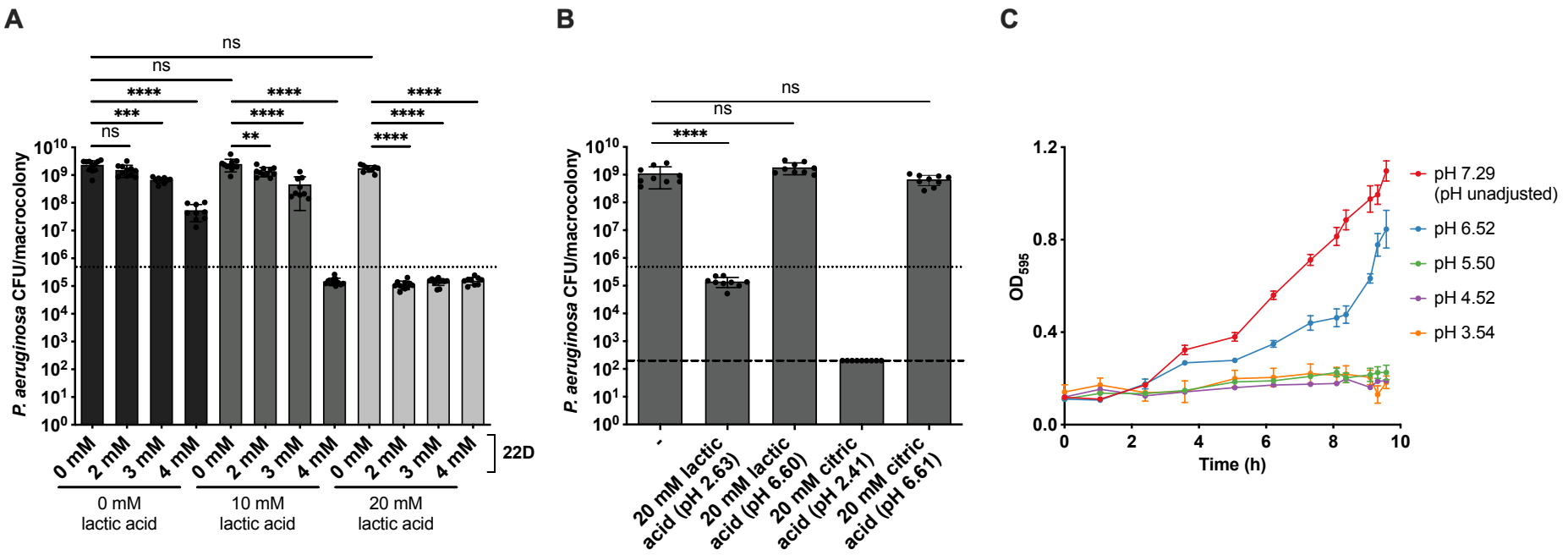

Figure 2.5 *P. aeruginosa* growth inhibition is due to lowered environmental pH under iron-restricted conditions.
(A) Enumeration of PADP6 from 48 h single-species macrocolonies grown in TSBG media supplemented without and with increasing 22D concentrations (2, 3 and 4 mM), which is then further supplemented without and with lactic acid (10 and 20 mM). Dotted lines represent inoculum of bacteria spotted. N ≥ 3 with 3 technical replicates; error bars represent SD from the mean. Statistical analysis was performed using Mann-Whitney U test, *p < 0.05, **p < 0.01, ***p < 0.001, ****p < 0.0001. **(B)** Enumeration of PADP6 from 48 h single-species macrocolonies grown in 2 mM 22D-chelated TSBG media supplemented without and with 20 mM lactic acid (pH unadjusted and pH adjusted to pH 6.6) or 20 mM citric acid (pH unadjusted and pH adjusted to pH 6.61). Dotted lines represent inoculum of bacteria spotted and dashed lines represent limit of detection. N = 3 with 3 technical replicates; error bars represent SD from the mean. Statistical analysis was performed using Mann-Whitney U test, *p < 0.05, **p < 0.01, ***p < 0.001, ****p < 0.0001. **(C)**

Planktonic growth of PADP6 in pH unadjusted (pH 7.29) and pH adjusted (pH 6.52, 5.50, 4.52 and 3.54) TSBG media supplemented with 2 mM 22D. N = 3 with 3 technical replicates; error bars represent SD from the mean.

2.3.5 Decreased environmental pH under iron restriction inhibits *P. aeruginosa* growth.

Next, we investigated why PADP6 viability was lost in the presence of L-lactate under iron-restricted conditions. Upon export of lactic acid by *E. faecalis*, it is deprotonated into L-lactate and H^+. We therefore examined whether a lowered environmental pH contributes to PADP6 growth inhibition when iron was restricted. Supplementation of iron-restricted media with 20 mM pH unadjusted lactic acid (pH 2.69) resulted in significant PADP6 growth inhibition compared to the absence of lactic acid supplementation **(Figure 2.5B)**. In contrast, PADP6 growth was unaffected when we supplemented the media with 20 mM pH adjusted lactic acid (pH 6.60) using sodium hydroxide (NaOH) when iron was otherwise restricted **(Figure 2.5B)**. To examine if other organic acids had the ability to inhibit *P. aeruginosa* growth, we also supplemented the iron-restricted media with citric acid to lower the environmental pH. Supplementation with pH unadjusted citric acid (pH 2.41) significantly inhibited PADP6 growth to below the limit of detection, while no significant growth difference was observed upon supplementation with 20 mM pH adjusted citric acid using NaOH (pH 6.61) or in the absence of citric acid supplementation **(Figure 2.5B)**. Moreover, alleviation of the low pH in iron-restricted media with PIPES, MOPS or HEPES buffer partially rescued *P. aeruginosa* growth in the mixed-species macrocolonies **(Appendix Figure 2.5)**. To further assess the impact of low pH on *P. aeruginosa* growth, we grew PADP6 planktonically in pH unadjusted and pH adjusted 22D-chelated media. When grown in 22D-chelated media at pH 5.50 and lower, we observed minimal to no PADP6 growth **(Figure 2.5C)**, suggesting that *P. aeruginosa* growth is generally inhibited when grown in low

pH environments as previously shown (Bushell et al., 2019; Tanner & James, 1992). These data also helps in explaining an interesting observation seen in **Figure 2.1F** and **Figure 2.4A**, whereby when PADP6 was grown in mixed-species macrocolonies with OG1RF, the CFU/macrocolony was ~2 × 10^7 for 24 h macrocolonies **(Figure 2.1F)** and ~9 × 10^5 for 48 h macrocolonies **(Figure 2.4A)**, suggesting that *P. aeruginosa* grows from its initial inoculum of ~5 × 10^5 CFU but eventually dies off likely due to the drop in pH and competitive depletion of iron. Altogether, these data show that the lowered environmental pH as a consequence of *E. faecalis* lactic acid export, coupled with L-lactate-mediated chelation of iron, plays a critical role in *P. aeruginosa* growth under iron-restricted conditions.

2.3.6 *P. aeruginosa* mixed-species infection augments *E. faecalis* growth in a mouse wound excisional model.

Since *E. faecalis* and *P. aeruginosa* are often co-isolated in wounds (Gjødsbøl et al., 2006) and to validate our *in vitro* findings in *in vivo* settings, we co-infected these two bacteria in a mouse wound excisional model. We first assessed the *in vivo* polymicrobial interactions using PAO1-WT, PADP6 and OG1RF to determine whether there were any differences between PAO1-WT and PADP6 in wound colonization. Based on a previous study profiling *P. aeruginosa* transcriptomes during wound infection, genes involved in siderophores biosynthesis were significantly upregulated, suggesting that iron availability was indeed restricted during wound infection (Turner et al., 2014). Therefore, it was not surprising that PADP6 single-species infection colonized the wound better than PAO1-WT, probably attributed by the higher tolerance to

iron starvation in PADP6 **(Figure 2.6A)**. However, contrary to our *in vitro* findings, both PAO1-WT and PADP6 growth were similar in the single- and mixed-species infected wounds at 24 h post-infection (hpi) **(Figure 2.6A)**. Additionally, we observed an augmentation of OG1RF growth in the mixed-species infection with PAO1-WT (1.43-log increase) and PADP6 (0.72-log increase) compared to OG1RF single-species infection **(Figure 2.6B)**. Nonetheless, we went on to examine whether *E. faecalis ldh1* would impact these *in vivo* polymicrobial interactions with PAO1-WT as PAO1-WT resulted in a larger OG1RF growth augmentation than PADP6 in mixed-species infection. Again, we observed that PAO1-WT growth remained relatively similar in the single- and mixed-species wound infection **(Figure 2.6C)**, while OG1RF growth was augmented in the mixed-species compared to OG1RF single-species infection (1.59-log increase) **(Figure 2.6D)**. Likewise, OG1RF Δ*ldh1* growth was augmented in the mixed-species compared to OG1RF Δ*ldh1* single-species infection (1.39-log increase) **(Figure 2.6D)**, suggesting that *ldh1* does not contribute to the *E. faecalis* augmentation when co-infected with *P. aeruginosa*. Collectively, rather than an antagonistic relationship observed in *in vitro*, our *in vivo* findings suggest that *E. faecalis* and *P. aeruginosa* exists in symbiosis.

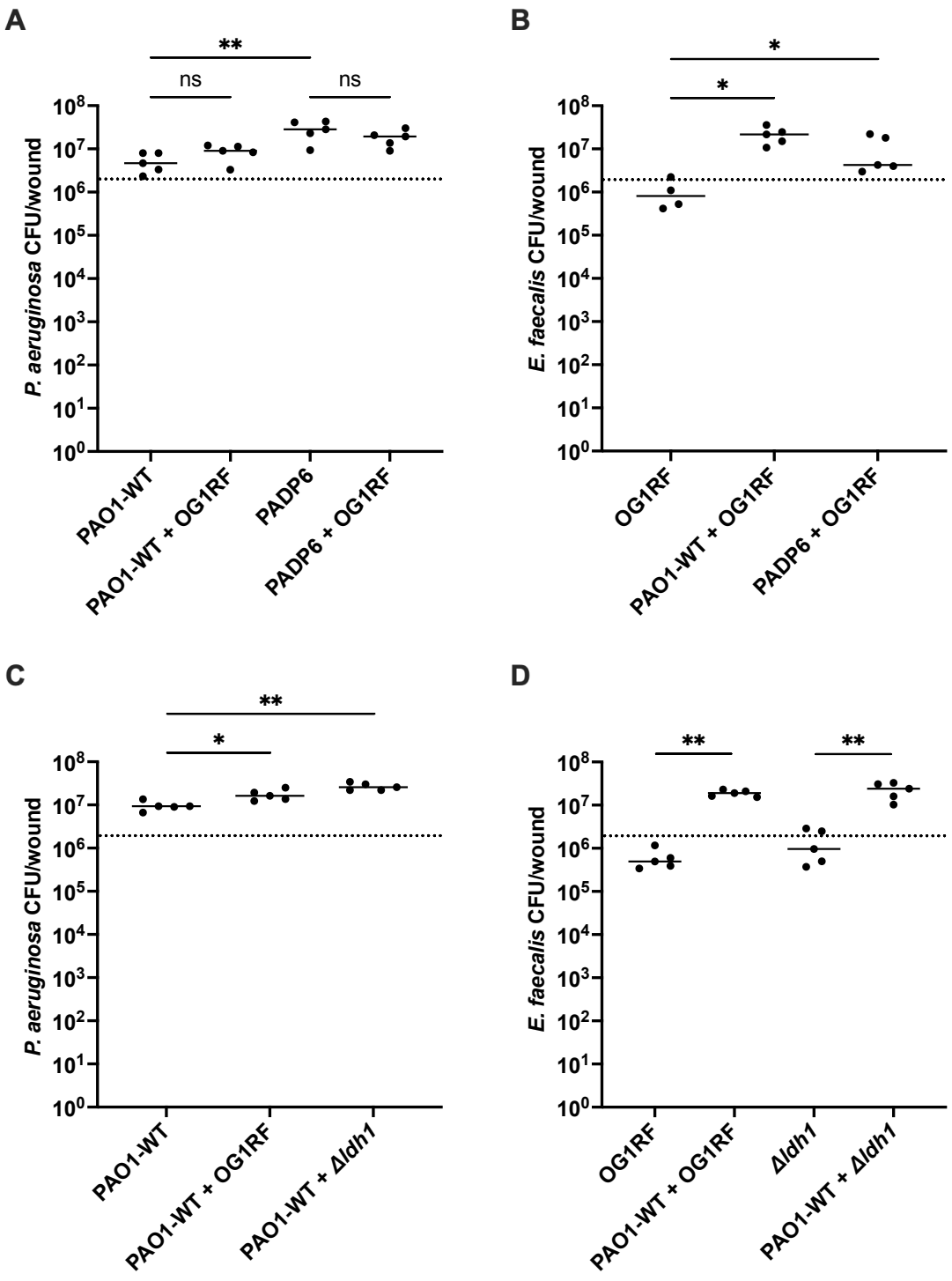

Figure 2.6 *P. aeruginosa* mixed-species infection augments the growth of *E. faecalis* in a mouse wound excisional model.

Male C57BL/6 mice were wounded and infected with single- and mixed-species (1:1 ratio) inoculums at 2 – 4 × 10^6 CFU/wound. Wounds were harvested at 24 hpi and the recovered bacteria were enumerated on selection agar plates. Enumeration of **(A)** PAO1-WT, PADP6 and **(B)** OG1RF from single- and mixed-species infected wounds with PAO1-WT, PADP6 and OG1RF. Enumeration of **(C)** PAO1-WT, **(D)** OG1RF and Δ*ldh1* from single- and mixed-species infected

wounds with PAO1-WT, OG1RF and Δ*ldh1*. Each data point represents one mouse and horizontal lines indicate the median, N = 1, n = 5 mice. Statistical analysis was performed using Mann-Whitney U test, *p < 0.05, **p < 0.01, ***p < 0.001, ****p < 0.0001.

2.4 Discussion

In this study, we sought to characterize the polymicrobial interactions between commonly co-isolated *E. faecalis* and *P. aeruginosa* in an iron-restricted condition. We show that *E. faecalis* inhibits *P. aeruginosa* growth in biofilms when iron availability is restricted in an LDH-dependent manner. Since *E. faecalis* Ldh1 catalyzes the reduction of pyruvate to L-lactate, the increased *ldh1* expression translates to an increased L-lactate production in *E. faecalis*. The L-lactate produced is then exported as lactic acid which then gets deprotonated into L-lactate releasing H^+ in the surrounding environment. Together, the chelation of iron by L-lactate and lowered pH environment contributes to *P. aeruginosa* growth inhibition under iron-restricted conditions.

An outstanding question from this work is how iron restriction leads to an upregulation of *E. faecalis ldh1*. *E. faecalis* possesses two copies of the *ldh* gene, *ldh1* and *ldh2*, both encoding for L-lactate dehydrogenase (Ramsey et al., 2014). Both isoenzymes contributes to L-lactate production through catalyzing the reduction of pyruvate to L-lactate (Ramsey et al., 2014). The activity of both isoenzymes is regulated by fructose 1,6-bisphosphate, intracellular phosphate and pH levels (Feldman-Salit et al., 2013). The principal L-lactate dehydrogenase, encoded by *ldh1*, was suggested to be post-transcriptionally regulated upon different growth rates (Mehmeti et al., 2012). The transcription of *ldh1* is also activated by CcpA, a global transcription regulator of carbon catabolite repression, by binding to a catabolite-responsive elements (*cre*) box identified upstream of *ldh1* gene (Leboeuf et al., 2000). However, little is known if iron levels play any role in regulating *ldh1* expression. We show that *E. faecalis*

ldh1 expression is increased in iron-restricted media and this is supported by an increased amount of L-lactate measured in the surrounding environment of macrocolonies grown. Ferric uptake regulator (Fur) is a transcription factor involved in regulating iron uptake and homeostasis (Hassan & Troxell, 2013). The DNA-binding sequence of Fur is well-studied (Latorre et al., 2018; Quatrini et al., 2007; Yu, C. & Genco, 2012) and we tried using different DNA Fur binding motifs to identify possible Fur binding sites upstream of *ldh1*, but we did not find any that resemble known binding motifs. Despite this, a previous study reported that *ldh1* is differentially expressed between *E. faecalis* OG1RF and OG1RF Δ*fur* mutant, suggesting that *ldh1* expression is directly or indirectly influenced by Fur (Latorre et al., 2018). An upregulation of *ldh1* and several genes involved in iron transport is also observed in another transcriptome study done when *E. faecalis* was exposed to urine (Vebø et al., 2010). It is therefore consistent that in iron-restricted environments, such as urine or *E. faecalis* macrocolonies growing in iron-restricted media, *ldh1* expression is induced. This observation is not limited to *E. faecalis* as *ldh1* expression is similarly induced under iron-restricted conditions for the anaerobe *Clostridium acetobutylicum* (Vasileva et al., 2012). Although it remains unclear how iron levels influence *ldh1* expression in *E. faecalis*, it is tempting to speculate that there is an interplay between iron levels and energy metabolism during growth under iron-restricted conditions.

Lactic acid exported by *E. faecalis* is deprotonated to L-lactate and H^+. We show that the consequential lowered environmental pH contributes to *P. aeruginosa* growth inhibition when iron is restricted. This is not surprising as *P. aeruginosa* growth is generally affected at low pH and prefers to grow in a more

neutral pH range (Bushell et al., 2019; Tanner & James, 1992). In fact, *E. faecalis* V583 adopts a similar strategy of lowering environmental pH as a result of lactic acid export to inhibit *Klebsiella pneumoniae* growth in polymicrobial biofilms (Ballén et al., 2020). *P. aeruginosa* siderophores pyoverdine and pyochelin have an iron formation stability constant of approximately 10^{24} and 10^{5} M^{-1}, respectively (Cox & Graham, 1979; Lamont et al., 2009), while L-lactate has a stability constant of approximately 10^{2} M^{-1} (Gorman & Clydesdale, 1984). The binding affinity for iron and zinc of *Escherichia coli* Nissle siderophore yersiniabactin changes accordingly to pH, in which yersiniabactin preferentially binds to zinc as pH increases (Behnsen et al., 2021). In addition, a high concentration of H^{+} is required for dechelation of iron-siderophore complexes (Boukhalfa & Crumbliss, 2002). As such, the low pH environment around *E. faecalis* likely affects the binding affinity of iron and promotes dissociation of iron from its siderophore complexes before it can be taken up by specific outer membrane receptors into *P. aeruginosa*. Moreover, varying pH of the medium alters the production of pyoverdine and pyochelin (Dumas et al., 2013). Even though a *P. aeruginosa* PADP6 strain that is able to grow under iron-restricted conditions is used to study the polymicrobial interactions with *E. faecalis*, the lowered iron availability resulted from 22D-mediated iron chelation and L-lactate-mediated iron chelation is likely an added stress apart from the lowered pH environment. Afterall, iron is an essential element for many cellular and metabolite processes (Andreini et al., 2008; Frawley & Fang, 2014). Together, the low pH environment created by *E. faecalis* might possibly affect *P. aeruginosa* siderophore-mediated iron uptake and consequently, negatively impacting its growth due to insufficient intracellular iron.

Interestingly, *P. aeruginosa* did not inhibit *E. faecalis* growth in the presence or absence of iron restriction. *P. aeruginosa* is known to produce antimicrobial metabolites that are toxic toward other Gram-positive bacteria such as *Staphylococcus aureus*. For example, the antimicrobial metabolite 2-heptyl-4-hydroxyquinoline N-oxide (HQNO) inhibits both the growth of *S. aureus* (Machan et al., 1992) and the activity of succinate:quinone oxidoreductase from *Bacillus subtilis* (Smirnova et al., 1995). Moreover, *P. aeruginosa* produces rhamnolipids which alter the cell surface of *S. aureus* resulting in increasing membrane permeability (Bharali et al., 2013). Despite these antimicrobial metabolites, *P. aeruginosa* and *S. aureus* are often co-isolated in infections (Gjødsbøl et al., 2006; Limoli & Hoffman, 2019) as *P. aeruginosa* attenuates its virulence when co-colonized with *S. aureus* and hence is more permissive to *S. aureus* growth (Baldan et al., 2014; Wakeman et al., 2016). We hypothesize the inability of *P. aeruginosa* to inhibit *E. faecalis* growth may also be due to a similar attenuation of *P. aeruginosa* virulence when grown with *E. faecalis*. In addition, rather than being in an antagonistic relationship, *P. aeruginosa* and *E. faecalis* could be symbiotic when iron is not restricted or in different environmental conditions. There is evidence between *E. faecalis* and *E. coli, P. aeruginosa* and *S. aureus* as well as *S. aureus* and *E. faecalis*, whereby interspecies metabolic feeding benefits one species and promotes polymicrobial biofilms and infections (Al Mahmud et al., 2021; Ch'ng et al., 2022; Keogh et al., 2016). Thus, although *P. aeruginosa* possesses the ability to produce antimicrobial metabolites, *E. faecalis* might be cross feeding metabolite(s) that are beneficial to *P. aeruginosa* and as a result, *P. aeruginosa* may tolerate *E. faecalis* in the right environment.

Even though we showed that *E. faecalis* antagonize *P. aeruginosa* under iron-restricted conditions *in vitro*, our *in vivo* findings suggest that these two bacteria exist in symbiosis. This is not surprising as *E. faecalis* and *P. aeruginosa* are often co-isolated *in vivo* (Citron et al., 2007; Giacometti et al., 2000; Gjødsbøl et al., 2006; Tsuchimori et al., 1994). The contrasting observation that we observed *in vitro* and *in vivo* could be due to in-host bacterial or host mechanism that negate or override the antagonism. Our findings show that, in addition to iron-restrictive effects, *P. aeruginosa* growth inhibition is largely dependent on the effects of pH arising from export of *E. faecalis* lactic acid into the environment. As such, co-existence of *E. faecalis* and *P. aeruginosa in vivo* may be due to host influence on *E. faecalis* L-lactate production, or that the host buffers the environmental pH, negating *E. faecalis* L-lactate effects (Schneider et al., 2007). Another possibility could be differences in *in vitro* and *in vivo* spatial organization of *E. faecalis* and *P. aeruginosa*. When *P. aeruginosa* and *E. faecalis* were grown *in vitro*, they exhibit distinct spatial separation in which *P. aeruginosa* forms a structured biofilm above the *E. faecalis* biofilm (Lee et al., 2017). Whereas during polymicrobial wound infection (*P. aeruginosa*, *E. faecalis*, *S. aureus*, and *Fineglodia magna*), *P. aeruginosa* is seen throughout the wound bed as well as at the leading edge of wound (Dalton et al., 2011). Host factors might also contribute and affect spatial organization as this is evident in gut microbiome spatial organization (Chang & Kao, 2019; Tropini et al., 2017). Spatial structuring that keeps the two bacteria physically separated could therefore blunt any local pH and iron-competition effects.

Based on the current findings, we propose a working model of *E. faecalis* and *P. aeruginosa* polymicrobial interactions *in vitro* **(Figure 2.7)**. During co-culture of *E. faecalis* and *P. aeruginosa* in unchelated media, L-lactate produced by *E. faecalis* is exported out via a symporter with H^+ as lactic acid. Since the pKa of lactic acid is lower than pH of the environment, lactic acid gets deprotonated into L-lactate and H^+, acidifying the environment. The L-lactate in the environment then chelates iron in the media **(Figure 2.7A)**. In contrast, during co-culture under iron-restricted conditions, there is an upregulation of *E. faecalis ldh1* expression which translates to an increased L-lactate production and lactic acid exported, further acidifying the environment. As *E. faecalis* continues to grow and lactic acid accumulates over time, the L-lactate in the environment further restricts iron availability in the iron-restricted media and the acidity of the environment subsequently exceeds a pH threshold at which *P. aeruginosa* can no longer grow **(Figure 2.7B)**.

Many infections are often polymicrobial and our work emphasizes the importance of how changes in the microenvironment such as iron or pH levels can significantly influence the interactions between two bacterial species. Despite the contrasting observation for *E. faecalis* and *P. aeruginosa* antagonism *in vitro* and *in vivo*, exploration of the mechanistic basis of antagonistic relationships between bacteria is informative because knowledge of such *in vitro* antagonism between bacteria has the potential to be used as a basis for additional control strategies against specific bacterial pathogens in the management of infections.

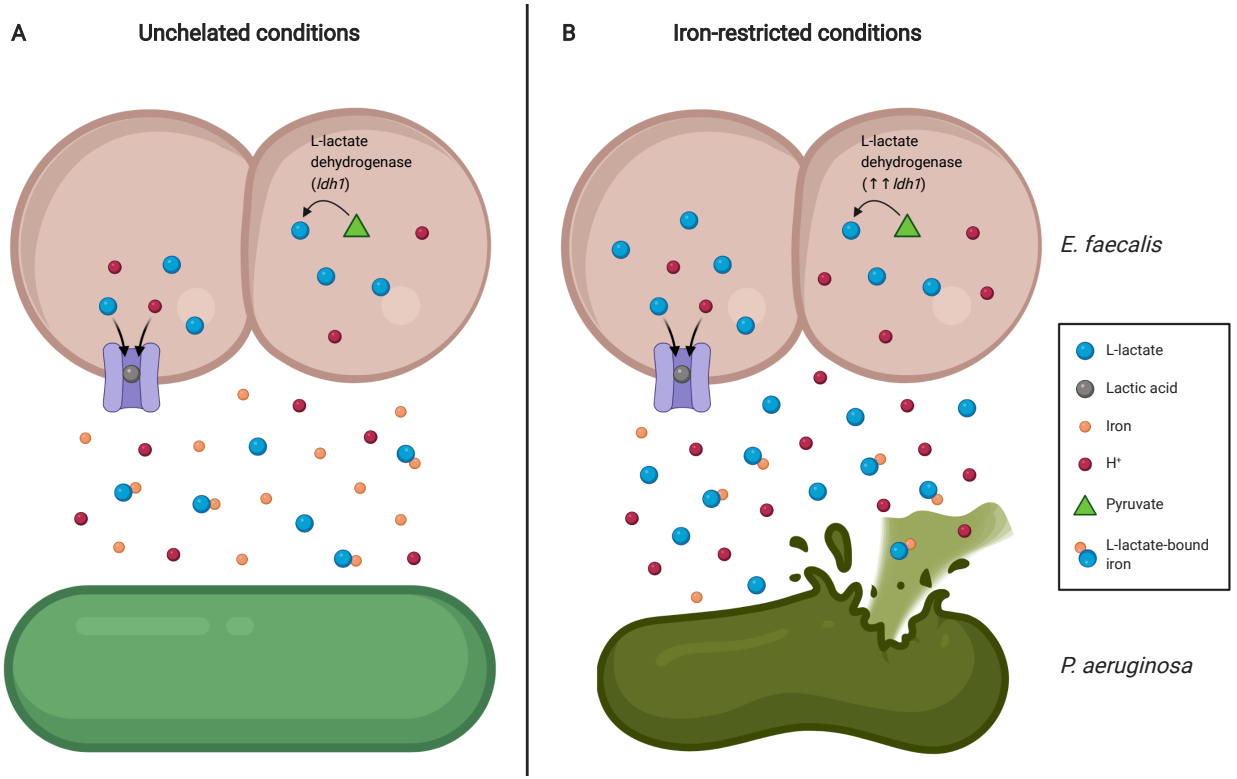

Figure 2.7 Proposed working model of *E. faecalis* and *P. aeruginosa in vitro* polymicrobial interactions.
Interactions between *E. faecalis* and *P. aeruginosa* under **(A)** unchelated and **(B)** iron-restricted conditions. **(A)** Under unchelated conditions, L-lactate produced in *E. faecalis* is exported with hydrogen ions via a symporter (purple) as lactic acid, which is then deprotonated in the environment into L-lactate and hydrogen ions (H^+). These L-lactate then chelates iron in the environment. **(B)** Under iron-restricted conditions, *E. faecalis ldh1* expression is upregulated. Consequently, as *E. faecalis* grows, L-lactate production and lactic acid secretion increase. This further chelates iron under iron-restricted conditions and lowers the environmental pH to a point at which *P. aeruginosa* cannot grow.

2.5 Author contributions

I designed the study of this project, performed, and analyzed all the *in vitro* experiments, occasionally assisted by my student Ms. Toh Xiao Wei from Temasek Polytechnic during her internship. All *in vitro* experiments involving PAO1 BAA-47 strain was designed, performed, and analyzed by Dr. Lam Ling Ning. Dr. Goran Biukovic constructed the PADP6 and PADP6-mCherry strains, designed and performed the *E. faecalis* transposon library screen. I designed, performed, and analyzed the *in vivo* experiments, assisted by Dr. Wong Jun Jie or Dr. Brenda Tien Yin Qi. I performed the transcriptomic analysis of the macrocolonies and constructed the OG1RF Δ*ldh1* and OG1RF Δ*ldh1::ldh1* strains. I wrote and edited the manuscript published for this study.

Chapter 3 – Purine and carbohydrate availability drive *Enterococcus faecalis* fitness during wound infection

3.1 Introduction

Globally, 7 – 15% of hospitalized patients are affected by wound infections (WHO, 2016). *Enterococcus faecalis* is an opportunistic pathogen and is suggested to colonize a range of host niches due to its ability to grow in high pH, temperatures, and salt concentrations (Sherman, 1937). *E. faecalis* is capable of infecting various wound types that can develop into chronic infections (Dowd et al., 2008; Dworniczek et al., 2012; Fisher & Phillips, 2009; Giacometti et al., 2000; Shettigar et al., 2018). Additionally, *E. faecalis* is among the top five most commonly isolated pathogens from surgical sites infections (Gjødsbøl et al., 2006) and diabetic wounds (Citron et al., 2007; Mottola et al., 2016). Worryingly, it has been increasingly challenging to treat *E. faecalis* infections because of their intrinsic and acquired antibiotic resistance (Hollenbeck & Rice, 2012).

A bacterial wound infection usually starts with pathogens colonizing the dermal layer of skin which can develop into an infection and become chronic if left untreated. Most infected wounds are a result of bacterial colonization from either the normal skin flora, outside environment, or pathogens from other parts of the body such as the oral cavity or gut (Bowler et al., 2001). *E. faecalis* wound infection involves a rapid replication of *E. faecalis* to establish an infection by 8 h post-infection (hpi), followed by a gradual decrease (but not clearance) of *E.*

faecalis burden by 3 days post-infection (dpi) (Chong et al., 2017). To successfully colonize different host niches, *E. faecalis* express microbial surface components recognizing adhesive matrix molecules (MSCRAMMs) such as the cell-wall anchored protein, Ebp pilus (Sillanpää et al., 2004). Flores-Mireles et al. (2014) demonstrated that *E. faecalis* EbpA mediates its attachment to host fibrinogen during catheter-associated urinary tract infections (CAUTI), which suggests the importance of Ebp in surface adhesion during infections. *E. faecalis* also encodes for collagen binding protein, Ace, to facilitate colonization of different niches. Ace can bind to host fibrinogen and collagen (Nallapareddy & Murray, 2008), and is important for *E. faecalis* colonization during urinary tract infections (UTI) (Lebreton et al., 2009) and infective endocarditis (Singh et al., 2010). Although *E. faecalis* possess numerous factors known to play a role during different infections **(Table 1.1)**, none of these factors has been implicated in wound infection and the pathogenic requirements of *E. faecalis* during wound infection remains poorly understood. Therefore, the goal of this chapter is to identify *E. faecalis* genetic determinant(s) that is/are crucial for *E. faecalis* acute replication at 8 hpi and persistence at 3 dpi.

To achieve this goal, an *in vivo* transposon (Tn-seq) and RNA sequencing (RNA-seq) approach was adopted to discover possible genetic determinant(s) that are important for the acute replication and persistence during *E. faecalis* wound infection. An *E. faecalis* transposon mutant library consisting of ~15,000 mutants were pooled together for the *in vivo* Tn-seq to uncover genetic determinants that contributes to wound infection (Kristich et al., 2008). Tn- and RNA-seq approaches have been used in combination to identify

genetic determinants that are important during infections such as genetic determinants of *Enterococcus faecium* during growth in human serum (Zhang et al., 2017) and *Pseudomonas aeruginosa* during wound infection (Turner et al., 2014), but this is the first study that adopts both approaches to identify *E. faecalis* genetic determinants contributing to wound infection.

In this study, *de novo* purine biosynthesis genes were found to be indispensable for *E. faecalis* acute replication during wound infection from the Tn- and RNA-seq analysis. Liquid chromatography-mass spectrometry (LC-MS) analysis of mouse wound samples showed that exogenous purine metabolites in the wound microenvironment are low, and thus likely insufficient to support *E. faecalis* rapid growth during wound infection. Through Tn-seq analysis, the *E. faecalis* MptABCD phosphotransferase system (PTS) was found to be crucial for persistence in wounds. Here, *E. faecalis* MptABCD PTS was characterized as a galactose and mannose transporter, and that carbohydrate availability such as glucose, galactose and mannose changes as the wound infection progresses. In addition to a role in wound infection pathogenesis, both *E. faecalis de novo* purine biosynthesis and the MptABCD PTS also contribute to *E. faecalis* fitness during catheter-associated urinary tract infections (CAUTI). Altogether, this study suggests that changes in the wound microenvironment affects *E. faecalis* pathogenesis and raises the possibility of purine biosynthesis and/or MptABCD PTS as future therapeutic targets to curb difficult-to-treat wound infections.

3.2 Materials and methods

3.2.1 Bacterial strains and growth conditions

Bacterial strains used in this study are listed in **Table 3.1**. Unless stated, all *E. faecalis* bacterial strains were grown in Brain Heart Infusion broth (BHI; Neogen, USA) at 37 °C in static conditions for 16 – 18 h. Cells were harvested by centrifugation at 5,000 rpm for 5 min and cell pellets were washed twice with 1 mL of 1X sterile phosphate buffered saline (PBS). The final pellet was resuspended in 5 mL of 1X sterile PBS prior to optical density (OD) measurement at 600 nm. Cell suspensions were then normalized to the required cell number for the various experimental assays. When applicable, BHI were supplemented with 25 µg/mL erythromycin (Sigma-Aldrich, USA) for maintenance of pTCV and pMSP3535 plasmids.

Table 3.1 Bacterial strains used in Chapter 3.

Strain	Description	Reference
OG1X	Wild-type, str^r	Ike et al. (1983)
OG1RF	Wild-type, rif^r	Dunny et al. (1978)
OG1RF pTCV::P_{tet}-Empty	OG1RF with pTCV empty vector, erm^r, kan^r	This study
OG1RF pMSP3535::P_{nisA}-Empty	OG1RF with pMSP3535 empty vector, erm^r	This study
OG1RF Δ*purEK*	OG1RF with *purE* and *purK* deletion	This study
OG1RF Δ*purEK* pTCV::P_{tet}-Empty	Δ*purEK* with pTCV empty vector, erm^r, kan^r	This study
OG1RF Δ*purEK* pTCV::P_{tet}-*purEK*	Δ*purEK* with *purEK* complemented on pTCV vector, erm^r, kan^r	This study
OG1RF Δ*mptD*	OG1RF with *mptD* deletion	This study
OG1RF Δ*mptD* pMSP3535::P_{nisA}-Empty	Δ*mptD* with pMSP3535 empty vector, erm^r	This study
OG1RF Δ*mptD* pMSP3535::P_{nisA}-*mptD*	Δ*mptD* with *mptD* complemented on pMSP3535 vector, erm^r	This study

Str^r, rif^r, erm^r and kan^r represents streptomycin, rifampicin, erythromycin, and kanamycin resistance, respectively.

3.2.2 Mouse wound excisional model

Bacterial cultures were normalized to 2 – 4 × 10^8 CFU/mL in 1X sterile PBS. Mouse wound infections were performed similarly to a previous study (Chong et al., 2017). Briefly, male C57BL/6 mice (7 – 8 weeks old, InVivos, Singapore) were anesthetized by inhalation of 3% isoflurane and the dorsal hair trimmed. A depilatory cream (Nair™ cream, Church and Dwight Co, USA) was then applied, and fine hair was removed through shaving with a scalpel. The skin was subsequently disinfected with 70% ethanol and a wound was created using a 6 mm biopsy punch (Integra Miltex, USA). This was followed by inoculation with 10 µL of respective bacterial cultures per wound before the wound site was sealed with a transparent dressing (Tegaderm™ 3M, USA). At indicated time points, mice were euthanized and a 1 × 1 cm piece of skin encompassing the wound site was excised into 1 mL of 1X sterile PBS. Excised wounds were homogenized, and viable bacteria were enumerated by spotting onto respective selection agars. For OG1X and OG1RF selection, bacteria were spotted onto BHI solidified with 1.5% agar (Oxoid Technical No. 3) supplemented with 500 µg/mL streptomycin (MP Biomedicals, USA) or 25 µg/mL rifampicin (Sigma-Aldrich, USA), respectively. Animals without the wound dressing at the time of sacrifice were excluded from data analysis. For competitive infection experiments, the competitive index (CI) was determined with the following formula:

$$\mathrm{CI} = \frac{\mathrm{OG1RF}_{\mathrm{output}}/\mathrm{OG1X}_{\mathrm{output}}}{\mathrm{OG1RF}_{\mathrm{input}}/\mathrm{OG1X}_{\mathrm{input}}}$$

3.2.3 Transposon sequencing

The *E. faecalis* transposon library containing ~15,000 mutants was constructed and kindly provided to us by Gary Dunny (Kristich et al., 2008). Transposon mutants were arrayed into 384 wells with the transposon sequence of each mutant being known. Initial pools consisting of 100 transposon mutants per pool were made and glycerol stocked. Fifty transposon pools of 100 were then combined to achieve a final pool size of 5,000 to be used for subsequent transposon sequencing, with a total of 3 pools of 5,000 covering the whole transposon library. Glycerol stocks of the 5,000 mutants were grown overnight in BHI medium (Neogen, Lansing, USA) for 15 - 18 h at 37 °C. Overnight cultures were washed twice with 1X sterile PBS after pelleting at 5,000 rpm for 4 min and normalized to OD_{600} of 0.35 corresponding to 2×10^8 CFU/mL. Wounds were made on the dorsal back of the mice as described above and 10 µL of the normalized inocula was inoculated into wounds to achieve an infection CFU of 2×10^6 CFU.

3.2.4 Genomic DNA extraction for transposon sequencing

Mice were euthanized and wounds were excised at the indicated time points. Excised wounds were subsequently homogenized in 1 mL of 1X sterile PBS. To reduce biological variance, 500 mL from two wound homogenates containing the same transposon mutants were pooled together into 4 mL of BHI to a final volume of 5 mL at 37 °C for 3 h. The remaining wound homogenates were subjected to CFU enumeration on BHI agar (Acumedia, USA) supplemented with rifampicin or BHI agar without any antibiotics to check for the presence of contamination. Homogenates containing contaminants were

excluded from subsequent library preparation. *In vitro* comparator pools were made by incubating 10 µL of normalized transposon overnight cultures into 4 mL of BHI broth at 37 °C for 3 h as well. To recover as much transposon mutants as possible, we adopted an enrichment step of transposon pools for all mice samples by incubating the mixture at 37 °C for 3 h, and DNA were extracted using the Qiagen DNeasy Blood and Tissue Kit (Qiagen, Germany). A total of 3 biological replicates of DNA samples were made from 6 wounds per transposon pool.

3.2.5 Transposon library construction and sequencing

DNA extracted was used for DNA library construction using NEBNext Ultra™ II DNA Library Prep Kit for Illumina (New England Biolabs, USA) according to the manufacturer's instructions. DNA was subjected to acoustic shearing to obtain fragment sizes of approximately 300 bp using g-Tube (Covaris, USA). We adopted and modified the TraDIS protocol published by Barquist et al. (2016) by using the proposed splinkerette design for adapter ligation and subsequent enrichment of transposon pools using an amplicon-based sequencing approach. TraDIS adapters were used for adapter ligation and PCR amplified for final library construction using the Nextera XT DNA kit (Illumina, USA) as per manufacturer's instructions. Constructs were normalized and sequenced as 150 bp single read using the MiSeqV3.

3.2.6 Analysis of transposon sequencing results

Reads obtained from sequencing were checked using FastQC (version 0.11.5) and adapter trimmed using bbduk from the BBMap tools (version 34.49)

(Bushnell, 2015). Trimmed reads containing the 15 bp transposon sequence at the 5' region was obtained using a customized python script and subsequently trimmed to obtain sequences for mapping. Reads were mapped onto the *E. faecalis* OG1RF (NCBI accession: GCF_000172575.2) reference genome using BWA (version 0.7.15-r1140) (Li, H. & Durbin, 2009). Reads mapping to predicted open reading frames of each genome were quantified using HTSeq (Anders et al., 2015) and differential gene expression analysis was performed under the R environment (version 3.4.4) using Bioconductor package, edgeR (Robinson et al., 2010). Reads were normalized based on sequencing depth, scaled for the respective library sizes using trimmed mean of M-values (TMM), with common and tagwise dispersions being estimated for downstream analysis. Genes were considered differentially expressed under false discovery rate (FDR) <0.05 under correction by the Benjamin-Hochberg procedure. Gene annotation was performed using the database from the Kyoto Encyclopedia of Genes and Genomes (KEGG).

3.2.7 RNA extraction from *in vivo* wound samples

A 1 × 1 cm of mouse skin encompassing the wound site was excised into 2 mL of RNA*later*™ stabilization solution (Invitrogen, USA) and incubated overnight at 4 °C. The mouse skin was then transferred into 1 mL of TRIzol (Life Technologies, USA) and cut into smaller pieces. The entire suspension was transferred into Lysing Matrix B 2-mL tubes (MP Biomedicals, USA) and homogenized using a FastPrep-24 tissue grinder (MP Biomedicals, USA) for 2 rounds of 40 s at 6.0 m/s with 2 min rest on ice in between. To each sample, 200 µL of chloroform (Sigma-Aldrich, USA) was added, vortexed vigorously for

30 s and centrifuged at 12,000 x g for 10 min at 4 °C. The top layer (aqueous phase) containing RNA was transferred to 1.5 mL tubes containing 500 µL of ice-cold ethanol and shaken vigorously before loading into the RNeasy Mini spin columns (Qiagen, Germany). Subsequent RNA extraction steps were performed according to manufacturer's protocol of the RNeasy® Mini Kit (Qiagen, Germany). Briefly, samples were washed once with Buffer RW1, followed by 2 washes with Buffer RPE and elution of RNA with RNase-free water. The RNA and potential DNA contamination concentrations were quantified using Qubit™ RNA BR and Qubit™ dsDNA HS assay kits, respectively. The extracted RNA was quality checked using the RNA ScreenTape on a TapeStation instrument (Agilent Technologies, USA). Every sample had a minimum RNA concentration of 100 ng/µL, a maximum of 10% DNA contamination and a RINe value ≥ 8.0 before it was used for library preparation. Library preparation was done using the Ribo-Zero Plus rRNA depletion kit (Illumina, USA) to remove mouse and bacterial rRNA from the extracted total RNA samples. The RNA samples were sequenced as 75 bp paired-end reads on an Illumina HiSeq2500. Library preparation and sequencing was done by the sequencing facility at Singapore Centre for Environmental Life Sciences Engineering (SCELSE).

3.2.8 RNA extraction from *in vitro* bacterial cultures

Overnight cultures of wild-type OG1RF and OG1RF Δ*mptD* were sub-cultured to OD_{600} of 0.01 in a 24-well microtiter plate containing 1 mL of Tryptone Soya Broth without dextrose (TSBd, Sigma-Aldrich, USA) supplemented with or without mannose (Sigma-Aldrich, USA) in biological triplicates. Bacteria were harvested at late log/early stationary phase in RNAprotect™ Bacteria Reagent

(Qiagen, Germany) and incubated at room temperature for 5 min before centrifuging at 10,000 *g* for 10 min. The supernatant was decanted, and bacteria pellets collected were subjected to total RNA extraction using the Qiagen RNeasy® Mini Kit (Qiagen, Germany) with slight modifications. Briefly, cell pellets were resuspended in TE buffer containing 20 mg/mL lysozyme (Sigma-Aldrich, USA), further supplemented with 20 µL proteinase K (Qiagen, Germany), and incubated at 37 °C for 1 h. Subsequent RNA extraction steps were performed according to manufacturer's protocol. The extracted RNA samples were treated with DNase (TURBO DNA-*free*™ kit, Invitrogen, USA) for removal of genomic DNA before it was purified using the Monarch® RNA cleanup kit (New England Biolabs, USA). The RNA and potential DNA contamination concentrations were quantified using Qubit™ RNA BR and Qubit™ dsDNA HS assay kits, respectively. The extracted RNA was quality checked using the RNA ScreenTape on a TapeStation instrument (Agilent Technologies, USA) before it was sent for sequencing. Every sample had a minimum RNA concentration of 40 ng/µL, a maximum of 10% DNA contamination and a RIN value ≥ 8.0 before being used for library preparation and subsequent sequencing as 75 bp paired-end reads on an Illumina HiSeq2500. Similarly, library preparation and sequencing were done by SCELSE sequencing facility.

3.2.9 *In vivo* and *in vitro* transcriptomic analysis

All raw reads obtained were checked using FastQC (Version 0.11.9) and adaptor trimmed using bbduk from BBMap tools (Version 39.79) (Bushnell, 2015). The trimmed reads were then mapped against *E. faecalis* OG1RF (NCBI

accession: CP002621) reference genome using bwa-mem of BWA (Version 0.7.17-r1188) with default options. Reads mapped to open reading frames were quantified using htseq-count of HTSeq (Version 0.12.4) with option "-m intersection-strict" (Anders et al., 2015). All rRNA counts were manually removed from all data sets. Differential gene expression analysis was performed in R using *edgeR* (Version 3.28.1) (Robinson et al., 2010). The log2 fold change values extracted were based on the false discovery rate (FDR) ≤ 0.05. A gene set enrichment analysis (GSEA) was also done in R using the clusterProfiler package (Version 3.16.1) (Wu et al., 2021; Yu, G. et al., 2012).

For *in vitro* transcriptome analysis, common differentially expressed genes (DEGs) identified between without and with carbohydrate supplementation in TSBd media were removed, and only unique DEGs were used for downstream GSEA.

3.2.10 Molecular cloning

The primers used in this study are listed in **Table 3.2**. Transformants were screened using respective selection agar as follows: (1) *Escherichia coli* strains, LB with 500 µg/mL erythromycin (pGCP213 and pMSP3535) or 50 µg/mL kanamycin (pTCV); and (2) *E. faecalis* strains, BHI with 25 µg/mL erythromycin (pGCP213, pMSP3535 and pTCV). The generation of *E. faecalis* deletion mutants were done by allelic replacement using pGCP213 temperature-sensitive shuttle vector described previously (Nielsen et al., 2012). For the construction of OG1RF Δ*purEK* and OG1RF Δ*mptD*, vector pGCP213 was linearized using *Bam*HI and *Not*I (New England Biolabs, USA). Linearized

pGCP213 and inserts were ligated using In-Fusion® HD Cloning Kit (Clontech, Takara, Japan) and transformed into Stellar™ competent cells. Successful plasmid constructs were verified by Sanger sequencing and transformed into wild-type OG1RF. Transformants were selected with erythromycin at 30 °C, then passaged at non-permissive temperature at 42 °C with erythromycin to select for bacteria with successful plasmid integration into the chromosome. For plasmid excision, bacteria were serially passaged at 37 °C without erythromycin for erythromycin-sensitive colonies. These colonies were then subjected to PCR screening for detection of deletion mutants.

For the complementation of *purEK*, vector pTCV was linearized using *Bam*HI and *Sph*I (New England Biolabs, USA). Whereas, for the complementation of *mptD*, vector pMSP3535 was linearized using inverse PCR with iPCR_pMSP3535_F and iPCR_pMSP3535_R primers. Similarly, linearized pTCV and pMSP3535 as well as the respective inserts were ligated using In-Fusion® HD Cloning Kit and transformed into Stellar™ competent cells. Successful plasmid constructs were verified by Sanger sequencing and transformed into OG1RF Δ*purEK* or OG1RF Δ*mptD*.

Table 3.2 Primers used in Chapter 3.

Purpose	Primer name	Sequence (5' to 3')	Reference
Construction of OG1RF Δ*purEK*	1-Δ*purEK*_UpF	CATGCTCGAGCGGCCGTGTAGAGGTTATCGAAACACGG	This study
	2-Δ*purEK*_UpR	GTTGCTCCGACTTTTAAAGGTTTACATGAATGTAATAACTCCTTCCG	This study
	3-Δ*purEK*_DownF	CGGAAGGAGTTATTACATTCATGTAAACCTTTAAAAGTCGGAGCAAC	This study
	4-Δ*purEK*_DownR	TACCGAGCTCGGATCTGTCCTTTTCCATCGTATCCACC	This study
	screen-Δ*purEK*_F	GAACAGATCGAAGAAGGGCA	This study
	screen-Δ*purEK_R*	AGGGGCAATCTTACAGCCAA	This study
Construction of OG1RF Δ*mptD*	1-Δ*mptD*_UpF	CATGCTCGAGCGGCC GTGTTAAAGGTGTTCCTTCAGCGA	This study
	2-Δ*mptD*_UpR	AAGCCGATTAAGTGGCCGACTGCCATTTTCTTTGCTCCTCC	This study
	3-Δ*mptD*_DownF	GGAGGAGCAAAGAAAATGGCAGTCGGCCACTTAATCGGCTT	This study
	4-Δ*mptD*_DownR	TACCGAGCTCGGATC CCCAATCGAGAGAATCCCTCT	This study
	screen-Δ*mptD*_F	GTATGGTCGTTGCCGTAGGT	This study
	screen-Δ*mptD_R*	TCCTGTAAATGCCGTCGCA	This study
Construction of OG1RF Δ*purEK* pTCV::P_{tet}-*purEK*	*purEK*compl_F	CTGAGGATCCCAGTGAAAAAAGGCGGAAGGAGT	This study
	*purEK*compl_R	ACTGGCATGCCTTGCTTGGAGCAAGCATTTATTAAG	This study
	screen-*purEK*compl_F	GTAAAACGACGGCCAGT	This study
	screen-*purEK*compl_R	CAGGAAACAGCTATGAC	This study
Linearizing pMSP3535	iPCR_pMSP3535_F	GATCCGGTACCACTAGTCCCG	This study
	iPCR_pMSP3535_R	CATGCAGAGTCTCCTGTTTTACAAC	This study
Construction of OG1RF Δ*mptD* pMSP3535::P_{nisA}-*mptD*	*mptD*compl_F	AGGAGACTCTGCATGCTAATTCTGAAGGAGGAGCAAA	This study
	*mptD*compl_R	TAGTGGTACCGGATCGACTAGTTTATAATAAGCCGATT	This study
	screen-*mptD*compl_F	GGTTGCAAATTTTGAAAACCGC	This study
	screen-*mptD*compl_R	TAATACGACTCACTATAGGG	This study

3.2.11 Growth kinetic assay

Overnight cultures of the respective bacteria strains were diluted to OD_{600} of 0.01 in: (1) RPMI 1640 medium, no phenol red (Gibco, USA) supplemented with 1% (w/v) casamino acids (RPMI-CA; BD Biosciences, USA) with or without IMP; or (2) TSBd supplemented with 40 ng/mL nisin with or without 1% (w/v) galactose, mannose, or glucose (all purchased from Sigma-Aldrich, USA). A total of 200 µL of the diluted cell suspensions were inoculated per well in a 96-well polystyrene microtiter plate (Thermo Fisher Scientific, USA). Bacterial growth was measured at OD_{600} using a Tecan Infinite© M200 Pro spectrophotometer (Tecan Group Ltd, Switzerland) every 15 min for 16 h at 37 °C under static conditions.

3.2.12 Purine metabolites quantification

Purine metabolites in mouse wounds were quantified using LC-MS performed by Singapore Phenome Centre (SPC). A 1 × 1 cm of mouse skin encompassing the wound site was excised into 1.5 mL tubes, snap frozen in liquid nitrogen and submitted to SPC for sample preparation, LC-MS profiling and data processing. Briefly, tissue samples were weighed into tubes containing zirconium beads, 200 µL of 0.1M NaOH and 600 µL of methanol. The tubes were vortexed, homogenized and centrifuged at 10,000 rpm for 10 min at 4 °C. Two aliquots of 300 µL supernatant were taken, dried down and reconstituted as follows: (1) for purine quantification, 100 µL of 80:20 acetonitrile:water, 15 mM of ammonium acetate, pH 9.2; and (2) for phosphate quantification, 100 µL of water, 20 mM of ammonium acetate, 0.1% of formic acid.

Purine and phosphate quantification was performed on a Xevo TQ-S (Waters, UK). The source temperature was set at 150 °C with a cone gas flow of 150 L/h and a desolvation gas temperature of 450 °C with a desolvation gas flow of 900 L/h. The capillary voltage was set to 2.5 kV in the ESI positive or negative ionization mode for purine and phosphate quantification, respectively. For purine quantification (adenine, guanine, xanthine, adenosine, guanosine and inosine), samples were injected into 2.1 mm × 100 mm, 1.7 µm UPLC BEH C18 column (Waters, UK) held at 45 °C. Mobile phase A is water with 15 mM of ammonium acetate (pH 9.2) and mobile phase B is 90:10 acetonitrile:water with 15 mM of ammonium acetate (pH 9.2). The column flow rate was 0.4 to 0.5 mL/min. For phosphate quantification (AMP), samples were injected into 2.1 mm × 150 mm, 1.7 µm UPLC HSS T3 column (Waters, UK) held at 45 °C. Mobile phase A is water with 20 mM of ammonium acetate and 0.1% of formic acid. The column flow rate was 0.4 mL/min.

The weight of all tissue samples were measured prior to purine metabolites quantification, and the concentration of purine metabolites were normalized accordingly to the weight of the respective samples.

3.2.13 Carbohydrate metabolism assay

Carbohydrate metabolism of *E. faecalis* strains were tested using API® 50 CH (bioMérieux, France). Briefly, bacterial cultures were prepared to a turbidity equivalent of 2 McFarland standard and added to API 50 CHL Medium supplemented with 40 ng/mL nisin for induction of plasmid expression. The bacterial suspension was then distributed into all 50 microtubes and sealed with

mineral oil. The tray was then incubated at 37 °C under static condition for 48 h to 72 h. The results for each microtube, positive (+), negative (-) and doubtful (?), were recorded on the result sheet provided.

3.2.14 Enzyme-linked immunosorbent assay

A 1 × 1 cm of mouse skin encompassing the wound site was first rinsed in ice-cold 1X sterile PBS and homogenized in 1 mL ice-cold 1X sterile PBS. The homogenates then undergo two freeze-thaw cycles to break the cell membranes and centrifuged at 5,000 x g for 5 min at 4 °C. The supernatants were collected and stored at -80 °C until assessment by Mouse Glucose ELISA, Mouse Galactose ELISA and Mannose ELISA kits (MyBioSource, USA) as per manufacturer's protocol. Optical density of each well was determined at OD_{450} using a Tecan Infinite© M200 Pro spectrophotometer (Tecan Group Ltd, Switzerland).

3.2.15 Catheterization and bacterial infection

Bacterial cultures were normalized to 2 – 4 × 10^8 CFU/mL in 1X sterile PBS. Implantation of catheters into mouse was performed as previously described (Hung et al., 2009). Briefly, female C57BL/6 mice (8 – 9 weeks old, InVivos, Singapore) were anesthetized by inhalation of 3% isoflurane. Mice were inoculated with 50 µL of bacteria suspension (~10^7 CFU) into the urethra after catheterization. At 24 hpi, mice were euthanized. The bladders and kidneys were aseptically removed and homogenized in 1 mL and 800 µL of 1X sterile PBS, respectively. Catheters removed from the bladders were sonicated at 37 kHz and 30% power for 15 mins in 1 mL 1X sterile PBS (Elma Ultrasonic,

Germany), followed by vortexing at maximum speed for another 15 mins. All the samples were then serially diluted and viable bacteria were enumerated by spotting onto the respective selection agars. For OG1X and OG1RF selection, bacteria were spotted onto BHI agar supplemented with 500 μg/mL streptomycin (MP Biomedicals, USA) or 25 μg/mL rifampicin (Sigma-Aldrich, USA), respectively for competitive infection enumeration. Animals without catheters at the time of sacrifice were excluded from data analysis.

3.2.16 Statistical analysis

Statistical analyses were performed with GraphPad Prism software (Version 9.0.0, California, USA) and are described in the respective figure legends.

3.2.17 Ethics statement

All procedures were approved and performed in accordance with the Institutional Animal Care and Use Committee in Nanyang Technological University (ARF SBS/NIE-A19061 and ARF SBS/NIE-A18063).

3.2.18 Data availability

All the sequences have been deposited in the National Center for Biotechnology Information (NCBI) Gene Expression Omnibus (GEO) database under accession number GSE206751 (https://www.ncbi.nlm.nih.gov/geo/query/acc.cgi?acc=GSE206751).

3.3 Results

3.3.1 *E. faecalis de novo* purine biosynthesis genes contribute to *E. faecalis* acute replication during wound infection.

Although *E. faecalis* is a common wound pathogen, little is known about the genetic determinants that contribute to wound infection. To identify these genetic determinants, using a mouse wound infection model that was previously characterized for *E. faecalis* (Chong et al., 2017) and an *E. faecalis* OG1RF transposon mutant library consisting of ~15,000 mutants (Kristich et al., 2008), a Tn-seq at 8 h post-infection (hpi) and 3 days post-infection (dpi) following infection was performed. Mutants disrupted in the *pur* operon (9 out of 11 genes) were found to be significantly less abundant at 8 hpi compared to the pre-inoculation pool **(Table 3.3 and Appendix Figure 3.1)**, indicating the importance of purine biosynthesis genes for *E. faecalis* during acute wound replication. The *E. faecalis pur* operon consists of 11 genes **(Figure 1.2A)** and *de novo* purine biosynthesis undergoes 11 reactions from L-glutamine and 5-phosphoribosyl diphosphate (PRPP) to inosine monophosphate (IMP) before branching into specific pathways that produces guanosine and adenosine monophosphate (GMP and AMP) (Ramsey et al., 2014) **(Figure 1.2B)**. At the same time, an *in vivo* RNA-seq on *E. faecalis* wild-type OG1RF from infected wounds was also performed to provide a genome-wide analysis of differentially expressed genes during wound infection. Genes identified as important for wound fitness using Tn-seq was predicted to display an increased expression in the RNA-seq analysis (correlation coefficient of Tn-seq and RNA-seq should be close to -1). However, the calculated Spearman rank correlation coefficient between fold change of mutant abundance and fold change of differential

expression among statistically significant genes was only -0.0311 **(Appendix Figure 3.2A)**, which was similar to a previous study looking at genetic determinants and gene expression during *P. aeruginosa* wound infection (Turner et al., 2014). Despite the poor correlation between mutant fitness and differential expression, all 11 genes in the *pur* operon were significantly upregulated at 8 hpi compared to inoculum **(Table 3.4 and Appendix Figure 3.2B)**.

Table 3.3 *E. faecalis* transposon mutant abundance profiled by Tn-seq from 8 hpi wounds.

Locus tag	Name	Description	log2FC	p-value	FDR
OG1RF_10019	*mptAB*	PTS mannose transporter subunit EIIAB	-1.15	5.75E-06	2.11E-05
OG1RF_10020	*mptC*	PTS mannose/fructose/sorbose transporter subunit IIC	-0.92	3.54E-10	1.58E-09
OG1RF_10021	*mptD*	PTS mannose transporter subunit IID	-1.11	8.90E-18	7.46E-17
OG1RF_11489	*purD*	phosphoribosylamine--glycine ligase	-1.70	1.12E-06	3.48E-06
OG1RF_11490	*purH*	inosine monophosphate cyclohydrolase	-2.29	1.61E-37	5.62E-36
OG1RF_11491	*purN*	phosphoribosylglycinamide formyltransferase	-1.16	1.63E-02	3.03E-02
OG1RF_11492	*purM*	phosphoribosylformylglycinamidine cyclo-ligase	-2.06	1.87E-15	1.30E-14
OG1RF_11493	*purF*	amidophosphoribosyltransferase	-3.19	3.23E-27	1.82E-26
OG1RF_11494	*purL*	phosphoribosylformylglycinamidine synthase II	-1.79	1.38E-11	3.68E-11
OG1RF_11495	*purL2*	phosphoribosylformylglycinamidine synthase subunit PurQ	-3.03	2.91E-37	2.59E-36
OG1RF_11496	*purS*	phosphoribosylformylglycinamidine synthase	-2.68	7.75E-15	5.12E-14
OG1RF_11498	*purK*	5-(carboxyamino)imidazole ribonucleotide synthase	-2.15	9.76E-13	5.37E-12

*Complete table can be found in **Supplementary File 2** at https://bit.ly/3tOvqhy.*

Table 3.4 *E. faecalis* purine biosynthesis genes are differentially regulated from 8 hpi wounds.

Locus tag	Name	Description	log2FC	p-value	FDR
OG1RF_11489	*purD*	phosphoribosylamine--glycine ligase	6.47	5.40E-199	4.36E-197
OG1RF_11490	*purH*	inosine monophosphate cyclohydrolase	6.26	2.78E-182	1.50E-180
OG1RF_11491	*purN*	phosphoribosylglycinamide formyltransferase	6.27	1.91E-115	3.48E-114
OG1RF_11492	*purM*	phosphoribosylformylglycinamidine cyclo-ligase	7.02	7.40E-132	1.73E-130
OG1RF_11493	*purF*	amidophosphoribosyltransferase	7.40	1.57E-141	4.15E-140
OG1RF_11494	*purL*	phosphoribosylformylglycinamidine synthase II	6.58	9.95E-152	3.10E-150
OG1RF_11495	*purL2*	phosphoribosylformylglycinamidine synthase subunit PurQ	6.12	1.16E-82	1.35E-81
OG1RF_11496	*purS*	phosphoribosylformylglycinamidine synthase	6.35	7.15E-22	2.25E-21
OG1RF_11497	*purC*	phosphoribosylaminoimidazolesuccinocarboxamide synthase	7.29	6.75E-118	1.28E-116
OG1RF_11498	*purK*	5-(carboxyamino)imidazole ribonucleotide synthase	5.37	1.57E-62	1.20E-61
OG1RF_11499	*purE*	5-(carboxyamino)imidazole ribonucleotide mutase	5.24	1.24E-75	1.29E-74

*Complete table can be found in **Supplementary File 3** at https://bit.ly/3tOvqhy.*

To confirm the role of *de novo* purine biosynthesis for *E. faecalis* replication during wound infection, an in-frame deletion mutant of the first two genes in the *pur* operon was created (OG1RF Δ*purEK*). An *in vivo* competitive infection was then performed with OG1RF Δ*purEK* and OG1X at 8 hpi. *E. faecalis* OG1X is a closely related strain with *E. faecalis* OG1RF and expresses different antibiotic resistance genes which enables differential selection (Ike et al., 1983). In accordance with the Tn-seq and RNA-seq results, OG1RF Δ*purEK* (CI = 0.93) displayed significantly reduced fitness compared to wild-type OG1RF (CI = 1.69) **(Figure 3.1A)**. Subsequently, a single-strain infection was performed and OG1RF Δ*purEK* CFU (8.33×10^6 CFU/wound) was found to be significantly lower than wild-type OG1RF (2.77×10^7 CFU/wound) at 8 hpi **(Figure 3.1B)**.

Tn-seq analysis at 3 dpi also showed the importance of *de novo* purine biosynthesis for *E. faecalis* persistence in wounds, as two genes in the *pur* operon (*purH* and *purM*) were significantly fewer in the post-infection transposon pools **(Table 3.5)**. Hence, to validate the contribution of purine biosynthesis at 3 dpi, an *in vivo* competitive infection with OG1X was similarly performed. Although OG1RF Δ*purEK* (CI = 1.43) displayed significantly reduced fitness compared to wild-type OG1RF (CI = 1.85) at 3 dpi **(Figure 3.1C)**, the difference in CI was not as large as compared to 8 hpi **(Figure 3.1A)**. Overall, these results demonstrate that *E. faecalis de novo* purine biosynthesis contributes significantly to *E. faecalis* replication during acute infection as well as to persistence during wound infection.

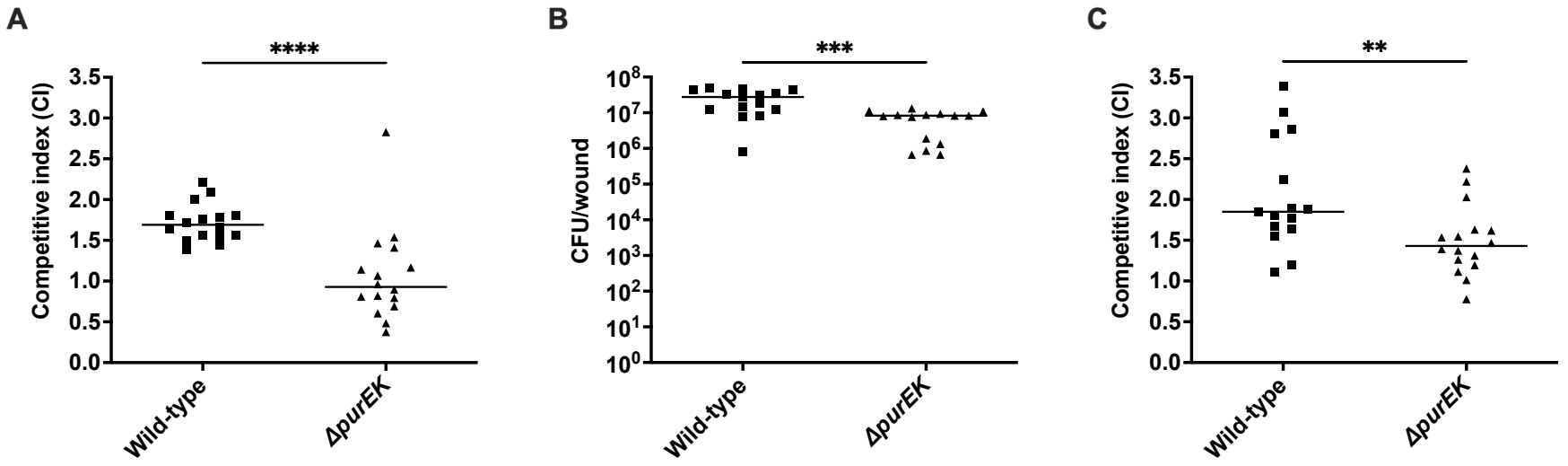

Figure 3.1 *De novo* purine biosynthesis contributes to *E. faecalis* fitness during early stages of wound infection.
Male C57BL/6 mice were wounded and infected with **(A)** a 1:1 ratio of *E. faecalis* OG1X:wild-type OG1RF or OG1X:OG1RF Δ*purEK* at 2 – 4 × 10^6 CFU/wound, **(B)** 2 – 4 × 10^6 CFU of wild-type OG1RF or OG1RF Δ*purEK* in single-strain infection and CFU determined at 8 hpi, or **(C)** a 1:1 ratio of *E. faecalis* OG1X:wild-type OG1RF or OG1X:OG1RF Δ*purEK* at 2 – 4 × 10^6 CFU/wound and CFU determined at 3 dpi. The recovered bacteria were enumerated on selective agar plates for each strain. Each data point represents one mouse and horizontal lines indicate the median, N = 3, n = 5 - 6 mice per group per experiment. Statistical analysis was performed using the Mann-Whitney U test, **p < 0.01, ***p < 0.001, ****p < 0.0001.

Table 3.5 *E. faecalis* transposon mutant abundance profiled by Tn-seq from 3 dpi wounds.

Locus tag	Name	Description	log2FC	p-value	FDR
OG1RF_10019	*mptAB*	PTS mannose transporter subunit EIIAB	-9.75	5.64E-05	2.93E-03
OG1RF_10020	*mptC*	PTS mannose/fructose/sorbose transporter subunit IIC	-10.36	3.81E-06	8.53E-05
OG1RF_10021	*mptD*	PTS mannose transporter subunit IID	-10.86	1.10E-08	6.29E-07
OG1RF_11490	*purH*	inosine monophosphate cyclohydrolase	-10.30	2.52E-06	6.12E-05
OG1RF_11492	*purM*	phosphoribosylformylglycinamidine cyclo-ligase	-9.01	4.66E-03	2.42E-02
OG1RF_11280	*aroE*	shikimate dehydrogenase	-9.76	7.37E-05	3.34E-03
OG1RF_11281	*aroF*	3-deoxy-7-phosphoheptulonate synthase	-9.20	2.70E-03	1.60E-02

*Complete table can be found in **Supplementary File 4** at https://bit.ly/3tOvqhy.*

Next, the predicted requirement of *de novo* purine biosynthesis for *E. faecalis* growth was validated by growing *E. faecalis* in RPMI-CA medium lacking purines. As expected, the deletion of *purEK* (OG1RF Δ*purEK* pTCV::P_{tet}-Empty) resulted in severe growth attenuation compared to wild-type (OG1RF pTCV::P_{tet}-Empty), and complementation of *purEK* on a plasmid (OG1RF Δ*purEK* pTCV::P_{tet}-*purEK*) restored growth to near wild-type levels **(Figure 3.2A)**. To confirm that the growth attenuation observed was due to the disruption of purine biosynthesis pathway, RPMI-CA medium was supplemented with 10 and 100 µM IMP (end-product of purine biosynthesis). With supplementation of IMP, the growth of OG1RF Δ*purEK* pTCV::P_{tet}-Empty was restored to wild-type levels in a dose-dependent manner **(Figure 3.2B and C)**. These findings suggest the importance of *E. faecalis pur* operon during growth in a purine-deficient environment.

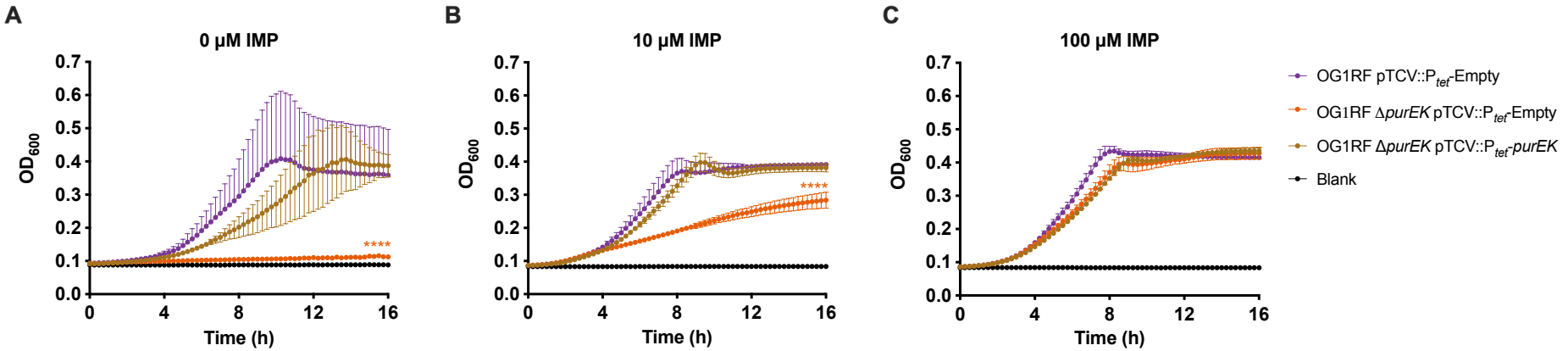

Figure 3.2 *De novo* purine biosynthesis is required for the growth of *E. faecalis* in purine-deficient medium.
Growth kinetics of wild-type OG1RF pTCV::P_{tet}-Empty, OG1RF Δ*purEK* pTCV::P_{tet}-Empty, and OG1RF Δ*purEK* pTCV::P_{tet}-*purEK* in RPMI-CA media supplemented with **(A)** 0, **(B)** 1 or **(C)** 100 µM IMP over 16 h. Baseline readings are indicated by Blank, containing only the growth media. Data are mean values of three independent biological replicates and vertical lines represent SD from the mean. Statistical analysis was performed at 16 h OD_{600} measurement with wild-type OG1RF pTCV::P_{tet}-Empty as the comparator using the Mann-Whitney U test, ****$p < 0.0001$.

3.3.2 Purine metabolites in wounds are low during the replication phase of *E. faecalis*.

De novo purine biosynthesis is necessary for *Staphylococcus aureus* pathogenesis during bacteremia because disruption of purine biosynthesis results in reduced bacterial virulence as measured by bacterial burden and animal weight loss (Goncheva et al., 2020). Moreover, previous Tn-seq revealed that purines were among the metabolites deemed "not available" to *P. aeruginosa* during both burn and chronic wound infections (Turner et al., 2014). Collectively, these studies demonstrate the significance of purine biosynthesis for virulence across various bacteria and infections. Hence, purines availability in the wound microenvironment was predicted to be low, which would explain the importance of *de novo* purine biosynthesis for successful *E. faecalis* wound infection. To assess whether purines were indeed limited during wound infection, purine metabolites were quantified from *E. faecalis* wild-type OG1RF-infected wounds compared to PBS-treated control wounds at 8 hpi and 3 dpi using LC-MS. Following infection with wild-type *E. faecalis*, a trend towards decreased purine metabolites compared to PBS-treated wounds at 8 hpi was observed, which was significant for adenine, guanine, xanthine, and AMP (**Figure 3.3A – D**, compare blue bars), suggesting that there may be consumption of purine metabolites during acute wound infection which could explain the high demand for purine metabolites when *E. faecalis* is rapidly replicating in the wounds (Chong et al., 2017). By contrast, the levels of purine metabolites remain largely similar between PBS-treated and wild-type OG1RF-infected wounds at 3 dpi, except for xanthine and AMP (**Figure 3.3C and D**, compare green bars). Differences following infection were not observed for adenosine, guanosine, and

inosine **(Appendix Figure 3.3)**. Taken together, these results demonstrate that the importance of *de novo* purine biosynthesis for *E. faecalis* replication during acute wound infection is driven by its consumption of purine metabolites in the wound microenvironment.

3.3.3 *E. faecalis* MptABCD phosphotransferase system is more important for *E. faecalis* persistence during wound infection.

Tn-seq analysis at 8 hpi and 3 dpi also identified *mptABCD* as significantly contributing to *E. faecalis* fitness at both timepoints **(Table 3.3 and Table 3.5)**. Therefore, the contribution of *mptABCD* to *E. faecalis* virulence in wound infection was investigated, especially at 3 dpi when transposon insertions in all genes of the *mpt* operon were among the most significantly underrepresented following Tn-seq **(Appendix Figure 3.4)**. *E. faecalis mptABCD* encodes a phosphotransferase system that is used by bacteria for the transport of carbohydrates (Deutscher et al., 2006), suggesting the importance of carbohydrates import during *E. faecalis* wound infection. An *in vivo* RNA-seq on wild-type OG1RF-infected wounds at 3 dpi was also attempted. However, due to the low amount of wild-type OG1RF recovered from the wounds (~10^5 CFU/wound) and as a result lower bacterial raw counts, the *E. faecalis* transcriptome at 3 dpi could not be accurately profiled.

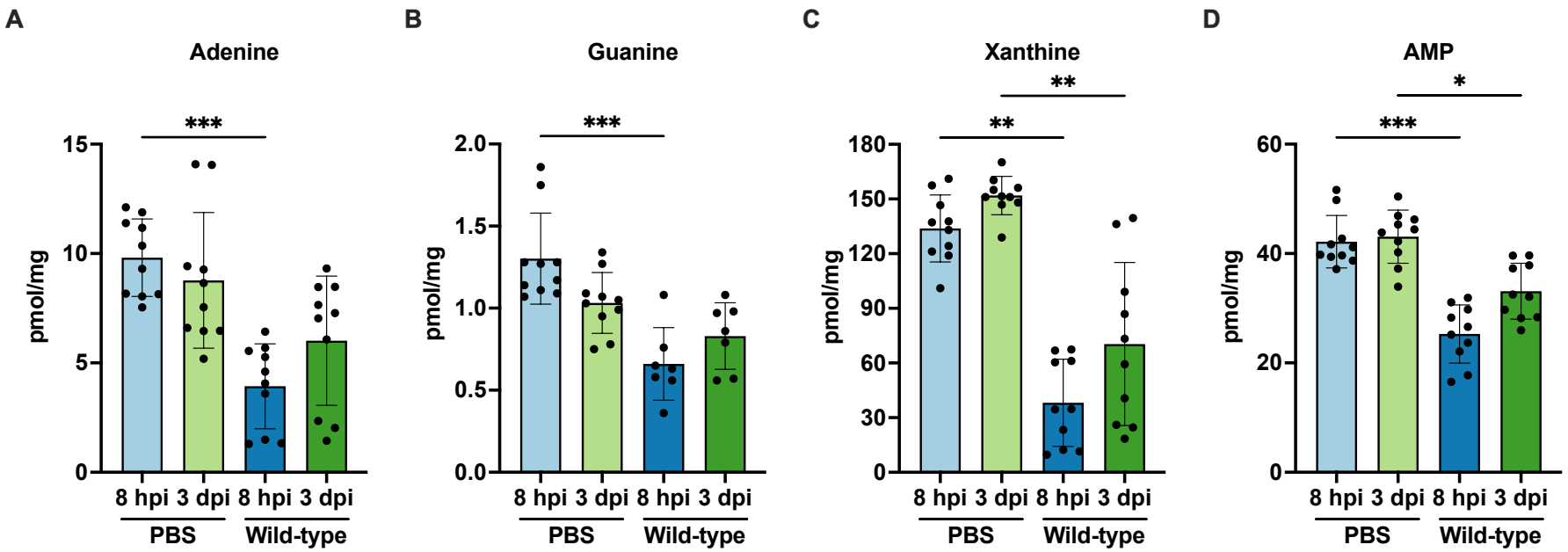

Figure 3.3 Purine metabolites are low during early *E. faecalis* wound infection.
Male C57BL/6 mice were wounded and inoculated with PBS or 2 – 4 × 10^6 CFU of wild-type OG1RF. Wounds were harvested at 8 hpi and 3 dpi for quantification of **(A)** adenine, **(B)** guanine, **(C)** xanthine, and **(D)** AMP using LC-MS. Each data point represents one mouse and error bars represent SD from the mean; N = 2, n = 5 mice per group per experiment. Statistical analysis was performed using the Mann-Whitney U test, *$p < 0.05$, **$p < 0.01$, ***$p < 0.001$.

To validate the role of *E. faecalis* MptABCD PTS during wound infections, an in-frame deletion mutant of *mptD* was created (OG1RF Δ*mptD*), and an *in vivo* competitive infection was performed with OG1X at 8 hpi and 3 dpi. In agreement with the Tn-seq results, OG1RF Δ*mptD* had reduced fitness compared to wild-type OG1RF at both 8 hpi and 3 dpi **(Figure 3.4A and B)**. However, a bigger difference in CI at 3 dpi (CI_{OG1RF} = 1.89, $CI_{\Delta mptD}$ = 0.23) compared to 8 hpi (CI_{OG1RF} = 1.53, $CI_{\Delta mptD}$ = 1.08) was observed, which may explain the more pronounced decrease in log2FC that was seen in the post-infection transposon pools at 3 dpi **(Table 3.3 and Table 3.5)**. Similarly, a single-strain infection was performed and OG1RF Δ*mptD* (3.50×10^4 CFU/wound) was found to colonize poorer than wild-type OG1RF (2.47×10^5 CFU/wound) at 3 dpi **(Figure 3.4C)**. Although the *mptD* complement strain was created (OG1RF Δ*mptD* pMSP3535::P_{nisA}-*mptD*), it was not tested *in vivo* as the bacteria would likely lose the plasmid without antibiotic pressure added to the mice (especially for 3 dpi). Together, these results indicate that MptABCD PTS plays a significant role during *E. faecalis* persistence in wounds infection.

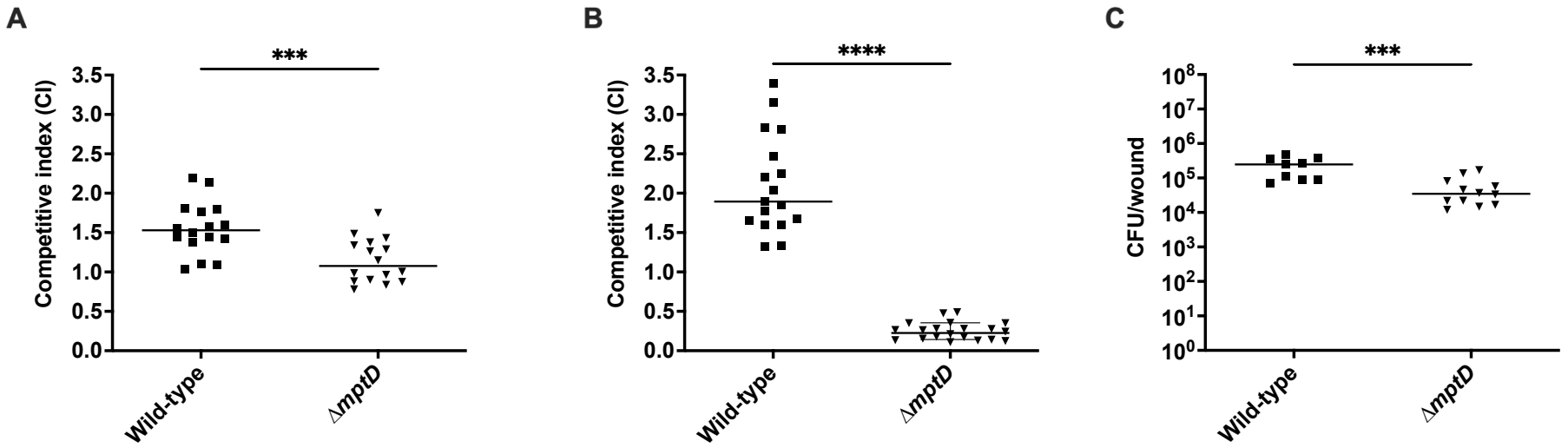

Figure 3.4 MptABCD phosphotransferase system contributes to *E. faecalis* wound fitness during persistence.
Male C57BL/6 mice were wounded and infected with **(A)** a 1:1 ratio of *E. faecalis* OG1X:wild-type OG1RF or OG1X:OG1RF Δ*mptD* at 2 – 4 × 10^6 CFU/wound (N = 3, n = 5 - 6 mice) and CFU determined at 8 hpi or **(B)** a 1:1 ratio of *E. faecalis* OG1X:wild-type OG1RF or OG1X:OG1RF Δ*mptD* at 2 – 4 × 10^6 CFU/wound (N = 4, n = 5 - 6 mice) and CFU determined at 3 dpi or **(C)** 2 – 4 × 10^6 CFU of wild-type OG1RF or OG1RF Δ*mptD* (N = 2, n = 5 - 6 mice) and CFU determined at 3 dpi. The recovered bacteria were enumerated on selective agar plates for each strain. Each data point represents one mouse and horizontal lines indicate the median. Statistical analysis was performed using the Mann-Whitney U test, ***$p < 0.001$, ****$p < 0.0001$.

3.3.4 *E. faecalis* MptABCD phosphotransferase system is responsible for the import of galactose and mannose.

Based on KEGG genome, *E. faecalis mptABCD* is predicted to encode PTS mannose/fructose/sorbose transporter subunits. Therefore, to determine the carbohydrate(s) transported by the MptABCD PTS, the ability of *E. faecalis* to metabolize 50 different carbohydrates was tested. Across all 50 carbohydrates, the deletion of *mptD* (OG1RF Δ*mptD* pMSP3535::P_{nisA}-Empty) only affected the metabolism of galactose and mannose when compared to wild-type (OG1RF pMSP3535::P_{nisA}-Empty), and complementation of *mptD* on an inducible plasmid (OG1RF Δ*mptD* pMSP3535::P_{nisA}-*mptD*) restored mannose and galactose metabolism **(Figure 3.5A)**. To validate that the *mptD* deletion mutant was indeed unable to metabolize galactose and mannose, growth kinetic assays of wild-type OG1RF, *mptD* deletion, and complement strains was performed in TSBd (TSB broth lacking dextrose) growth media supplemented with different carbohydrates. No growth differences were observed between all three strains in TSBd in the absence of carbohydrate supplementation **(Figure 3.5B)**. When TSBd was supplemented with either galactose or mannose, the growth of OG1RF pMSP3535::P_{nisA}-Empty was augmented, but OG1RF Δ*mptD* pMSP3535::P_{nisA}-Empty growth was not **(Figure 3.5C and D)**. Complementation of *mptD* in the deletion mutant resulted in significantly improved growth compared to OG1RF pMSP3535::P_{nisA}-Empty levels when supplemented with galactose **(Figure 3.5C)** and was almost identical to OG1RF pMSP3535::P_{nisA}-Empty levels with mannose supplementation **(Figure 3.5D)**. As a control, TSBd was supplemented with glucose, and minimal or no growth differences was expected between the three strains as metabolism of glucose

was unaffected when *mptD* was deleted **(Figure 3.5A)**. As expected, growth differences were similar between all strains, at least through log phase, when supplemented with glucose **(Figure 3.5E)**. Collectively, these results indicate that MptABCD PTS is responsible for the import for galactose and mannose into *E. faecalis*, and that the import of these carbohydrates may contribute to *E. faecalis* persistence in wounds.

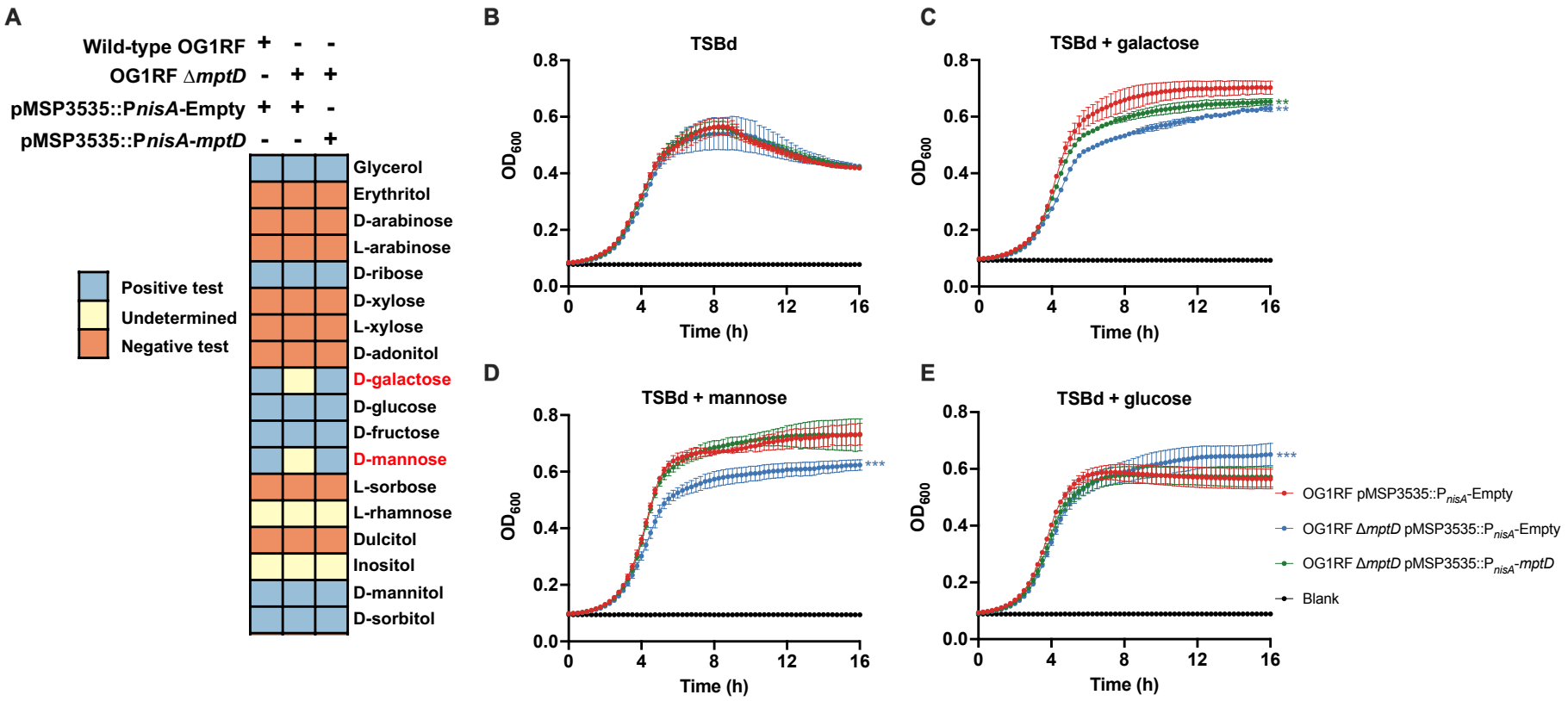

Figure 3.5 *E. faecalis* MptABCD phosphotransferase system is responsible for the transport of galactose and mannose. **(A)** Carbohydrate fermentation test (API CH50) of wild-type OG1RF pMPSP3535::P*nisA*-Empty, OG1RF Δ*mptD* pMSP3535::P*nisA*-Empty, and OG1RF Δ*mptD* pMSP3535::*PnisA*-*mptD*. Plasmid-based *mptD* expression was induced with 40 ng/mL nisin. Results shown are a subset of the 50 carbohydrates; differences were only detected for D-galactose and D-mannose (see **Appendix Table 3.1** for complete table). Positive tests were determined by a change of the bromcresol purple indicator in the medium to yellow. For undetermined test results, the bromcresol purple indicator did not change to yellow nor did remain purple. Negative tests occurred

when the bromcresol purple indicator remained purple. Growth kinetics of wild-type OG1RF pMPSP3535::P_{nisA}-Empty, OG1RF Δ*mptD* pMSP3535::P_{nisA}-Empty, and OG1RF Δ*mptD* pMSP3535::*P_{nisA}-mptD* in TSBd media supplemented **(B)** without additional carbohydrates and with 1% (w/v) of **(C)** galactose, **(D)** mannose and **(E)** glucose over 16 h. Plasmid-based *mptD* expression was induced with 40 ng/mL nisin. Baseline readings are indicated by Blank, containing only the growth media. Data are mean values of three independent biological replicates and vertical lines represent SD from the mean. Statistical analysis was performed at 16 h OD_{600} measurement with wild-type OG1RF pMPSP3535::P_{nisA}-Empty as the comparator using the Mann-Whitney U test, **$p < 0.01$, ***$p < 0.001$.

3.3.5 Carbohydrate availability changes as the wound infection progresses.

The import of galactose and mannose appear more important at 3 dpi than at 8 hpi **(Figure 3.4A and B)**, possibly due to changes in carbohydrate availability in the wound microenvironment as the wound infection progresses. The changing carbohydrate availability was hypothesized to influence the natural course of wound pathogenesis and healing, as well as *E. faecalis* depletion of preferred carbohydrate sources such as glucose during acute infection, thus wound would necessitate a switch to other carbohydrates such as mannose and galactose at later timepoints. To test this hypothesis, PBS-treated, *E. faecalis* wild-type OG1RF- and OG1RF Δ*mptD*-infected wounds were harvested at 8 hpi and 3 dpi, and the concentrations of glucose, galactose and mannose were measured. Consistent with the prediction, lower glucose concentrations were detected at 3 dpi compared to 8 hpi in PBS-treated wounds **(Figure 3.6A)**, and concordant higher galactose and mannose concentrations at 3 dpi compared to 8 hpi **(Figure 3.6B and C)**. Additionally, *E. faecalis* wild-type OG1RF infection further decreased glucose, galactose and mannose concentrations compared to PBS-treated wounds at 8 hpi **(Figure 3.6A – C)**, suggesting that *E. faecalis* can use all three carbohydrates during early phases of wound infection, which may support its rapid growth. At 3 dpi however, no significant differences in glucose concentrations were detected in any wounds **(Figure 3.6A)**, and that *E. faecalis* wild-type OG1RF- and OG1RF Δ*mptD*-infected wounds had less galactose than PBS-treated wounds **(Figure 3.6B)**. Likewise, less mannose was detected compared to PBS-treated wounds when infected with *E. faecalis* wild-type OG1RF at 3 dpi **(Figure 3.6C)**. These results

indicate that *E. faecalis* can import and deplete galactose and mannose during wound infection. Consistent with this conclusion, mannose concentrations were similar between PBS-treated and OG1RF Δ*mptD*-infected wounds at 8 hpi and higher in OG1RF Δ*mptD*-infected wounds compared to OG1RF-infected wounds at 3 dpi (albeit not significant) **(Figure 3.6C)**, suggesting that disruption of MptABCD PTS indeed leads to decreased mannose import (i.e. mannose accumulation) *in vivo*. Unexpectedly, no significant differences in galactose concentration was detected between wild-type OG1RF- and OG1RF Δ*mptD*-infected wounds at any time point **(Figure 3.6B)**, despite a role for MptABCD in galactose metabolism *in vitro* **(Figure 3.5A)**. Taken together, these results suggest that as the wound infection progresses, glucose becomes depleted and other carbohydrates, such as galactose and mannose, become more available in the wounds. As such, *E. faecalis* undergo a metabolic switch towards galactose and mannose metabolism as wound infection progresses.

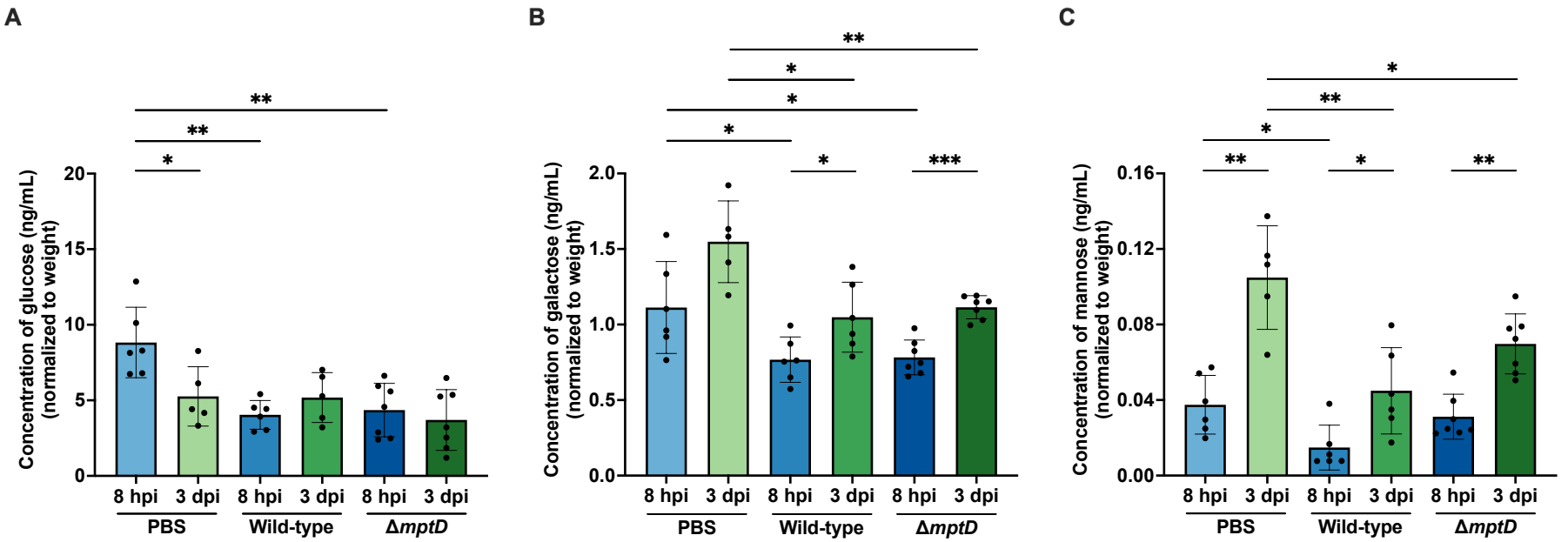

Figure 3.6 Carbohydrate availability changes as *E. faecalis* wound infection progresses.
Male C57BL/6 mice were wounded and inoculated with sterile PBS, wild-type OG1RF or OG1RF Δ*mptD* at 2 – 4 × 10^6 CFU/wound. Wounds were harvested at 8 hpi and 3 dpi, and subjected to **(A)** glucose, **(B)** galactose and **(C)** mannose quantification by ELISA. Each data point represents measurement from one mouse; error bars represent SD from the mean; N = 1, n = 6 - 7 mice. Statistical analysis was performed using the Mann-Whitney U test, *p < 0.05, **p < 0.01, ***p < 0.001.

3.3.6 MptABCD phosphotransferase system-mediated mannose import contributes to *E. faecalis de novo* purine and shikimate biosynthesis.

Since MptABCD PTS imports galactose and mannose which contributes to *E. faecalis* virulence *in vivo*, there could be other galactose and/or mannose-dependent changes in gene expression that are important during wound infection. To examine this, an *in vitro* RNA-seq was performed with wild-type OG1RF and OG1RF Δ*mptD* grown in TSBd without and with supplementation of galactose or mannose. Based on gene set enrichment analysis (GSEA), there was no gene sets enriched with the supplementation of galactose. By contrast, when wild-type OG1RF and OG1RF Δ*mptD* were grown in TSBd supplemented with mannose, several processes/pathways such as purine metabolism, PTS, fructose and mannose metabolism, biosynthesis of secondary metabolites and amino acids were enriched **(Figure 3.7A)**. Among the enriched processes/pathways, 7 out of 8 genes in the shikimate biosynthesis operon (*aroF*, *aroE*, *aroC*, *tyrA*, *aroA*, *aroK*, and *pheA*) and 6 out of 11 genes in the *pur* operon (*purH*, *purN*, *purM*, *purF*, *purL* and *purL2*) were significantly downregulated in OG1RF Δ*mptD* when grown in TSBd supplemented with mannose **(Figure 3.7A)**, suggesting that shikimate and purine biosynthesis are attenuated when import of mannose is hindered. KEGG pathway analysis showed that mannose imported by MptABCD PTS was functionally linked to shikimate and purine biosynthesis **(Figure 3.7B)**. Following mannose import, it can undergo a series of reactions that leads to the production of PEP (a substrate of shikimate pathway) or production of PRPP (a substrate for purine biosynthesis) **(Figure 3.7B)**. These results were also supported by Tn-seq analysis whereby transposon mutants for some genes of the shikimate

biosynthesis and *pur* operon were significantly underrepresented in the post-infection transposon pools at 3 dpi **(Table 3.5)**.

To assess whether purine biosynthesis was impeded when mannose import was hindered, a growth kinetic assay was performed with OG1RF Δ*mptD* in RPMI-CA medium lacking purines. In agreement with the *in vitro* RNA-seq analysis, OG1RF Δ*mptD* growth was attenuated compared to wild-type OG1RF in RPMI-CA medium **(Figure 3.7C)**. These results confirm that hindered mannose import by MptABCD PTS also reduces *de novo* purine biosynthesis.

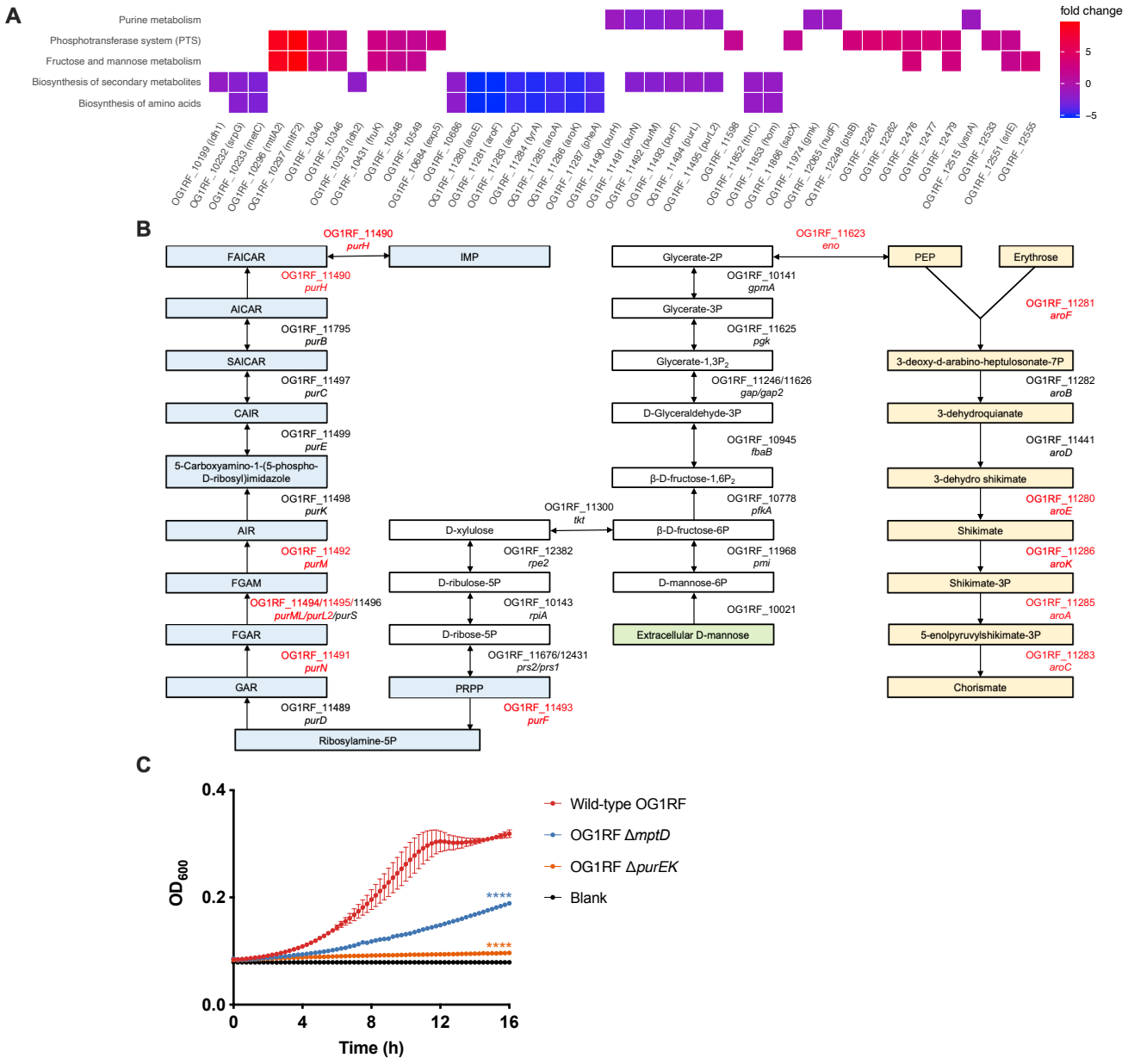
A
Purine metabolism
Phosphotransferase system (PTS)
Fructose and mannose metabolism
Biosynthesis of secondary metabolites
Biosynthesis of amino acids
fold change
5
0
−5
OG1RF_10199 (folH1)
OG1RF_10232 (srpG)
OG1RF_10233 (metC)
OG1RF_10296 (mtlA2)
OG1RF_10297 (mtlF2)
OG1RF_10340
OG1RF_10346
OG1RF_10373 (folH2)
OG1RF_10431 (fruK)
OG1RF_10548
OG1RF_10549
OG1RF_10634 (exp5)
OG1RF_10686
OG1RF_11280 (aroE)
OG1RF_11281 (aroF)
OG1RF_11283 (aroC)
OG1RF_11284 (tyrA)
OG1RF_11285 (aroA)
OG1RF_11286 (aroK)
OG1RF_11287 (pheA)
OG1RF_11490 (purH)
OG1RF_11491 (purN)
OG1RF_11492 (purM)
OG1RF_11493 (purF)
OG1RF_11494 (purL)
OG1RF_11495 (purL2)
OG1RF_11598
OG1RF_11852 (thrC)
OG1RF_11853 (hom)
OG1RF_11896 (sacX)
OG1RF_11974 (gmk)
OG1RF_12065 (hudF)
OG1RF_12248 (ptsB)
OG1RF_12261
OG1RF_12262
OG1RF_12476
OG1RF_12477
OG1RF_12479
OG1RF_12515 (ysnA)
OG1RF_12533
OG1RF_12551 (srlE)
OG1RF_12555
B
OG1RF_11490
purH
FAICAR
IMP
OG1RF_11490
purH
AICAR
OG1RF_11795
purB
SAICAR
OG1RF_11497
purC
CAIR
OG1RF_11499
purE
5-Carboxyamino-1-(5-phospho-D-ribosyl)imidazole
OG1RF_11498
purK
AIR
OG1RF_11492
purM
FGAM
OG1RF_11494/11495/11496
purML/purL2/purS
FGAR
OG1RF_11491
purN
GAR
OG1RF_11489
purD
Ribosylamine-5P
OG1RF_11300
tkt
D-xylulose
OG1RF_12382
rpe2
D-ribulose-5P
OG1RF_10143
rpiA
D-ribose-5P
OG1RF_11676/12431
prs2/prs1
PRPP
OG1RF_11493
purF
OG1RF_11623
eno
Glycerate-2P
PEP
Erythrose
OG1RF_10141
gpmA
Glycerate-3P
OG1RF_11625
pgk
Glycerate-1,3P2
OG1RF_11246/11626
gap/gap2
D-Glyceraldehyde-3P
OG1RF_10945
fbaB
β-D-fructose-1,6P2
OG1RF_10778
pfkA
β-D-fructose-6P
OG1RF_11968
pmi
D-mannose-6P
OG1RF_10021
Extracellular D-mannose
OG1RF_11281
aroF
3-deoxy-d-arabino-heptulosonate-7P
OG1RF_11282
aroB
3-dehydroquianate
OG1RF_11441
aroD
3-dehydro shikimate
OG1RF_11280
aroE
Shikimate
OG1RF_11286
aroK
Shikimate-3P
OG1RF_11285
aroA
5-enolpyruvylshikimate-3P
OG1RF_11283
aroC
Chorismate
C
OD600
0.4
0.2
0.0
0
4
8
12
16
Time (h)
****
****
Wild-type OG1RF
OG1RF ΔmptD
OG1RF ΔpurEK
Blank

Figure 3.7 Mannose imported by *E. faecalis* MptABCD phosphotransferase system is functionally linked to *de novo* purine and shikimate biosynthesis.
(A) Gene set enrichment pathways identified based on differentially expressed genes between wild-type OG1RF and OG1RF Δ*mptD* grown in TSBd supplemented with 1% (w/v) of mannose. Complete table of differentially expressed genes can be found in **Supplementary File 5** at https://bit.ly/3tOvqhy. **(B)** KEGG pathways depicting how import of extracellular D-mannose by MptD (green) acts as a substrate for *de novo* purine (blue) and shikimate (yellow) biosynthesis. **(C)** Growth kinetics of wild-type OG1RF, OG1RF Δ*mptD*, and OG1RF Δ*purEK* in RPMI-CA over 16 h. Baseline readings are indicated by Blank, containing only the growth media. Data are mean values of three independent biological replicates and vertical lines represent SD from the mean. Statistical analysis was performed at 16 h OD_{600} measurement with wild-type OG1RF as the comparator using the Mann-Whitney U test, ****$p < 0.0001$.

3.3.7 *E. faecalis de novo* purine biosynthesis and MptABCD phosphotransferase system are important for catheter-associated urinary tract infection.

Purine biosynthesis is essential in a variety of infection types (Goncheva et al., 2020; Kim et al., 2003; Li, L. et al., 2018; Mei et al., 1997; Samant et al., 2008; Sause et al., 2019). As such, *E. faecalis de novo* purine biosynthesis and MptABCD PTS could similarly contribute to other *E. faecalis* infections. In addition to being a common wound pathogen, *E. faecalis* is also a frequently isolated uropathogen (Kline & Lewis, 2016). Hence, the contribution of purine biosynthesis and MptABCD PTS was tested in a CAUTI model through assessing *in vivo* competitive infections of OG1RF Δ*purEK* and OG1RF Δ*mptD* with OG1X at 1 dpi. OG1RF Δ*purEK* (CI = 8.99) and OG1RF Δ*mptD* (CI = 6.01) had significantly reduced fitness compared to wild-type OG1RF (CI = 46.19) on catheters **(Figure 3.8A)**, while only OG1RF Δ*mptD* (CI = 4.83) had significantly reduced fitness compared to wild-type OG1RF (CI = 33.33) in the bladder **(Figure 3.8B)**, and neither *purEK* nor *mptD* contributed to fitness in the kidneys **(Figure 3.8C)**. These results suggest that *de novo* purine biosynthesis and the MptABCD PTS may be central and niche-independent virulence factors of *E. faecalis*.

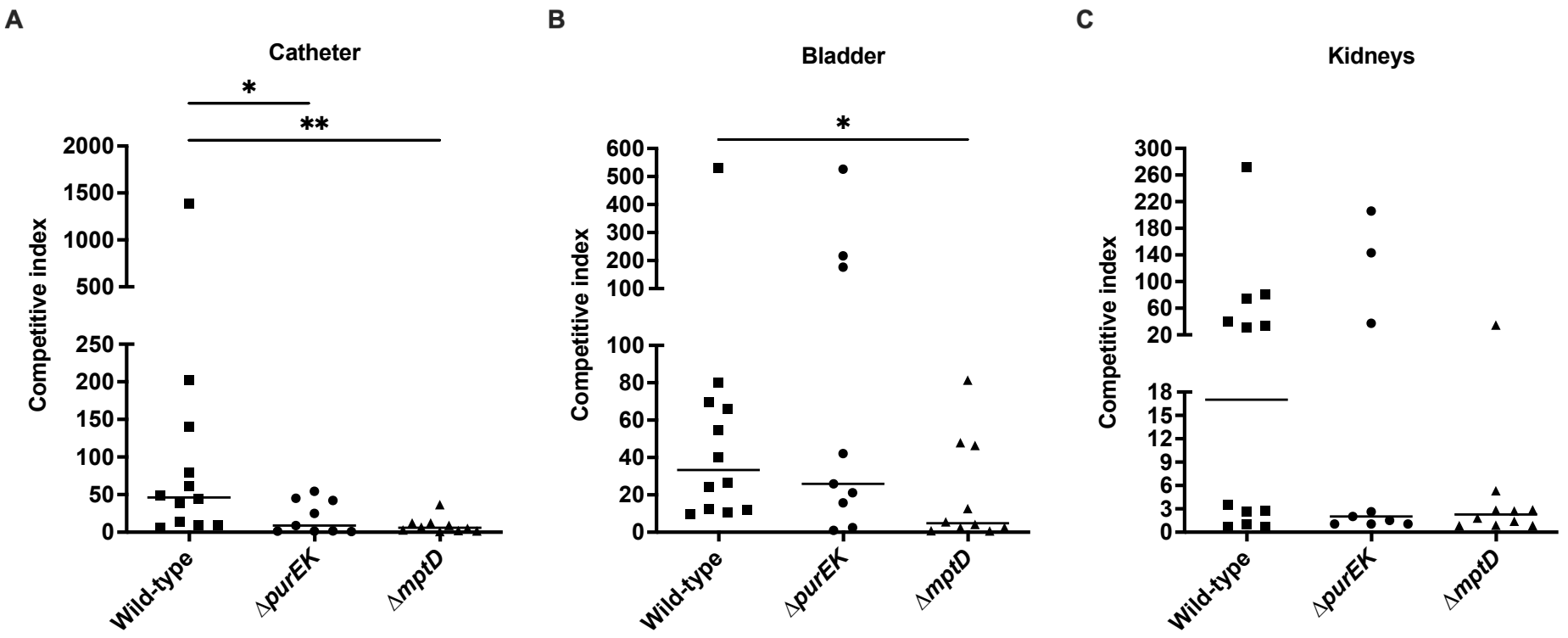

Figure 3.8 *De novo* purine biosynthesis and MptABCD phosphotransferase system contributes to *E. faecalis* fitness during catheter-associated urinary tract infection.

Female C57BL/6 mice were implanted with 5 mm silicon catheters in the bladders and infected with a 1:1 ratio of 10^7 CFU of *E. faecalis* OG1X:wild-type OG1RF, OG1X:OG1RF Δ*purEK* or OG1X:OG1RF Δ*mptD*. **(A)** Catheters, **(B)** bladders and **(C)** kidneys were harvested at 24 hpi and the recovered bacteria were enumerated on selective agar plates for each strain. Each data point represents one mouse and horizontal lines indicate the median; N = 2, n = 6 mice per group per experiment. Statistical analysis was performed using the Mann-Whitney U test, *$p < 0.05$, **$p < 0.01$.

3.4 Discussion

This study aims to identify genetic determinants that are crucial for acute *E. faecalis* replication and later persistence in wounds. Both *E. faecalis de novo* purine biosynthesis and MptABCD PTS are shown to be important for *E. faecalis* acute replication and persistence, respectively. Here, purine metabolites are reported to be lower at the wound site during the early stages of wound infection compared to later persistent stages, explaining the importance of *de novo* purine biosynthesis for acute *E. faecalis* wound infection. Also, this study shows that carbohydrate availability in the wound microenvironment favors galactose and mannose as the wound infection progresses, providing a reason for the requirement of the *E. faecalis* MptABCD galactose and mannose transporter during persistent *E. faecalis* wound infection.

Nucleotide plays an important role in cell physiology of both prokaryotes and eukaryotes, such as DNA and RNA synthesis, enzyme cofactors (NAD^+ and FAD^+), energy carriers (ATP and GTP), and are also involved in the biosynthesis of riboflavin (Abbas & Sibirny, 2011; Jensen et al., 2008). *De novo* purine biosynthesis is necessary for many pathogens to establish a successful infection. For example, purine biosynthesis is necessary for successful proliferation of Gram-negative *E. coli* and *Salmonella typhimurium* in human serum (Samant et al., 2008) and *P. aeruginosa* in wounds (Turner et al., 2014) as well as for Gram-positive *Streptococcus pyogenes* growth in human blood (Le Breton et al., 2013), *E. faecium* growth in human serum (Zhang et al., 2017) and *Bacillus anthracis* growth in human serum and virulence in a mouse bacteremia model (Samant et al., 2008). Likewise, purine biosynthesis is

necessary for *S. aureus* growth in bovine and human serum (Connolly et al., 2017), virulence in mouse models of bacteremia (Goncheva et al., 2020; Sause et al., 2019) and endocarditis infections (Li, L. et al., 2018). Therefore, it is not surprising that purine biosynthesis is also required for *E. faecalis* to establish a successful colonization in wounds, especially during the early phases of wound infection where *E. faecalis* is rapidly replicating (Chong et al., 2017). Together, these studies demonstrate that *de novo* purine biosynthesis probably is a common metabolic pathway that is generally required by bacterial pathogens in most infections. Hence, detailed exploration of enzymes involved in the purine biosynthesis can be considered as potential targets for the treatment of *E. faecalis* wound infections or in general bacterial infections.

Carbohydrates are essential for their metabolism into glucose, which serves as a primary energy source for most bacteria. These large uncharged polar molecules cannot cross the bacterial plasma membrane freely (Cooper & Hausman, 2000). Consequently, bacteria encode PTS to import carbohydrates from the environment (Deutscher et al., 2006). A PTS is made up of several functional subunits, of which the EII subunits of each PTS determines its substrate carbohydrate specificity (Deutscher et al., 2006). As such, most bacteria encode multiple PTS to enable the transport of different carbohydrates. As the wound infection progresses, *E. faecalis* encounters changing carbohydrate availability in the wound microenvironment from higher glucose during acute wound infection to higher galactose and mannose in late stages of the infection, hinting that there is a metabolic switch in the carbohydrate phosphotransferase system in *E. faecalis* and that wound infection is a

"controlled" process. As a result, any disturbance introduced (e.g. hindered mannose import) to this "controlled" process would then lead to reduced competitive index as observed with the OG1RF Δ*mptD* mutant during wound infection. However, there is still limited information on carbohydrate availability in wounds in experimental models or in human wounds, hence we cannot discount the presence of other carbohydrates in the wound microenvironment and the importance of other PTS that might be contributing to *E. faecalis* persistence. Apart from *E. faecalis*, the impact of carbohydrates metabolism and import is also evident in the pathogenesis of several other Gram-positive bacteria. For example, sucrose-6-phosphate hydrolase and its sucrose ABC transporter contributes to *Streptococcus pneumoniae in vivo* fitness during lung infection in mouse (Iyer & Camilli, 2007). Based on comparative genomic analysis, a PTS locus in *Enterococcus faecium* clinical isolates is found to play an important role in mouse intestinal colonization and the deletion of an EII subunit of this PTS resulted in reduced intestinal colonization (Zhang et al., 2013). Garnett et al. (2014) similarly showed the importance of *S. aureus* PTS in importing carbohydrates from the airway surface liquid to support its growth. Given the significance of PTS on the pathogenesis of various infections caused by different bacteria, drugs and/or inhibitors targeting carbohydrate import process(s) seems like an attractive alternative to control infections.

As aforementioned, purine biosynthesis may be a common metabolic pathway that is required for virulence. Fittingly, *E. faecalis de novo* purine biosynthesis also contributes to its fitness during CAUTI. The notion that purines are limiting in the urinary tract is consistent with studies of uropathogenic *E. coli*,

in which a *guaA* mutant that has defective guanine biosynthesis was unable to grow in human urine *in vitro* and was significantly less virulent than the parental wild-type strain in a mouse model of urinary tract infection (UTI) (Russo et al., 1996). The OG1RF Δ*mptD* mutant was less fit than wild-type during CAUTI, suggesting that galactose and mannose availability in the urinary tract are likely limited, which is in contrast with uropathogenic *E. coli* that preferentially take advantage of amino acids and small peptides as a carbon source, since mutants with defective peptide import had significantly reduced fitness during UTI (Alteri et al., 2009). However, future studies will be needed to confirm whether purines are similarly limited in the mice bladders and the carbohydrates profile during CAUTI.

E. faecalis de novo purine biosynthesis and MptABCD PTS are functionally linked **(Figure 3.7B)**. There are multiple pathways like pentose phosphate pathway, alanine, aspartate and glutamate metabolism, thiamine metabolism, and histidine metabolism that contributes to purine biosynthesis (efi00230) (Kanehisa & Goto, 2000), and it is possible that in order to maintain healthy levels of purine to support active cell division during *E. faecalis* acute replication, the presence of all the contributing pathways are likely required. This could explain why there is a growth attenuation of OG1RF Δ*mptD* mutant in purine lacking medium as purine biosynthesis is affected in the absence of mannose transport. However, the OG1RF Δ*mptD* mutant is strongly outcompeted compared to OG1RF Δ*purEK* in wounds at 3 dpi, suggesting that the import of galactose and mannose has a more significant role as a carbon source for *E. faecalis* persistence in wounds other than for purine biosynthesis.

These observations suggest that genes can have a functional shift depending on the state/phase during *E. faecalis* wound infection.

An outstanding question from this study is whether shikimate biosynthesis might be contributing to *E. faecalis* persistence in wounds. The production of secondary metabolites are usually not critical for cell growth, but instead serve as a survival strategy for organisms during adverse conditions likely triggered by depletion of nutrients or environmental stress (Gokulan et al., 2014). The end-product of the shikimate pathway is chorismate, which is essential for subsequent biosynthesis of aromatic amino acids such as phenylalanine, tryptophan and tyrosine as well as aromatic secondary metabolites (Averesch & Krömer, 2018; Herrmann & Weaver, 1999). For example, chorismate branching into the synthesis of para-aminobenzoic acid (PABA), which is a precursor for folate metabolism (Averesch & Krömer, 2018). Interestingly, Turner et al. (2014) not only showed that purines were unavailable to *P. aeruginosa* during wound infection, chorismate, phenylalanine, tyrosine, and PABA were also unavailable. Moreover, shikimate pathway intermediates are also potential substrates leading to other metabolic pathways (Herrmann & Weaver, 1999). Thereby, it is tempting to hypothesize that the shikimate pathway is important as it is a central metabolic route that leads to the production of other aromatic metabolites that might be essential for *E. faecalis* persistence in wounds. However, further studies will be needed to examine the role of *E. faecalis* shikimate biosynthesis in wound infection.

Based on the current findings, a working model of *E. faecalis* wound infection dynamics is proposed **(Figure 3.9)**. During the early phase of wound infection, *E. faecalis* undergoes acute replication and therefore, the demand for purines is high. However, purine metabolites in the wound microenvironment are low, which makes *E. faecalis de novo* purine biosynthesis indispensable for acute replication **(Figure 3.9A)**. Carbohydrate availability during acute infection differs from persistence, in which glucose is higher while galactose and mannose are lower during earlier stages of infection. Despite these differences in availability, it is likely that *E. faecalis* can use all three carbohydrates to support its rapid growth. By contrast, during *E. faecalis* persistence in wounds, galactose and mannose availability are higher than glucose in the wound microenvironment and that there was minimal depletion of glucose by *E. faecalis*, suggesting that galactose and mannose are a preferred carbohydrate source by *E. faecalis* during persistence **(Figure 3.9B)**.

Overall, this study provides insights into the pathogenic requirements and potential of *E. faecalis* during wound infection, and factors that are required for *E. faecalis* to replicate and persist in this niche. Given the suggested importance of *E. faecalis de novo* purine biosynthesis and MptABCD PTS during acute replication and persistence in wounds, this work raises the possibility for future drugs and/or inhibitors to target enzymes involved in purine biosynthesis or MptABCD PTS or in general *E. faecalis* carbohydrate utilization processes as a novel approach to curb infections.

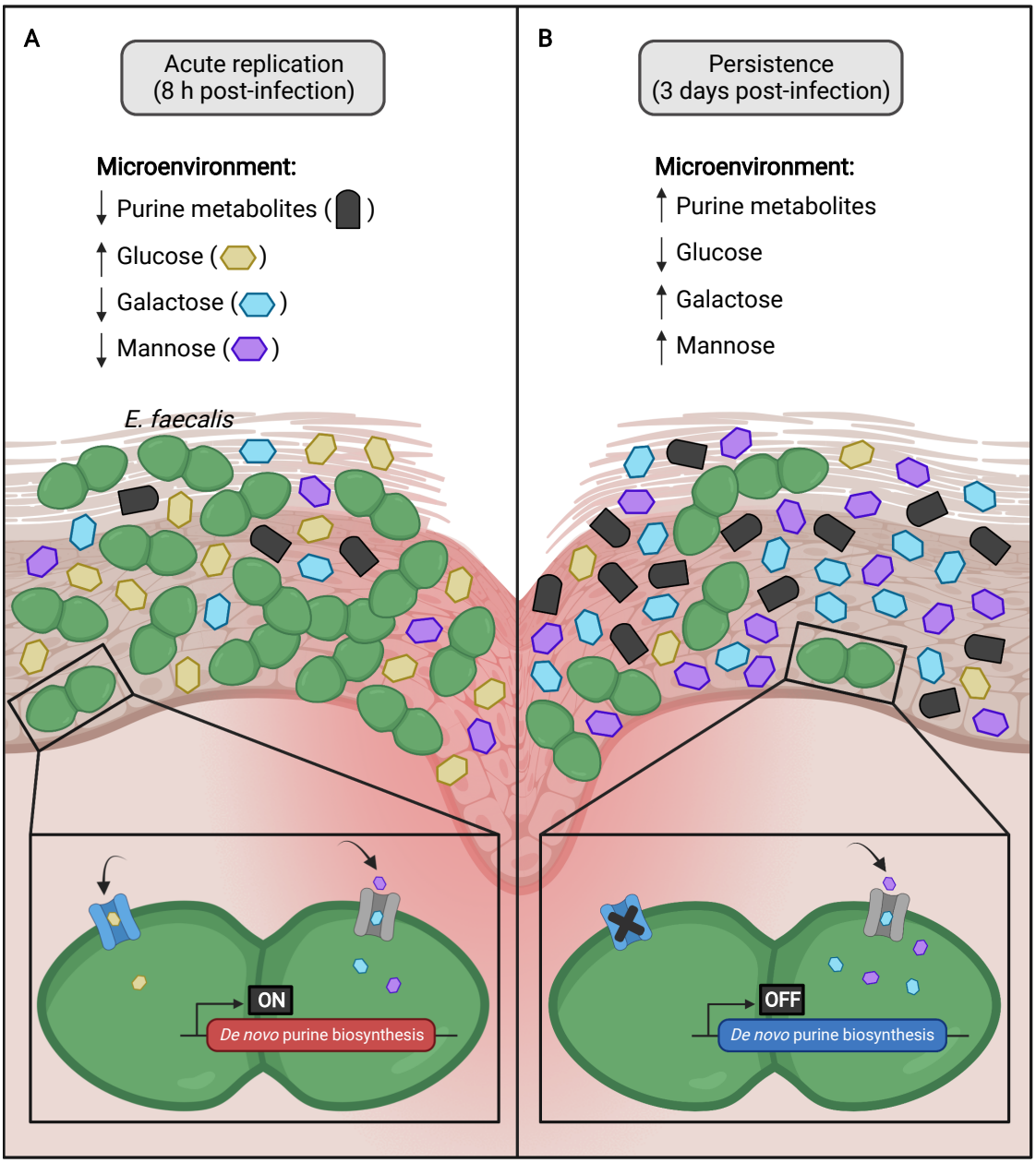

Figure 3.9 Proposed working model of *E. faecalis* wound infection dynamics.

(A) During *E. faecalis* acute replication (8 h post-infection), purine metabolites, galactose and mannose availability in the wound microenvironment are low while glucose is high. As a result, *de novo* purine biosynthesis is induced and *E. faecalis* imports all three carbohydrates to support its rapid growth. **(B)** However, as the wound infection progresses to persistence (3 days post-infection), purine metabolites, galactose and mannose availability are high while glucose is low. Since *E. faecalis* is not actively dividing and purine metabolites are abundant in the wound microenvironment, *de novo* purine biosynthesis is likely not induced in *E. faecalis*. Additionally, given that there was minimal depletion of glucose and increased uptake of galactose and mannose by *E. faecalis*, it suggests that

galactose and mannose are the preferred carbohydrates by *E. faecalis* during persistence.

3.5 Author contributions

I designed the study of this project, performed, and analyzed all the *in vitro* experiments. I designed, performed, and analyzed all the *in vivo* experiments, assisted by Dr. Wong Jun Jie, Dr. Brenda Tien Yin Qi, Mr. Thong Chor Ming, Ms. Alicia Tan Qian Ler, Mr. Daryl Yeong Yu Xuan or Ms. Ng Hui Min Celine. Dr. Chong Kian Long Kelvin designed, performed, and analyzed the *in vivo* Tn-seq experiments. I performed the *in vivo* transcriptomic analysis of wound samples and constructed all the mutant and complement strains, except for OG1RF Δ*purEK*, which is constructed by Ms. Ng Hui Min Celine from School of Biological Sciences (SBS) during her final year project (FYP). I performed the *in vitro* transcriptomic analysis of *E. faecalis* growing in the absence and presence of mannose, assisted by my student Mr. Daryl Yeong Yu Xuan from SBS during his FYP. I wrote (except for materials and methods **section 3.2.3 – 3.2.6** which was written by Dr. Chong Kian Long Kelvin) and edited the pre-print that is available on BioRxiv for this study. The pre-print was revised by Dr. Chong Kian Long Kelvin and Prof. Kimberly Kline.

Chapter 4 – General discussions and conclusions

4.1 Our current understanding of *E. faecalis* wound infection

Enterococcus faecalis can colonize many host niches and is responsible for numerous biofilm-associated infections such as catheter-associated urinary tract infection (CAUTI), infective endocarditis, and wound infection (Arias & Murray, 2012). Although the pathogenesis of *E. faecalis* have been extensively studied in some of these infections, pathogenesis during wound infection remains underexplored. *E. faecalis* is a common wound pathogen, yet it is usually not the only microorganism in wounds, and it is often co-isolated with other microorganisms such as *Pseudomonas aeruginosa* (Gjødsbøl et al., 2006). As such, the overall goal of this dissertation was to gain a deeper understanding of *E. faecalis* wound pathogenesis. To achieve this goal, I undertook the following: (1) explored the nature and mechanistic underpinning for *E. faecalis* and *P. aeruginosa* mixed-species interactions within biofilms under *in vitro* iron-restricted conditions and *in vivo* mouse wound excisional model, and (2) determined and characterized *E. faecalis* genetic determinants involved in *E. faecalis* wound pathogenesis. In this last chapter, I will review and briefly summarize the findings as well as discuss the limitations and how this dissertation can help in deciding future studies to enhance our knowledge regarding *E. faecalis* wound pathogenesis.

There is no study on the mixed-species interactions during wound infection between commonly co-isolated wound pathogens, *E. faecalis* and *P. aeruginosa*. Therefore, I first sought to study the *in vitro* mixed-species

interactions between these two bacterial species in an infection-relevant, low iron condition. This study began by exploring the nature of the mixed-species interactions using static biofilm and macrocolony biofilm assays with both laboratory and clinical isolates of *E. faecalis* and *P. aeruginosa*. These two species were found to engage in an antagonistic relationship, in which *E. faecalis* inhibits *P. aeruginosa* growth in biofilms under *in vitro* iron-restricted conditions. To determine the mechanism underlying this antagonism observed, an *in vitro E. faecalis* transposon library screen was performed, and *E. faecalis ldh1* was identified to be responsible for the phenotype under iron-restricted conditions. I subsequently showed that *E. faecalis ldh1* expression was induced when grown in iron-restricted media, which resulted in an increased lactic acid secretion, and consequently decreasing the local environmental pH. The findings in **Chapter 2** suggests that under *in vitro* iron-restricted conditions, *E. faecalis* changes the local microenvironment by increasing lactic acid secretion to further chelate the limited iron in the environment and lowers the local pH to antagonize *P. aeruginosa* growth. In addition, instead of engaging in an antagonistic relationship, *P. aeruginosa* augmented *E. faecalis* growth in a mouse wound excisional model. I hypothesize that the spatial organization of these two bacterial species in wounds might dampen any local pH and iron-competition effects observed under *in vitro* conditions. Hence, it will be interesting to investigate the spatial organization of *E. faecalis* and *P. aeruginosa* during wound infection, which will be discussed further in the following section. Taken together, these findings provide insights into the mixed-species interactions between different bacterial species and highlights the

importance of microenvironment manipulation in influencing growth trajectory of bacterial communities.

Next, in **Chapter 3**, I sought to identify and characterize *E. faecalis* genetic determinants that contributes to *E. faecalis* wound pathogenesis, specifically the factors that are important for acute *E. faecalis* replication and persistence in wounds, using *in vivo* transposon (Tn-seq) and RNA sequencing (RNA-seq) approaches. I found that *E. faecalis de novo* purine biosynthesis genes and MptABCD phosphotransferase system (PTS) were indispensable for *E. faecalis* acute replication and persistence, respectively. Moreover, *E. faecalis* MptABCD PTS was characterized to be responsible for the import of galactose and mannose from the environment. To further understand how purine biosynthesis genes and MptABCD PTS contributed to *E. faecalis* wound infection, I investigated the wound microenvironment during the infection, explicitly in terms of purine metabolite and carbohydrate availability. Through profiling of the wound microenvironment, purine metabolites were found to be low during the period of acute replication, and that the availability of carbohydrates changes as *E. faecalis* progresses from acute replication to a persistence phase during wound infection. These observations suggest that *E. faecalis de novo* purine biosynthesis and MptABCD PTS play a vital role in the progression of wound infection and may represent a novel target for increased efficacy in the treatment of *E. faecalis* wound infection. Furthermore, a functional link between MptABCD PTS and *de novo* purine and shikimate biosynthesis was identified. However, it remains unclear whether *E. faecalis* shikimate biosynthesis similarly contributes to wound pathogenesis. Thus, it is worthwhile

to further investigate and understand the significance of shikimate biosynthesis during *E. faecalis* wound infection which will be discussed further in the subsequent section. These findings suggest that other than classical virulence factors as discussed in section **1.1.4**, metabolic processes such as purine biosynthesis and carbohydrate import can also similarly contribute to the pathogenesis of infections. Additionally, these findings once again emphasize the importance of how dynamic microenvironment changes can influence the pathogenic requirements of *E. faecalis* during wound infection. This is the first study that identifies and explores the genetic determinants that are crucial for *E. faecalis* wound infection.

In summary, the overall goal of this dissertation has been achieved, and the findings presented in **Chapter 2** and **Chapter 3** has set the foundation for further exploration of *E. faecalis* wound pathogenesis. We are just beginning to understand the *E. faecalis* pathogenesis during wound infection and there are still many aspects worth investigating in both the single- and mixed-species infections.

4.2 Limitations of this study

The *in vitro* findings in **Chapter 2** emphasize the importance of iron and pH in the microenvironment in influencing *E. faecalis* and *P. aeruginosa* mixed-species interactions. However, a limitation of the *in vivo* experiments is that the pH of single- and mixed-species infected wounds were not measured. Even though *E. faecalis* did not inhibit *P. aeruginosa* growth when co-infected in wounds **(Figure 2.6A)**, the pH of the infected wounds can be measured so that

it can be correlated to the *in vitro* results. Additionally, the *in vivo* experiments were performed in C57BL/6 mice and given the importance of low iron conditions in inducing *E. faecalis ldh1* expression, the wound excisional model can be performed in iron-deficient mice or C57BL/6 mice fed with low iron diet over a period of time.

Although an *in vivo* RNA-seq on *E. faecalis* wild-type OG1RF from 3 dpi wounds was attempted in **Chapter 3**, the number of raw counts were significantly lower as compared to 8 hpi wounds. As such, it was not possible to analyze the differentially expressed *E. faecalis* genes at 3 dpi and correlate it to the Tn-seq results. This is likely due to the low *E. faecalis* cell numbers in the 3 dpi wounds (~10^5 – 10^6 CFU/wound) compared to 8 hpi wounds (~10^7 – 10^8 CFU/wound). A possibility to overcome the low *E. faecalis* cell numbers at 3 dpi is to pool wound samples from different mice and combine them together as 1 sample, which will increase the number of *E. faecalis* per sample and hence, increase the amount of RNA extracted per sample. Alternatively, a single-cell RNA sequencing approach (Kuchina et al., 2021) can be taken to overcome the limitation of low reads in 3 dpi wounds and at the same time also enables us to elucidate heterogeneity of *E. faecalis* gene expression in the wounds.

4.3 Future perspectives

The spatial localization between *E. faecalis* and *P. aeruginosa* during wound infection could be contributing to the contrasting observations reported between the *in vitro* and *in vivo* conditions in **Chapter 2**, in which *E. faecalis* inhibited *P. aeruginosa* growth *in vitro* but *P. aeruginosa* augmented *E. faecalis*

growth *in vivo*. Stacy et al. (2016) introduced the concept of "biogeography" in which microorganisms within a polymicrobial community are spatially organized or segregated during infections. In a four-species wound infection involving *E. faecalis*, *P. aeruginosa*, *Staphylococcus aureus* and *Finegoldia magna*, spatial segregation was reported between *E. faecalis* and *P. aeruginosa*, in which *P. aeruginosa* was found deeper in the wound bed compared to *E. faecalis* (Dalton et al., 2011). Thus, it is highly possible that *E. faecalis* and *P. aeruginosa* are also similarly segregated during mixed-species wound infection and as a result, negating the inhibitory effect we observed *in vitro*. Moreover, to date, there is no study investigating the spatial localization between just *E. faecalis* and *P. aeruginosa* during wound infection. Hence, it will be interesting to visualize how these two pathogens are assembled during wound infection, as the spatial organization of any polymicrobial community can provide valuable information to help in designing strategies to stop or even eradicate infections. More importantly, the spatial localization between pathogens during infections can influence their virulence potential and disease progression significantly (Stacy et al., 2016).

Furthermore, in **Chapter 2**, *P. aeruginosa* was found to augment the growth of *E. faecalis* in wounds. However, the mechanism(s) underlying *E. faecalis* growth augmentation remains unclear. To elucidate the mechanism(s), an *in vivo* mixed-species Tn-seq using wild-type *P. aeruginosa* and a pooled *E. faecalis* transposon library can be conducted. By identifying *E. faecalis* transposon mutants that are "less fit" (denoted by a negative log2 fold change) during the mixed-species wound infection, we can identify *E. faecalis* bacterial

factors that contribute to the growth augmentation and subsequently, the mechanism(s) promoting the mixed-species wound infection. This knowledge may enable the development of targeted drugs or inhibitors to control mixed-species infections.

An outstanding question in **Chapter 3** is whether and how does *E. faecalis* shikimate biosynthesis contribute to wound infection. To investigate whether shikimate biosynthesis is essential for *E. faecalis* wound infection, we can apply the same strategy used in this dissertation, that is to create a mutant with disrupted shikimate biosynthesis and test it in the competitive mouse wound excisional model. There is evidence based on work in *P. aeruginosa* published by Turner et al. (2014) suggesting that the importance of shikimate biosynthesis could be due to limited chorismate (end-product of shikimate biosynthesis), phenylalanine, tyrosine and para-aminobenzoic acid (chorismate is required for the synthesis of these secondary metabolites) in the wound microenvironment. As such, similar to the purine metabolite quantification done in **Chapter 3**, a targeted metabolite screening can be performed to examine which metabolite(s) is/are limited during *E. faecalis* wound infection using mass spectrometry. Taking a step further, since mannose transported in by *E. faecalis* MptABCD PTS is functionally linked to purine and shikimate biosynthesis, double and triple deletion mutants with defective purine biosynthesis, MptABCD PTS, and shikimate biosynthesis can be created and tested in the competitive mouse wound excisional model, which would allow us to explore whether these pathways are acting independently or together. Collectively, examining the

wound microenvironment can help us to understand the mechanism(s) underlying *E. faecalis* wound pathogenesis.

Another question that is worth following up is what is/are the source(s) of carbohydrates that *E. faecalis* import to promote its persistence during wound infections? Free carbohydrates are likely scarce in the wound microenvironment, and *E. faecalis* might have to scavenge carbohydrates from N-linked or O-linked glycoconjugates present in the wound microenvironment. Subsequently, these released carbohydrates can then be imported by the respective PTS to be potentially used by *E. faecalis* as nutrients. This is evident in *Streptococcus pneumoniae*, whereby free carbohydrates are limited in the upper respiratory tract, and *S. pneumoniae* expresses a variety of glycosidases to cleave glycosidic linkage at the terminal monosaccharide of glycoconjugates to release free carbohydrates for uptake to promote nasopharyngeal colonization (Marion et al., 2009; Marion et al., 2012; Minhas et al., 2021; Paixão et al., 2015). Likewise, *E. faecalis* also encodes several putative glycosidases such as endoglycosidase EndoE, that is capable of cleaving N-linked glycans from glycoprotein lactoferrin (Garbe et al., 2014). Moreover, the presence of *E. faecalis* mannosidase activity was demonstrated with RNase B-derived glycans which releases free mannose to support *in vitro E. faecalis* growth (Roberts, G. et al., 2000). Therefore, it would be interesting to examine whether *E. faecalis* expresses these putative glycosidases during *in vivo* wound infection, as they could be an attractive target for designing drugs or inhibitors for enhanced treatment efficacy of *E. faecalis* wound infection.

Since **Chapter 3** highlights the importance of *E. faecalis de novo* purine biosynthesis and MptABCD PTS during wound infection, it will be worthwhile to investigate whether *E. faecalis* mutants defective in purine biosynthesis (OG1RF Δ*purEK*) and/or galactose and mannose transport (OG1RF Δ*mptD*) would play a role in mixed-species interactions with *P. aeruginosa* during wound infection **(Chapter 2)**. Additionally, findings in **Chapter 2** and **Chapter 3** suggest the importance of the wound microenvironment during bacterial wound pathogenesis, which can impact the outcome of bacteria-bacteria and/or bacteria-host interactions. Thus, it will be meaningful to analyze the wound metabolome during different phases of wound infection (e.g. acute replication and persistence). This could potentially identify metabolites that are limited (or important) during wound infection as well as the metabolite changes in the wound microenvironment as the infection progresses. Also, combining the metabolomics analysis with our Tn-seq and RNA-seq results, we could possibly reconstruct the *in vivo* metabolic network of *E. faecalis* during wound infection.

4.4 Managing wound infections through the microenvironment

Collectively, the findings in **Chapter 2** and **Chapter 3** highlight the significance of the microenvironment in wound pathogenesis. Several studies have suggested that lowering pH in wounds (e.g. lactic acid) improves wound healing (Haller et al., 2021). Combining this information with the *in vitro* findings in **Chapter 2**, could we inhibit *P. aeruginosa* growth in single- and/or mixed-species wound infections, while simultaneously improve healing by further acidifying the microenvironment to fight infection? For example, the pH of the wound microenvironment can be fine-tuned using a micro-gel during wound

infection (Cui et al., 2022). Moreover, the knowledge gained on nutritional requirements by *E. faecalis* during wound infection in **Chapter 3** can be exploited to fight infection. Can the *E. faecalis de novo* purine biosynthesis and/or MptABCD PTS be inhibited? A drug discovery or drug repurposing approach can be adopted to identify any potential inhibitor(s) that blocks only *E. faecalis* purine biosynthesis and/or galactose and mannose uptake by MptABCD PTS, while having no effect on the host. These inhibitor(s) would likely affect *E. faecalis* capability in colonizing and persisting in the wounds and hence, lowering pathogenicity of *E. faecalis*.

Overall, my dissertation provides insights into how the microenvironment can be manipulated to influence the interactions between *E. faecalis* and *P. aeruginosa*, and how temporal wound microenvironment changes can affect the pathogenic requirements and potential of *E. faecalis* during wound infection. In addition, I have discovered and characterized several *E. faecalis* genetic determinants underlying *E. faecalis* wound pathogenesis and together, these findings can be used as a basis for further studies to explore the possibility of developing inhibitors to target these genetic determinants identified as an alternative treatment option to better manage *E. faecalis* wound infection.

References

Abbas, C. A., & Sibirny, A. A. (2011). Genetic control of biosynthesis and transport of riboflavin and flavin nucleotides and construction of robust biotechnological producers. *Microbiology and Molecular Biology Reviews, 75*(2), 321-360.

Al Mahmud, H., Baishya, J., & Wakeman, C. A. (2021). Interspecies metabolic complementation in cystic fibrosis pathogens via purine exchange. *Pathogens, 10*(2), 146.

Alteri, C. J., Smith, S. N., & Mobley, H. L. (2009). Fitness of *Escherichia coli* during urinary tract infection requires gluconeogenesis and the TCA cycle. *PLoS Pathogens, 5*(5), e1000448.

Anders, S., Pyl, P. T., & Huber, W. (2015). HTSeq—a Python framework to work with high-throughput sequencing data. *Bioinformatics, 31*(2), 166-169.

Andreini, C., Bertini, I., Cavallaro, G., Holliday, G. L., & Thornton, J. M. (2008). Metal ions in biological catalysis: from enzyme databases to general principles. *JBIC Journal of Biological Inorganic Chemistry, 13*(8), 1205-1218.

Arias, C. A., & Murray, B. E. (2012). The rise of the *Enterococcus*: beyond vancomycin resistance. *Nature Reviews Microbiology, 10*(4), 266-278.

Averesch, N. J., & Krömer, J. O. (2018). Metabolic engineering of the shikimate pathway for production of aromatics and derived compounds—present and future strain construction strategies. *Frontiers in bioengineering and biotechnology, 6*, 32.

Bakaletz, L. O. (2004). Developing animal models for polymicrobial diseases. *Nature Reviews Microbiology, 2*(7), 552-568.

Bakaletz, L. O. (2007). Bacterial biofilms in otitis media: evidence and relevance. *The Pediatric Infectious Disease Journal, 26*(10), S17-S19.

Bakaletz, L. O. (2010). Immunopathogenesis of polymicrobial otitis media. *Journal of Leukocyte Biology, 87*(2), 213-222.

Bakar, M. B. A., McKimm, J., & Haque, M. (2018). Otitis media and biofilm: An overview. *International Journal of Nutrition, Pharmacology, Neurological Diseases, 8*(3), 70.

Baker, H. M., & Baker, E. N. (2012). A structural perspective on lactoferrin function. *Biochemistry and Cell Biology, 90*(3), 320-328.

Baldan, R., Cigana, C., Testa, F., Bianconi, I., De Simone, M., Pellin, D., . . . Cirillo, D. M. (2014). Adaptation of *Pseudomonas aeruginosa* in cystic fibrosis airways influences virulence of *Staphylococcus aureus in vitro* and murine models of co-infection. *PloS One, 9*(3), e89614.

Ballén, V., Ratia, C., Cepas, V., & Soto, S. M. (2020). *Enterococcus faecalis* inhibits *Klebsiella pneumoniae* growth in polymicrobial biofilms in a glucose-enriched medium. *Biofouling, 36*(7), 846-861.

Banla, L. I., Pickrum, A. M., Hayward, M., Kristich, C. J., & Salzman, N. H. (2019). Sortase-dependent proteins promote gastrointestinal colonization by enterococci. *Infection and Immunity, 87*(5), e00853-00818.

Barnes, A. M., Dale, J. L., Chen, Y., Manias, D. A., Greenwood Quaintance, K. E., Karau, M. K., . . . Dunny, G. M. (2017). *Enterococcus faecalis* readily

colonizes the entire gastrointestinal tract and forms biofilms in a germ-free mouse model. *Virulence, 8*(3), 282-296.
Barnes, A. M., Frank, K. L., Dale, J. L., Manias, D. A., Powers, J. L., & Dunny, G. M. (2021). *Enterococcus faecalis* colonizes and forms persistent biofilm microcolonies on undamaged endothelial surfaces in a rabbit endovascular infection model. *FEMS microbes, 2*.
Barquist, L., Mayho, M., Cummins, C., Cain, A. K., Boinett, C. J., Page, A. J., . . . Parkhill, J. (2016). The TraDIS toolkit: sequencing and analysis for dense transposon mutant libraries. *Bioinformatics, 32*(7), 1109-1111.
Behnsen, J., Zhi, H., Aron, A. T., Subramanian, V., Santus, W., Lee, M. H., . . . Green, K. D. (2021). Siderophore-mediated zinc acquisition enhances enterobacterial colonization of the inflamed gut. *Nature Communications, 12*(1), 1-15.
Bennison, L., Miller, C., Summers, R., Minnis, A., Sussman, G., & McGuiness, W. (2017). The pH of wounds during healing and infection: a descriptive literature review. *Wound Practice & Research: Journal of the Australian Wound Management Association, 25*(2), 63-69.
Bergqvist, S. W., Sandberg, A.-S., Andlid, T., & Wessling-Resnick, M. (2005). Lactic acid decreases Fe (II) and Fe (III) retention but increases Fe (III) transepithelial transfer by Caco-2 cells. *Journal of Agricultural and Food Chemistry, 53*(17), 6919-6923.
Bharali, P., Saikia, J., Ray, A., & Konwar, B. (2013). Rhamnolipid (RL) from *Pseudomonas aeruginosa* OBP1: a novel chemotaxis and antibacterial agent. *Colloids and Surfaces B: Biointerfaces, 103*, 502-509.
Black, C. E., & Costerton, J. W. (2010). Current concepts regarding the effect of wound microbial ecology and biofilms on wound healing. *Surgical Clinics, 90*(6), 1147-1160.
Black, J. R., Dyer, D., Thompson, M., & Sparling, P. (1986). Human immune response to iron-repressible outer membrane proteins of *Neisseria meningitidis*. *Infection and Immunity, 54*(3), 710-713.
Boukhalfa, H., & Crumbliss, A. L. (2002). Chemical aspects of siderophore mediated iron transport. *Biometals, 15*(4), 325-339.
Bowler, P., Duerden, B., & Armstrong, D. G. (2001). Wound microbiology and associated approaches to wound management. *Clinical Microbiology Reviews, 14*(2), 244-269.
Brandel, J., Humbert, N., Elhabiri, M., Schalk, I. J., Mislin, G. L., & Albrecht-Gary, A.-M. (2012). Pyochelin, a siderophore of *Pseudomonas aeruginosa*: physicochemical characterization of the iron (III), copper (II) and zinc (II) complexes. *Dalton Transactions, 41*(9), 2820-2834.
Braun, V., & Killmann, H. (1999). Bacterial solutions to the iron-supply problem. *Trends in Biochemical Sciences, 24*(3), 104-109.
Brogden, K. A., Guthmiller, J. M., & Taylor, C. E. (2005). Human polymicrobial infections. *The Lancet, 365*(9455), 253-255.
Bushell, F. M., Tonner, P. D., Jabbari, S., Schmid, A. K., & Lund, P. A. (2019). Synergistic impacts of organic acids and pH on growth of *Pseudomonas aeruginosa*: A comparison of parametric and Bayesian non-parametric methods to model growth. *Frontiers in Microbiology, 9*, 3196.
Bushnell, B. (2015). BBMap short-read aligner, and other bioinformatics tools. *University of California, Berkeley, CA*.

Cao, L., Srikumar, R., & Poole, K. (2004). MexAB-OprM hyperexpression in NalC-type multidrug-resistant *Pseudomonas aeruginosa*: identification and characterization of the *nalC* gene encoding a repressor of PA3720-PA3719. *Molecular Microbiology, 53*(5), 1423-1436.

Cao, S., Liu, P., Zhu, H., Gong, H., Yao, J., Sun, Y., . . . Han, M. (2015). Extracellular acidification acts as a key modulator of neutrophil apoptosis and functions. *PloS One, 10*(9), e0137221.

Cassat, J. E., & Skaar, E. P. (2013). Iron in infection and immunity. *Cell Host & Microbe, 13*(5), 509-519.

Castilla, D. M., Liu, Z.-J., & Velazquez, O. C. (2012). Oxygen: implications for wound healing. *Advances in Wound Care, 1*(6), 225-230.

Ch'ng, J.-H., Chong, K. K., Lam, L. N., Wong, J. J., & Kline, K. A. (2019). Biofilm-associated infection by enterococci. *Nature Reviews Microbiology, 17*(2), 82-94.

Ch'ng, J.-H., Muthu, M., Chong, K. K., Wong, J. J., Tan, C. A., Koh, Z. J., . . . Barkham, T. (2022). Heme cross-feeding can augment *Staphylococcus aureus* and *Enterococcus faecalis* dual species biofilms. *The ISME Journal*, 1-12.

Chakraborty, S., Karmakar, K., & Chakravortty, D. (2014). Cells producing their own nemesis: understanding methylglyoxal metabolism. *IUBMB life, 66*(10), 667-678.

Chang, C.-S., & Kao, C.-Y. (2019). Current understanding of the gut microbiota shaping mechanisms. *Journal of Biomedical Science, 26*(1), 1-11.

Chhibber, T., Gondil, V. S., & Sinha, V. (2020). Development of chitosan-based hydrogel containing antibiofilm agents for the treatment of *Staphylococcus aureus*–infected burn wound in mice. *AAPS PharmSciTech, 21*(2), 1-12.

Choi, K.-H., Gaynor, J. B., White, K. G., Lopez, C., Bosio, C. M., Karkhoff-Schweizer, R. R., & Schweizer, H. P. (2005). A Tn7-based broad-range bacterial cloning and expression system. *Nature methods, 2*(6), 443-448.

Choi, K.-H., & Schweizer, H. P. (2006). mini-Tn7 insertion in bacteria with single *att*Tn7 sites: example *Pseudomonas aeruginosa*. *Nature protocols, 1*(1), 153-161.

Chong, K. K. L., Tay, W. H., Janela, B., Yong, A. M. H., Liew, T. H., Madden, L., . . . Becker, D. L. (2017). *Enterococcus faecalis* modulates immune activation and slows healing during wound infection. *The Journal of Infectious Diseases, 216*(12), 1644-1654.

Chow, J., Thal, L., Perri, M., Vazquez, J. A., Donabedian, S., Clewell, D., & Zervos, M. (1993). Plasmid-associated hemolysin and aggregation substance production contribute to virulence in experimental enterococcal endocarditis. *Antimicrobial Agents and Chemotherapy, 37*(11), 2474-2477.

Chuang-Smith, O. N., Wells, C. L., Henry-Stanley, M. J., & Dunny, G. M. (2010). Acceleration of *Enterococcus faecalis* biofilm formation by aggregation substance expression in an *ex vivo* model of cardiac valve colonization. *PloS One, 5*(12), e15798.

Citron, D. M., Goldstein, E. J., Merriam, C. V., Lipsky, B. A., & Abramson, M. A. (2007). Bacteriology of moderate-to-severe diabetic foot infections and *in vitro* activity of antimicrobial agents. *Journal of Clinical Microbiology, 45*(9), 2819-2828.

Coburn, B., Wang, P. W., Caballero, J. D., Clark, S. T., Brahma, V., Donaldson, S., . . . Tullis, D. E. (2015). Lung microbiota across age and disease stage in cystic fibrosis. *Scientific Reports, 5*(1), 1-12.

Colombo, A., & Tanner, A. (2019). The role of bacterial biofilms in dental caries and periodontal and peri-implant diseases: a historical perspective. *Journal of Dental Research, 98*(4), 373-385.

Colombo, A. P. V., Magalhães, C. B., Hartenbach, F. A. R. R., do Souto, R. M., & da Silva-Boghossian, C. M. (2016). Periodontal-disease-associated biofilm: A reservoir for pathogens of medical importance. *Microbial Pathogenesis, 94*, 27-34.

Colombo, A. V., Barbosa, G. M., Higashi, D., di Micheli, G., Rodrigues, P. H., & Simionato, M. R. L. (2013). Quantitative detection of *Staphylococcus aureus*, *Enterococcus faecalis* and *Pseudomonas aeruginosa* in human oral epithelial cells from subjects with periodontitis and periodontal health. *Journal of Medical Microbiology, 62*(10), 1592-1600.

Connolly, J., Boldock, E., Prince, L. R., Renshaw, S. A., Whyte, M. K., & Foster, S. J. (2017). Identification of *Staphylococcus aureus* factors required for pathogenicity and growth in human blood. *Infection and Immunity, 85*(11), e00337-00317.

Cooper, G., & Hausman, R. (2000). The cell: a molecular approach. Sinauer Associates. *Sunderland, MA*.

Cooper, G. M., & Hausman, R. (2000). A molecular approach. *The Cell. 2nd ed. Sunderland, MA: Sinauer Associates*.

Cox, C. D., & Graham, R. (1979). Isolation of an iron-binding compound from *Pseudomonas aeruginosa*. *Journal of Bacteriology, 137*(1), 357-364.

Croxall, G., Weston, V., Joseph, S., Manning, G., Cheetham, P., & McNally, A. (2011). Increased human pathogenic potential of *Escherichia coli* from polymicrobial urinary tract infections in comparison to isolates from monomicrobial culture samples. *Journal of Medical Microbiology, 60*(1), 102-109.

Cui, T., Yu, J., Wang, C. F., Chen, S., Li, Q., Guo, K., . . . Ren, J. (2022). Micro‐gel ensembles for accelerated healing of chronic wound via pH regulation. *Advanced Science, 9*(22), 2201254.

Dalton, T., Dowd, S. E., Wolcott, R. D., Sun, Y., Watters, C., Griswold, J. A., & Rumbaugh, K. P. (2011). An *in vivo* polymicrobial biofilm wound infection model to study interspecies interactions. *PloS One, 6*(11).

Darveau, R. P. (2010). Periodontitis: a polymicrobial disruption of host homeostasis. *Nature Reviews Microbiology, 8*(7), 481-490.

Davies, C. E., Hill, K. E., Newcombe, R. G., Stephens, P., Wilson, M. J., Harding, K. G., & Thomas, D. W. (2007). A prospective study of the microbiology of chronic venous leg ulcers to reevaluate the clinical predictive value of tissue biopsies and swabs. *Wound Repair and Regeneration, 15*(1), 17-22.

del Mar Cendra, M., & Torrents, E. (2021). *Pseudomonas aeruginosa* biofilms and their partners in crime. *Biotechnology advances, 49*, 107734.

Delcaru, C., Alexandru, I., Podgoreanu, P., Grosu, M., Stavropoulos, E., Chifiriuc, M. C., & Lazar, V. (2016). Microbial biofilms in urinary tract infections and prostatitis: etiology, pathogenicity, and combating strategies. *Pathogens, 5*(4), 65.

DeLeon, S., Clinton, A., Fowler, H., Everett, J., Horswill, A. R., & Rumbaugh, K. P. (2014). Synergistic interactions of *Pseudomonas aeruginosa* and *Staphylococcus aureus* in an *in vitro* wound model. *Infection and Immunity, 82*(11), 4718-4728.

Demidova-Rice, T. N., Hamblin, M. R., & Herman, I. M. (2012). Acute and impaired wound healing: pathophysiology and current methods for drug delivery, part 1: normal and chronic wounds: biology, causes, and approaches to care. *Advances in skin & wound care, 25*(7), 304.

Deutscher, J., Francke, C., & Postma, P. W. (2006). How phosphotransferase system-related protein phosphorylation regulates carbohydrate metabolism in bacteria. *Microbiology and Molecular Biology Reviews, 70*(4), 939-1031.

Donlan, R. M., & Costerton, J. W. (2002). Biofilms: survival mechanisms of clinically relevant microorganisms. *Clinical Microbiology Reviews, 15*(2), 167-193.

Dowd, S. E., Sun, Y., Secor, P. R., Rhoads, D. D., Wolcott, B. M., James, G. A., & Wolcott, R. D. (2008). Survey of bacterial diversity in chronic wounds using Pyrosequencing, DGGE, and full ribosome shotgun sequencing. *BMC Microbiology, 8*(1), 43.

Dumas, Z., Ross-Gillespie, A., & Kümmerli, R. (2013). Switching between apparently redundant iron-uptake mechanisms benefits bacteria in changeable environments. *Proceedings of the Royal Society B: Biological Sciences, 280*(1764), 20131055.

Dunny, G. M., Brown, B. L., & Clewell, D. B. (1978). Induced cell aggregation and mating in *Streptococcus faecalis*: evidence for a bacterial sex pheromone. *Proceedings of the National Academy of Sciences, 75*(7), 3479-3483.

Dupont, H., Montravers, P., Mohler, J., & Carbon, C. (1998). Disparate findings on the role of virulence factors of *Enterococcus faecalis* in mouse and rat models of peritonitis. *Infection and Immunity, 66*(6), 2570-2575.

Dworniczek, E., Piwowarczyk, J., Bania, J., Kowalska-Krochmal, B., Wałecka, E., Seniuk, A., . . . Gościniak, G. (2012). *Enterococcus* in wound infections: virulence and antimicrobial resistance. *Acta Microbiologica et Immunologica Hungarica, 59*(2), 263-269.

Ebright, J. R. (2005). Microbiology of chronic leg and pressure ulcers: clinical significance and implications for treatment. *Nursing Clinics, 40*(2), 207-216.

Engelbert, M., Mylonakis, E., Ausubel, F. M., Calderwood, S. B., & Gilmore, M. S. (2004). Contribution of gelatinase, serine protease, and *fsr* to the pathogenesis of *Enterococcus faecalis* endophthalmitis. *Infection and Immunity, 72*(6), 3628-3633.

Eyal, A. M., & Canari, R. (1995). pH dependence of carboxylic and mineral acid extraction by amine-based extractants: effects of pKa, amine basicity, and diluent properties. *Industrial & Engineering Chemistry Research, 34*(5), 1789-1798.

Fallingborg, J. (1999). Intraluminal pH of the human gastrointestinal tract. *Danish medical bulletin, 46*(3), 183-196.

Featherstone, J., & Rodgers, B. (1981). Effect of acetic, lactic and other organic acids on the formation of artificial carious lesions. *Caries Research, 15*(5), 377-385.

Feldman-Salit, A., Hering, S., Messiha, H. L., Veith, N., Cojocaru, V., Sieg, A., . . . Fiedler, T. (2013). Regulation of the activity of lactate dehydrogenases from four lactic acid bacteria. *Journal of Biological Chemistry, 288*(29), 21295-21306.

Ferrando, M. L., van Baarlen, P., Orru, G., Piga, R., Bongers, R. S., Wels, M., . . . Wells, J. M. (2014). Carbohydrate availability regulates virulence gene expression in *Streptococcus suis*. *PloS One, 9*(3), e89334.

Filkins, L., Hampton, T., Gifford, A., Gross, M., Hogan, D., Sogin, M., . . . O'Toole, G. (2012). Prevalence of streptococci and increased polymicrobial diversity associated with cystic fibrosis patient stability. *Journal of Bacteriology, 194*(17), 4709-4717.

Fisher, K., & Phillips, C. (2009). The ecology, epidemiology and virulence of *Enterococcus*. *Microbiology, 155*(6), 1749-1757.

Flahaut, S., Hartke, A., Giard, J.-C., Benachour, A., Boutibonnes, P., & Auffray, Y. (1996). Relationship between stress response towards bile salts, acid and heat treatment in *Enterococcus faecalis*. *FEMS microbiology letters, 138*(1), 49-54.

Flemming, H.-C., Wingender, J., Szewzyk, U., Steinberg, P., Rice, S. A., & Kjelleberg, S. (2016). Biofilms: an emergent form of bacterial life. *Nature Reviews Microbiology, 14*(9), 563-575.

Flores-Mireles, A. L., Pinkner, J. S., Caparon, M. G., & Hultgren, S. J. (2014). EbpA vaccine antibodies block binding of *Enterococcus faecalis* to fibrinogen to prevent catheter-associated bladder infection in mice. *Science translational medicine, 6*(254), 254ra127-254ra127.

Frank, D. N., Wysocki, A., Specht‐Glick, D. D., Rooney, A., Feldman, R. A., St. Amand, A. L., . . . Trent, J. D. (2009). Microbial diversity in chronic open wounds. *Wound Repair and Regeneration, 17*(2), 163-172.

Frank, K. L., Colomer-Winter, C., Grindle, S. M., Lemos, J. A., Schlievert, P. M., & Dunny, G. M. (2014). Transcriptome analysis of *Enterococcus faecalis* during mammalian infection shows cells undergo adaptation and exist in a stringent response state. *PloS One, 9*(12), e115839.

Frawley, E. R., & Fang, F. C. (2014). The ins and outs of bacterial iron metabolism. *Molecular Microbiology, 93*(4), 609-616.

Garbe, J., Sjögren, J., Cosgrave, E. F., Struwe, W. B., Bober, M., Olin, A. I., . . . Collin, M. (2014). EndoE from *Enterococcus faecalis* hydrolyzes the glycans of the biofilm inhibiting protein lactoferrin and mediates growth. *PloS One, 9*(3), e91035.

Garnett, J. P., Braun, D., McCarthy, A. J., Farrant, M. R., Baker, E. H., Lindsay, J. A., & Baines, D. L. (2014). Fructose transport-deficient *Staphylococcus aureus* reveals important role of epithelial glucose transporters in limiting sugar-driven bacterial growth in airway surface liquid. *Cellular and Molecular Life Sciences, 71*(23), 4665-4673.

Garsin, D. A., Sifri, C. D., Mylonakis, E., Qin, X., Singh, K. V., Murray, B. E., . . . Ausubel, F. M. (2001). A simple model host for identifying Gram-positive virulence factors. *Proceedings of the National Academy of Sciences, 98*(19), 10892-10897.

Gethin, G. (2007). The significance of surface pH in chronic wounds. *Wounds uk, 3*(3), 52.

Ghio, C., Soukup, J. M., Dailey, L. A., Ghio, A. J., Schreinemachers, D. M., Koppes, R. A., & Koppes, A. N. (2021). Lactate production can function to increase human epithelial cell iron concentration. *BioRxiv*.

Giacometti, A., Cirioni, O., Schimizzi, A., Del Prete, M., Barchiesi, F., D'errico, M., . . . Scalise, G. (2000). Epidemiology and microbiology of surgical wound infections. *Journal of Clinical Microbiology, 38*(2), 918-922.

Gitton, C., Meyrand, M., Wang, J., Caron, C., Trubuil, A., Guillot, A., & Mistou, M.-Y. (2005). Proteomic signature of *Lactococcus lactis* NCDO763 cultivated in milk. *Applied and environmental microbiology, 71*(11), 7152-7163.

Gjødsbøl, K., Christensen, J. J., Karlsmark, T., Jørgensen, B., Klein, B. M., & Krogfelt, K. A. (2006). Multiple bacterial species reside in chronic wounds: a longitudinal study. *International Wound Journal, 3*(3), 225-231.

Gokulan, K., Khare, S., & Cerniglia, C. (2014). Metabolic pathways | Production of secondary metabolites of bacteria. In C. A. Batt & M. L. Tortorello (Eds.), *Encyclopedia of Food Microbiology (Second Edition)* (pp. 561-569). Oxford: Academic Press.

Goncheva, M. I., Flannagan, R. S., & Heinrichs, D. E. (2020). *De novo* purine biosynthesis is required for intracellular growth of *Staphylococcus aureus* and for the hypervirulence phenotype of a *purR* mutant. *Infection and Immunity, 88*(5), e00104-00120.

Gonzalez, M. I., Alvarez, S., Riera, F. A., & Álvarez, R. (2008). Lactic acid recovery from whey ultrafiltrate fermentation broths and artificial solutions by nanofiltration. *Desalination, 228*(1-3), 84-96.

Gorman, J., & Clydesdale, F. (1984). Thermodynamic and kinetic stability constants of selected carboxylic acids and iron. *Journal of Food Science, 49*(2), 500-503.

Grigg, J. C., Ukpabi, G., Gaudin, C. F., & Murphy, M. E. (2010). Structural biology of heme binding in the *Staphylococcus aureus* Isd system. *Journal of Inorganic Biochemistry, 104*(3), 341-348.

Guardabassi, L., Larsen, J., Skov, R., & Schønheyder, H. C. (2010). Gentamicin-resistant *Enterococcus faecalis* sequence type 6 with reduced penicillin susceptibility: diagnostic and therapeutic implications. *Journal of Clinical Microbiology, 48*(10), 3820-3821.

Guiton, P. S., Hung, C. S., Hancock, L. E., Caparon, M. G., & Hultgren, S. J. (2010). Enterococcal biofilm formation and virulence in an optimized murine model of foreign body-associated urinary tract infections. *Infection and Immunity, 78*(10), 4166-4175.

Gutschik, E., MØller, S., & Christensen, N. (1979). Experimental endocarditis in rabbits: 3. significance of the proteolytic capacity of the infecting strains of *Streptococcus faecalis*. *Acta Pathologica Microbiologica Scandinavica Section B Microbiology, 87*(1-6), 353-362.

Hall-Stoodley, L., & Stoodley, P. (2009). Evolving concepts in biofilm infections. *Cellular Microbiology, 11*(7), 1034-1043.

Haller, H. L., Sander, F., Popp, D., Rapp, M., Hartmann, B., Demircan, M., . . . Kamolz, L. P. (2021). Oxygen, pH, lactate, and metabolism—How old knowledge and new insights might be combined for new wound treatment. *Medicina, 57*(11), 1190.

Hammer, N. D., & Skaar, E. P. (2011). Molecular mechanisms of *Staphylococcus aureus* iron acquisition. *Annual Review of Microbiology, 65*, 129-147.

Hampton, S. (2008). Understanding the pH balance in wound healing. *Journal of Community Nursing, 22*(5), 34-37.

Hancock, L. E., & Perego, M. (2004). The *Enterococcus faecalis fsr* two-component system controls biofilm development through production of gelatinase. *Journal of Bacteriology, 186*(17), 5629-5639.

Harold, F. M., & Levin, E. (1974). Lactic acid translocation: terminal step in glycolysis by *Streptococcus faecalis*. *Journal of Bacteriology, 117*(3), 1141-1148.

Harrison‐Balestra, C., Cazzaniga, A. L., Davis, S. C., & Mertz, P. M. (2003). A wound‐isolated *Pseudomonas aeruginosa* grows a biofilm in vitro within 10 hours and is visualized by light microscopy. *Dermatologic Surgery, 29*(6), 631-635.

Hassan, H. M., & Troxell, B. (2013). Transcriptional regulation by Ferric Uptake Regulator (Fur) in pathogenic bacteria. *Frontiers in Cellular and Infection Microbiology, 3*, 59.

Hatt, J., & Rather, P. (2008). Role of bacterial biofilms in urinary tract infections. *Bacterial Biofilms*, 163-192.

Hava, D. L., & Camilli, A. (2002). Large‐scale identification of serotype 4 *Streptococcus pneumoniae* virulence factors. *Molecular Microbiology, 45*(5), 1389-1406.

Heming, T. A., Davé, S. K., Tuazon, D. M., Chopra, A. K., Peterson, J. W., & Bidani, A. (2001). Effects of extracellular pH on tumour necrosis factor-α production by resident alveolar macrophages. *Clinical science, 101*(3), 267-274.

Hentzer, M., Riedel, K., Rasmussen, T. B., Heydorn, A., Andersen, J. B., Parsek, M. R., . . . Høiby, N. (2002). Inhibition of quorum sensing in *Pseudomonas aeruginosa* biofilm bacteria by a halogenated furanone compound. *Microbiology, 148*(1), 87-102.

Herrmann, K. M., & Weaver, L. M. (1999). The shikimate pathway. *Annual review of plant biology, 50*(1), 473-503.

Hidron, A. I., Edwards, J. R., Patel, J., Horan, T. C., Sievert, D. M., Pollock, D. A., & Fridkin, S. K. (2008). Antimicrobial-resistant pathogens associated with healthcare-associated infections: annual summary of data reported to the National Healthcare Safety Network at the Centers for Disease Control and Prevention, 2006–2007. *Infection Control & Hospital Epidemiology, 29*(11), 996-1011.

Higuita, N. I. A., & Huycke, M. M. (2014). Enterococcal disease, epidemiology, and implications for treatment. *Enterococci: From commensals to leading causes of drug resistant infection (BioProject [Internet]. Bethesda (MD): National Library of Medicine (US))*: Massachusetts Eye and Ear Infirmary.

Hoffman, R., Noble, J., & Eagle, M. (1999). The use of proteases as prognostic markers for the healing of venous leg ulcers. *Journal of Wound Care, 8*(6), 273-276.

Hoffmann, J. P., Friedman, J. K., Wang, Y., McLachlan, J. B., Sammarco, M. C., Morici, L. A., & Roy, C. J. (2020). *In situ* treatment with novel microbiocide inhibits methicillin resistant *Staphylococcus aureus* in a murine wound infection model. *Frontiers in Microbiology, 10*, 3106.

Høiby, N. (2002). Understanding bacterial biofilms in patients with cystic fibrosis: current and innovative approaches to potential therapies. *Journal of Cystic Fibrosis, 1*(4), 249-254.
Høiby, N., Ciofu, O., & Bjarnsholt, T. (2010). *Pseudomonas aeruginosa* biofilms in cystic fibrosis. *Future Microbiology, 5*(11), 1663-1674.
Hollenbeck, B. L., & Rice, L. B. (2012). Intrinsic and acquired resistance mechanisms in *Enterococcus*. *Virulence, 3*(5), 421-569.
Hung, C.-S., Dodson, K. W., & Hultgren, S. J. (2009). A murine model of urinary tract infection. *Nature protocols, 4*(8), 1230-1243.
Hunt, T. K., & Beckert, S. (2005). Therapeutical and practical aspects of oxygen in wound healing. *The Wound Management Manual. McGraw-Hill Medical, New York*.
Ike, Y., Craig, R. A., White, B. A., Yagi, Y., & Clewell, D. B. (1983). Modification of *Streptococcus faecalis* sex pheromones after acquisition of plasmid DNA. *Proceedings of the National Academy of Sciences, 80*(17), 5369-5373. doi:10.1073/pnas.80.17.5369
Imperi, F., Massai, F., Facchini, M., Frangipani, E., Visaggio, D., Leoni, L., . . . Visca, P. (2013). Repurposing the antimycotic drug flucytosine for suppression of *Pseudomonas aeruginosa* pathogenicity. *Proceedings of the National Academy of Sciences, 110*(18), 7458-7463.
Iyer, R., & Camilli, A. (2007). Sucrose metabolism contributes to *in vivo* fitness of *Streptococcus pneumoniae*. *Molecular Microbiology, 66*(1), 1-13.
Jabado, N., Jankowski, A., Dougaparsad, S., Picard, V., Grinstein, S., & Gros, P. (2000). Natural resistance to intracellular infections: natural resistance–associated macrophage protein 1 (Nramp1) functions as a pH-dependent manganese transporter at the phagosomal membrane. *The Journal of Experimental Medicine, 192*(9), 1237-1248.
Jamal, M., Ahmad, W., Andleeb, S., Jalil, F., Imran, M., Nawaz, M. A., . . . Kamil, M. A. (2018). Bacterial biofilm and associated infections. *Journal of the chinese medical association, 81*(1), 7-11.
James, G. A., Swogger, E., Wolcott, R., Pulcini, E. d., Secor, P., Sestrich, J., . . . Stewart, P. S. (2008). Biofilms in chronic wounds. *Wound Repair and Regeneration, 16*(1), 37-44.
Jendresen, C. B., Martinussen, J., & Kilstrup, M. (2012). The PurR regulon in *Lactococcus lactis*–transcriptional regulation of the purine nucleotide metabolism and translational machinery. *Microbiology, 158*(8), 2026-2038.
Jensen, K. F., Dandanell, G., Hove-Jensen, B., & WillemoËs, M. (2008). Nucleotides, nucleosides, and nucleobases. *EcoSal Plus, 3*(1).
Jett, B., Jensen, H., Nordquist, R., & Gilmore, M. (1992). Contribution of the pAD1-encoded cytolysin to the severity of experimental *Enterococcus faecalis* endophthalmitis. *Infection and Immunity, 60*(6), 2445-2452.
Johnson, J. R., Clabots, C., Hirt, H., Waters, C., & Dunny, G. (2004). Enterococcal aggregation substance and binding substance are not major contributors to urinary tract colonization by *Enterococcus faecalis* in a mouse model of ascending unobstructed urinary tract infection. *Infection and Immunity, 72*(4), 2445-2448.
Jönsson, M., Saleihan, Z., Nes, I. F., & Holo, H. (2009). Construction and characterization of three lactate dehydrogenase-negative *Enterococcus faecalis* V583 mutants. *Appl. Environ. Microbiol., 75*(14), 4901-4903.

Jorth, P., Trivedi, U., Rumbaugh, K., & Whiteley, M. (2013). Probing bacterial metabolism during infection using high-resolution transcriptomics. *Journal of Bacteriology, 195*(22), 4991-4998.

Kaes, C., Katz, A., & Hosseini, M. W. (2000). Bipyridine: the most widely used ligand. A review of molecules comprising at least two 2,2'-bipyridine units. *Chemical Reviews, 100*(10), 3553-3590.

Kammler, M., Schön, C., & Hantke, K. (1993). Characterization of the ferrous iron uptake system of *Escherichia coli*. *Journal of Bacteriology, 175*(19), 6212-6219.

Kanehisa, M., & Goto, S. (2000). KEGG: kyoto encyclopedia of genes and genomes. *Nucleic Acids Research, 28*(1), 27-30.

Kang, D., Kirienko, D. R., Webster, P., Fisher, A. L., & Kirienko, N. V. (2018). Pyoverdine, a siderophore from *Pseudomonas aeruginosa*, translocates into *C. elegans*, removes iron, and activates a distinct host response. *Virulence, 9*(1), 804-817.

Kang, D., & Kirienko, N. V. (2017). High-throughput genetic screen reveals that early attachment and biofilm formation are necessary for full pyoverdine production by *Pseudomonas aeruginosa*. *Frontiers in Microbiology, 8*, 1707.

Kemp, K. D., Singh, K. V., Nallapareddy, S. R., & Murray, B. E. (2007). Relative contributions of *Enterococcus faecalis* OG1RF sortase-encoding genes, *srtA* and *bps* (*srtC*), to biofilm formation and a murine model of urinary tract infection. *Infection and Immunity, 75*(11), 5399-5404.

Keogh, D., Tay, W., Ho, Y., Dale, J., Chen, S., Umashankar, S., . . . Kline, K. (2016). Enterococcal metabolite cues facilitate interspecies niche modulation and polymicrobial infection. *Cell Host & Microbe, 20*(4), 493-503.

Kilstrup, M., Hammer, K., Ruhdal Jensen, P., & Martinussen, J. (2005). Nucleotide metabolism and its control in lactic acid bacteria. *FEMS Microbiology Reviews, 29*(3), 555-590.

Kilstrup, M., & Martinussen, J. (1998). A transcriptional activator, homologous to the *Bacillus subtilis* PurR repressor, is required for expression of purine biosynthetic genes in *Lactococcus lactis*. *Journal of bacteriology, 180*(15), 3907-3916.

Kim, Y. R., Lee, S. E., Kim, C. M., Kim, S. Y., Shin, E. K., Shin, D. H., . . . Hillman, J. D. (2003). Characterization and pathogenic significance of *Vibrio vulnificus* antigens preferentially expressed in septicemic patients. *Infection and Immunity, 71*(10), 5461-5471.

Kirienko, N. V., Ausubel, F. M., & Ruvkun, G. (2015). Mitophagy confers resistance to siderophore-mediated killing by *Pseudomonas aeruginosa*. *Proceedings of the National Academy of Sciences, 112*(6), 1821-1826.

Kline, K. A., & Lewis, A. L. (2016). Gram-positive uropathogens, polymicrobial urinary tract infection, and the emerging microbiota of the urinary tract. *Microbiology spectrum, 4*(2), 4.2. 04.

Kovach, K., Davis-Fields, M., Irie, Y., Jain, K., Doorwar, S., Vuong, K., . . . Gordon, V. D. (2017). Evolutionary adaptations of biofilms infecting cystic fibrosis lungs promote mechanical toughness by adjusting polysaccharide production. *NPJ Biofilms and Microbiomes, 3*(1), 1-9.

Kriebel, K., Hieke, C., Müller-Hilke, B., Nakata, M., & Kreikemeyer, B. (2018). Oral biofilms from symbiotic to pathogenic interactions and associated

disease–connection of periodontitis and rheumatic arthritis by peptidylarginine deiminase. *Frontiers in Microbiology, 9*, 53.
Kristich, C. J., Nguyen, V. T., Le, T., Barnes, A. M., Grindle, S., & Dunny, G. M. (2008). Development and use of an efficient system for random mariner transposon mutagenesis to identify novel genetic determinants of biofilm formation in the core *Enterococcus faecalis* genome. *Applied and Environmental Microbiology, 74*(11), 3377-3386.
Kristich, C. J., Rice, L. B., & Arias, C. A. (2014). Enterococcal infection—treatment and antibiotic resistance. *Enterococci: From commensals to leading causes of drug resistant infection (BioProject [Internet]. Bethesda (MD): National Library of Medicine (US))*: Massachusetts Eye and Ear Infirmary.
Kuchina, A., Brettner, L. M., Paleologu, L., Roco, C. M., Rosenberg, A. B., Carignano, A., . . . Seelig, G. (2021). Microbial single-cell RNA sequencing by split-pool barcoding. *Science, 371*(6531), eaba5257.
Lagendijk, E. L., Validov, S., Lamers, G. E., De Weert, S., & Bloemberg, G. V. (2010). Genetic tools for tagging Gram-negative bacteria with mCherry for visualization *in vitro* and in natural habitats, biofilm and pathogenicity studies. *FEMS Microbiology Letters, 305*(1), 81-90.
Lam, L. N., Wong, J. J., Chong, K. K. L., & Kline, K. A. (2020). *Enterococcus faecalis* manganese exporter MntE alleviates manganese toxicity and is required for mouse gastrointestinal colonization. *Infection and Immunity, 88*(6).
Lamont, I. L., Konings, A. F., & Reid, D. W. (2009). Iron acquisition by *Pseudomonas aeruginosa* in the lungs of patients with cystic fibrosis. *Biometals, 22*(1), 53-60.
Lardner, A. (2001). The effects of extracellular pH on immune function. *Journal of Leukocyte Biology, 69*(4), 522-530.
Lasserre, J. F., Brecx, M. C., & Toma, S. (2018). Oral microbes, biofilms and their role in periodontal and peri-implant diseases. *Materials, 11*(10), 1802.
Latorre, M., Quenti, D., Travisany, D., Singh, K. V., Murray, B. E., Maass, A., & Cambiazo, V. (2018). The role of Fur in the transcriptional and iron homeostatic response of *Enterococcus faecalis*. *Frontiers in Microbiology, 9*, 1580.
Le Breton, Y., Mistry, P., Valdes, K. M., Quigley, J., Kumar, N., Tettelin, H., & McIver, K. S. (2013). Genome-wide identification of genes required for fitness of group A *Streptococcus* in human blood. *Infection and Immunity, 81*(3), 862-875.
Leboeuf, C., Leblanc, L., Auffray, Y., & Hartke, A. (2000). Characterization of the *ccpA* gene of *Enterococcus faecalis*: identification of starvation-inducible proteins regulated by CcpA. *Journal of Bacteriology, 182*(20), 5799-5806.
Lebreton, F., Riboulet-Bisson, E., Serror, P., Sanguinetti, M., Posteraro, B., Torelli, R., . . . Giard, J.-C. (2009). *ace*, which encodes an adhesin in *Enterococcus faecalis*, is regulated by Ers and is involved in virulence. *Infection and Immunity, 77*(7), 2832-2839.
Lee, K., Lee, K.-M., Kim, D., & Yoon, S. S. (2017). Molecular determinants of the thickened matrix in a dual-species *Pseudomonas aeruginosa* and

Enterococcus faecalis biofilm. *Applied and Environmental Microbiology, 83*(21).

Legrain, M., Mazarin, V., Irwin, S. W., Bouchon, B., Quentin-Millet, M.-J., Jacobs, E., & Schryvers, A. B. (1993). Cloning and characterization of *Neisseria meningitidis* genes encoding the transferrin-binding proteins Tbp1 and Tbp2. *Gene, 130*(1), 73-80.

Leveen, H. H., Falk, G., Borek, B., Diaz, C., Lynfield, Y., Wynkoop, B. J., . . . Christoudias, G. C. (1973). Chemical acidification of wounds. An adjuvant to healing and the unfavorable action of alkalinity and ammonia. *Annals of surgery, 178*(6), 745.

Li, H., & Durbin, R. (2009). Fast and accurate short read alignment with Burrows–Wheeler transform. *Bioinformatics, 25*(14), 1754-1760.

Li, L., Abdelhady, W., Donegan, N. P., Seidl, K., Cheung, A., Zhou, Y.-F., . . . Xiong, Y. Q. (2018). Role of purine biosynthesis in persistent methicillin-resistant *Staphylococcus aureus* infection. *The Journal of Infectious Diseases, 218*(9), 1367-1377.

Limoli, D. H., & Hoffman, L. R. (2019). Help, hinder, hide and harm: what can we learn from the interactions between *Pseudomonas aeruginosa* and *Staphylococcus aureus* during respiratory infections? *Thorax, 74*(7), 684-692.

Lindenstrauß, A. G., Ehrmann, M. A., Behr, J., Landstorfer, R., Haller, D., Sartor, R. B., & Vogel, R. F. (2014). Transcriptome analysis of *Enterococcus faecalis* toward its adaption to surviving in the mouse intestinal tract. *Archives of microbiology, 196*(6), 423-433.

Lund, P., Tramonti, A., & De Biase, D. (2014). Coping with low pH: molecular strategies in neutralophilic bacteria. *FEMS Microbiology Reviews, 38*(6), 1091-1125.

Lund, P. A., De Biase, D., Liran, O., Scheler, O., Mira, N. P., Cetecioglu, Z., . . . Sauer, M. (2020). Understanding how microorganisms respond to acid pH is central to their control and successful exploitation. *Frontiers in Microbiology, 11*, 2233.

Lyczak, J. B., Cannon, C. L., & Pier, G. B. (2002). Lung infections associated with cystic fibrosis. *Clinical Microbiology Reviews, 15*(2), 194-222.

Machan, Z. A., Taylor, G. W., Pitt, T. L., Cole, P. J., & Wilson, R. (1992). 2-Heptyl-4-hydroxyquinoline N-oxide, an antistaphylococcal agent produced by *Pseudomonas aeruginosa*. *Journal of Antimicrobial Chemotherapy, 30*(5), 615-623.

Mäkinen, P., Clewell, D., An, F., & Mäkinen, K. (1989). Purification and substrate specificity of a strongly hydrophobic extracellular metalloendopeptidase ("gelatinase") from *Streptococcus faecalis* (strain 0G1-10). *Journal of Biological Chemistry, 264*(6), 3325-3334.

Mandlik, A., Livny, J., Robins, W. P., Ritchie, J. M., Mekalanos, J. J., & Waldor, M. K. (2011). RNA-Seq-based monitoring of infection-linked changes in *Vibrio cholerae* gene expression. *Cell Host & Microbe, 10*(2), 165-174.

Marion, C., Limoli, D. H., Bobulsky, G. S., Abraham, J. L., Burnaugh, A. M., & King, S. J. (2009). Identification of a pneumococcal glycosidase that modifies O-linked glycans. *Infection and Immunity, 77*(4), 1389-1396.

Marion, C., Stewart, J. M., Tazi, M. F., Burnaugh, A. M., Linke, C. M., Woodiga, S. A., & King, S. J. (2012). *Streptococcus pneumoniae* can utilize multiple

sources of hyaluronic acid for growth. *Infection and Immunity, 80*(4), 1390-1398.
Marom, T., Nokso-Koivisto, J., & Chonmaitree, T. (2012). Viral–bacterial interactions in acute otitis media. *Current Allergy and Asthma Reports, 12*(6), 551-558.
Martínez, D., Vermeulen, M., Trevani, A., Ceballos, A., Sabatté, J., Gamberale, R., . . . Coso, O. A. (2006). Extracellular acidosis induces neutrophil activation by a mechanism dependent on activation of phosphatidylinositol 3-kinase/Akt and ERK pathways. *The Journal of Immunology, 176*(2), 1163-1171.
Masson, P., Heremans, J., & Schonne, E. (1969). Lactoferrin, an iron-binbing protein Ni neutrophilic leukocytes. *The Journal of Experimental Medicine, 130*(3), 643-658.
McBride, S. M., Fischetti, V. A., LeBlanc, D. J., Moellering Jr, R. C., & Gilmore, M. S. (2007). Genetic diversity among *Enterococcus faecalis*. *PloS One, 2*(7), e582.
Mehmeti, I., Faergestad, E. M., Bekker, M., Snipen, L., Nes, I. F., & Holo, H. (2012). Growth rate-dependent control in *Enterococcus faecalis*: effects on the transcriptome and proteome, and strong regulation of lactate dehydrogenase. *Applied and Environmental Microbiology, 78*(1), 170-176.
Mei, J. M., Nourbakhsh, F., Ford, C. W., & Holden, D. W. (1997). Identification of *Staphylococcus aureus* virulence genes in a murine model of bacteraemia using signature‐tagged mutagenesis. *Molecular Microbiology, 26*(2), 399-407.
Mertz, P. M. (2003). Cutaneous biofilms: friend or foe? *Wounds, 15*, 129-132.
Meyer, J.-M., Neely, A., Stintzi, A., Georges, C., & Holder, I. A. (1996). Pyoverdin is essential for virulence of *Pseudomonas aeruginosa*. *Infection and Immunity, 64*(2), 518-523.
Milne, S. D., & Connolly, P. (2014). The influence of different dressings on the pH of the wound environment. *Journal of Wound Care, 23*(2), 53-57.
Minandri, F., Imperi, F., Frangipani, E., Bonchi, C., Visaggio, D., Facchini, M., . . . Visca, P. (2016). Role of iron uptake systems in *Pseudomonas aeruginosa* virulence and airway infection. *Infection and Immunity, 84*(8), 2324-2335.
Minhas, V., Paton, J. C., & Trappetti, C. (2021). Sickly sweet–how sugar utilization impacts pneumococcal disease progression. *Trends in Microbiology, 29*(9), 768-771.
Miyazaki, S., Ohno, A., Kobayashi, I., Uji, T., Yamaguchi, K., & Goto, S. (1993). Cytotoxic effect of hemolytic culture supernatant from *Enterococcus faecalis* on mouse polymorphonuclear neutrophils and macrophages. *Microbiology and Immunology, 37*(4), 265-270.
Miyazawa, K., & Inoue, K. (1990). Complement activation induced by human C-reactive protein in mildly acidic conditions. *The Journal of Immunology, 145*(2), 650-654.
Mobley, H., & Warren, J. W. (1987). Urease-positive bacteriuria and obstruction of long-term urinary catheters. *Journal of Clinical Microbiology, 25*(11), 2216-2217.
Mohamed, J. A., Huang, W., Nallapareddy, S. R., Teng, F., & Murray, B. E. (2004). Influence of origin of isolates, especially endocarditis isolates,

and various genes on biofilm formation by *Enterococcus faecalis*. *Infection and Immunity, 72*(6), 3658-3663.
Mottola, C., Mendes, J. J., Cristino, J. M., Cavaco-Silva, P., Tavares, L., & Oliveira, M. (2016). Polymicrobial biofilms by diabetic foot clinical isolates. *Folia Microbiologica, 61*(1), 35-43.
Naginyte, M., Do, T., Meade, J., Devine, D. A., & Marsh, P. D. (2019). Enrichment of periodontal pathogens from the biofilms of healthy adults. *Scientific Reports, 9*(1), 1-9.
Nakagawa, Y., Negishi, Y., Shimizu, M., Takahashi, M., Ichikawa, M., & Takahashi, H. (2015). Effects of extracellular pH and hypoxia on the function and development of antigen-specific cytotoxic T lymphocytes. *Immunology letters, 167*(2), 72-86.
Nallapareddy, S. R., & Murray, B. E. (2008). Role played by serum, a biological cue, in the adherence of *Enterococcus faecalis* to extracellular matrix proteins, collagen, fibrinogen, and fibronectin. *Journal of Infectious Diseases, 197*(12), 1728-1736.
Nallapareddy, S. R., Sillanpää, J., Mitchell, J., Singh, K. V., Chowdhury, S. A., Weinstock, G. M., . . . Murray, B. E. (2011). Conservation of Ebp-type pilus genes among enterococci and demonstration of their role in adherence of *Enterococcus faecalis* to human platelets. *Infection and Immunity, 79*(7), 2911-2920.
Nallapareddy, S. R., Singh, K. V., Sillanpää, J., Garsin, D. A., Höök, M., Erlandsen, S. L., & Murray, B. E. (2006). Endocarditis and biofilm-associated pili of *Enterococcus faecalis*. *The Journal of Clinical Investigation, 116*(10), 2799-2807.
Nallapareddy, S. R., Singh, K. V., Sillanpää, J., Zhao, M., & Murray, B. E. (2011). Relative contributions of Ebp Pili and the collagen adhesin *ace* to host extracellular matrix protein adherence and experimental urinary tract infection by *Enterococcus faecalis* OG1RF. *Infection and Immunity, 79*(7), 2901-2910.
Nelson, A., De Soyza, A., Perry, J. D., Sutcliffe, I. C., & Cummings, S. P. (2012). Polymicrobial challenges to Koch's postulates: ecological lessons from the bacterial vaginosis and cystic fibrosis microbiomes. *Innate Immunity, 18*(5), 774-783.
Nielsen, H. V., Guiton, P. S., Kline, K. A., Port, G. C., Pinkner, J. S., Neiers, F., . . . Hultgren, S. J. (2012). The metal ion-dependent adhesion site motif of the *Enterococcus faecalis* EbpA pilin mediates pilus function in catheter-associated urinary tract infection. *MBio, 3*(4), e00177-00112.
O'Hanlon, D. E., Come, R. A., & Moench, T. R. (2019). Vaginal pH measured *in vivo*: lactobacilli determine pH and lactic acid concentration. *BMC Microbiology, 19*(1), 1-8.
Ochsner, U. A., Johnson, Z., & Vasil, M. L. (2000). Genetics and regulation of two distinct haem-uptake systems, *phu* and *has*, in *Pseudomonas aeruginosa*. *Microbiology, 146*(1), 185-198.
Ollinger, J., Song, K.-B., Antelmann, H., Hecker, M., & Helmann, J. D. (2006). Role of the Fur regulon in iron transport in *Bacillus subtilis*. *Journal of Bacteriology, 188*(10), 3664-3673.
Paixão, L., Oliveira, J., Veríssimo, A., Vinga, S., Lourenço, E. C., Ventura, M. R., . . . Andrew, P. W. (2015). Host glycan sugar-specific pathways in

Streptococcus pneumonia: galactose as a key sugar in colonisation and infection. *PloS One, 10*(3), e0121042.

Park, S. Y., Kim, K. M., Lee, J. H., Seo, S. J., & Lee, I. H. (2007). Extracellular gelatinase of *Enterococcus faecalis* destroys a defense system in insect hemolymph and human serum. *Infection and Immunity, 75*(4), 1861-1869.

Park, S. Y., Shin, Y. P., Kim, C. H., Park, H. J., Seong, Y. S., Kim, B. S., . . . Lee, I. H. (2008). Immune evasion of *Enterococcus faecalis* by an extracellular gelatinase that cleaves C3 and iC3b. *The Journal of Immunology, 181*(9), 6328-6336.

Pastar, I., Nusbaum, A. G., Gil, J., Patel, S. B., Chen, J., Valdes, J., . . . Davis, S. C. (2013). Interactions of methicillin resistant *Staphylococcus aureus* USA300 and *Pseudomonas aeruginosa* in polymicrobial wound infection. *PloS One, 8*(2).

Peng, D., Li, X., Liu, P., Luo, M., Chen, S., Su, K., . . . Li, Y. (2018). Epidemiology of pathogens and antimicrobial resistanceof catheter-associated urinary tract infections in intensive care units: a systematic review and meta-analysis. *American Journal of Infection Control, 46*(12), e81-e90.

Peyssonnaux, C., Zinkernagel, A. S., Datta, V., Lauth, X., Johnson, R. S., & Nizet, V. (2006). TLR4-dependent hepcidin expression by myeloid cells in response to bacterial pathogens. *Blood, 107*(9), 3727-3732.

Pirnay, J.-P., Bilocq, F., Pot, B., Cornelis, P., Zizi, M., Van Eldere, J., . . . Pitt, T. (2009). *Pseudomonas aeruginosa* population structure revisited. *PloS One, 4*(11), e7740.

Poole, K., Heinrichs, D. E., & Neshat, S. (1993). Cloning and sequence analysis of an EnvCD homologue in *Pseudomonas aeruginosa*: regulation by iron and possible involvement in the secretion of the siderophore pyoverdine. *Molecular Microbiology, 10*(3), 529-544.

Poole, K., Krebes, K., McNally, C., & Neshat, S. (1993). Multiple antibiotic resistance in *Pseudomonas aeruginosa:* evidence for involvement of an efflux operon. *Journal of Bacteriology, 175*(22), 7363-7372.

Pourakbari, B., Yaslianifard, S., Yaslianifard, S., Mahmoudi, S., Keshavarz-Valian, S., & Mamishi, S. (2016). Evaluation of efflux pumps gene expression in resistant *Pseudomonas aeruginosa* isolates in an Iranian referral hospital. *Iranian journal of microbiology, 8*(4), 249.

Qin, X., Singh, K. V., Weinstock, G. M., & Murray, B. E. (2000). Effects of *Enterococcus faecalis fsr* genes on production of gelatinase and a serine protease and virulence. *Infection and Immunity, 68*(5), 2579-2586.

Quatrini, R., Lefimil, C., Veloso, F. A., Pedroso, I., Holmes, D. S., & Jedlicki, E. (2007). Bioinformatic prediction and experimental verification of Fur-regulated genes in the extreme acidophile *Acidithiobacillus ferrooxidans*. *Nucleic Acids Research, 35*(7), 2153-2166.

Quinn, M., Weyer, S., Lewis, L., Dyer, D., & Wagner, P. (1994). Insertional inactivation of the gene for the meningococcal lactoferrin binding protein. *Microbial Pathogenesis, 17*(4), 227-237.

Radlinski, L., Rowe, S. E., Kartchner, L. B., Maile, R., Cairns, B. A., Vitko, N. P., . . . Conlon, B. P. (2017). *Pseudomonas aeruginosa* exoproducts determine antibiotic efficacy against *Staphylococcus aureus*. *PLoS Biology, 15*(11), e2003981.

Rakita, R. M., Vanek, N. N., Jacques-Palaz, K., Mee, M., Mariscalco, M. M., Dunny, G. M., . . . Simon, S. I. (1999). *Enterococcus faecalis* bearing

aggregation substance is resistant to killing by human neutrophils despite phagocytosis and neutrophil activation. *Infection and Immunity, 67*(11), 6067-6075.

Ramsey, M., Hartke, A., & Huycke, M. (2014). The physiology and metabolism of enterococci. *Enterococci: From Commensals to Leading Causes of Drug Resistant Infection (BioProject [Internet]. Bethesda (MD): National Library of Medicine (US))*.

Ravel, J., & Cornelis, P. (2003). Genomics of pyoverdine-mediated iron uptake in pseudomonads. *Trends in Microbiology, 11*(5), 195-200.

Raymond, K. N., Dertz, E. A., & Kim, S. S. (2003). Enterobactin: an archetype for microbial iron transport. *Proceedings of the National Academy of Sciences, 100*(7), 3584-3588.

Roberts, F. A., & Darveau, R. P. (2015). Microbial protection and virulence in periodontal tissue as a function of polymicrobial communities: symbiosis and dysbiosis. *Periodontology 2000, 69*(1), 18-27.

Roberts, G., Tarelli, E., Homer, K. A., Philpott-Howard, J., & Beighton, D. (2000). Production of an endo-β-N-acetylglucosaminidase activity mediates growth of *Enterococcus faecalis* on a high-mannose-type glycoprotein. *Journal of Bacteriology, 182*(4), 882-890.

Robinson, M. D., McCarthy, D. J., & Smyth, G. K. (2010). edgeR: a Bioconductor package for differential expression analysis of digital gene expression data. *Bioinformatics, 26*(1), 139-140.

Rozdzinski, E., Marre, R., Susa, M., Wirth, R., & Muscholl-Silberhorn, A. (2001). Aggregation substance-mediated adherence of E*nterococcus faecalis* to immobilized extracellular matrix proteins. *Microbial Pathogenesis, 30*(4), 211-220.

Runci, F., Gentile, V., Frangipani, E., Rampioni, G., Leoni, L., Lucidi, M., . . . Stahl, J. (2019). Contribution of active iron uptake to *Acinetobacter baumannii* pathogenicity. *Infection and Immunity, 87*(4), e00755-00718.

Russo, T. A., Jodush, S. T., Brown, J. J., & Johnson, J. R. (1996). Identification of two previously unrecognized genes (*guaA* and *argC*) important for uropathogenesis. *Molecular Microbiology, 22*(2), 217-229.

Samant, S., Lee, H., Ghassemi, M., Chen, J., Cook, J. L., Mankin, A. S., & Neyfakh, A. A. (2008). Nucleotide biosynthesis is critical for growth of bacteria in human blood. *PLoS Pathogens, 4*(2), e37.

Sambrook, J., Fritsch, E. F., & Maniatis, T. (1989). *Molecular cloning: a laboratory manual*: Cold spring harbor laboratory press.

Sause, W. E., Balasubramanian, D., Irnov, I., Copin, R., Sullivan, M. J., Sommerfield, A., . . . Ueberheide, B. (2019). The purine biosynthesis regulator PurR moonlights as a virulence regulator in *Staphylococcus aureus*. *Proceedings of the National Academy of Sciences, 116*(27), 13563-13572.

Savli, H., Karadenizli, A., Kolayli, F., Gundes, S., Ozbek, U., & Vahaboglu, H. (2003). Expression stability of six housekeeping genes: a proposal for resistance gene quantification studies of *Pseudomonas aeruginosa* by real-time quantitative RT-PCR. *Journal of Medical Microbiology, 52*(5), 403-408.

Scalise, A., Bianchi, A., Tartaglione, C., Bolletta, E., Pierangeli, M., Torresetti, M., . . . Di Benedetto, G. (2015). *Microenvironment and microbiology of*

skin wounds: the role of bacterial biofilms and related factors. Paper presented at the Seminars in vascular surgery.
Schlievert, P. M., Chuang-Smith, O. N., Peterson, M. L., Cook, L. C., & Dunny, G. M. (2010). *Enterococcus faecalis* endocarditis severity in rabbits is reduced by IgG Fabs interfering with aggregation substance. *PloS One, 5*(10).
Schmid-Wendtner, M.-H., & Korting, H. C. (2006). The pH of the skin surface and its impact on the barrier function. *Skin pharmacology and physiology, 19*(6), 296-302.
Schneider, L. A., Korber, A., Grabbe, S., & Dissemond, J. (2007). Influence of pH on wound-healing: a new perspective for wound-therapy? *Archives of Dermatological Research, 298*(9), 413-420.
Schryvers, A. B., & Morris, L. (1988). Identification and characterization of the transferrin receptor from *Neisseria meningitidis*. *Molecular Microbiology, 2*(2), 281-288.
Schryvers, A. B., & Morris, L. J. (1988). Identification and characterization of the human lactoferrin-binding protein from *Neisseria meningitidis*. *Infection and Immunity, 56*(5), 1144-1149.
Sen, C. K., Gordillo, G. M., Roy, S., Kirsner, R., Lambert, L., Hunt, T. K., . . . Longaker, M. T. (2009). Human skin wounds: a major and snowballing threat to public health and the economy. *Wound repair and regeneration, 17*(6), 763-771.
Serralta, V. W., Harrison-Balestra, C., Cazzaniga, A. L., Davis, S. C., & Mertz, P. M. (2001). Lifestyles of bacteria in wounds: presence of biofilms? *Wounds, 13*(1), 29-34.
Severin, T., Müller, B., Giese, G., Uhl, B., Wolf, B., Hauschildt, S., & Kreutz, W. (1994). pH-dependent LAK cell cytotoxicity. *Tumor biology, 15*(5), 304-310.
Shankar, N., Lockatell, C. V., Baghdayan, A. S., Drachenberg, C., Gilmore, M. S., & Johnson, D. E. (2001). Role of *Enterococcus faecalis* surface protein Esp in the pathogenesis of ascending urinary tract infection. *Infection and Immunity, 69*(7), 4366-4372.
Sharpe, J., Harris, K., Jubin, K., Bainbridge, N., & Jordan, N. (2009). The effect of pH in modulating skin cell behaviour. *British Journal of Dermatology, 161*(3), 671-673.
Sherman, J. M. (1937). The streptococci. *Bacteriological reviews, 1*(1), 3-97.
Shettigar, K., Bhat, D. V., Satyamoorthy, K., & Murali, T. S. (2018). Severity of drug resistance and co-existence of *Enterococcus faecalis* in diabetic foot ulcer infections. *Folia Microbiologica, 63*(1), 115-122.
Shinzato, T., & Saito, A. (1995). The *Streptococcus milleri* group as a cause of pulmonary infections. *Clinical Infectious Diseases, 21*(Supplement_3), S238-S243.
Shukla, V., Shukla, D., Tiwary, S., Agrawal, S., & Rastogi, A. (2007). Evaluation of pH measurement as a method of wound assessment. *Journal of Wound Care, 16*(7), 291-294.
Sibley, C. D., Parkins, M. D., Rabin, H. R., Duan, K., Norgaard, J. C., & Surette, M. G. (2008). A polymicrobial perspective of pulmonary infections exposes an enigmatic pathogen in cystic fibrosis patients. *Proceedings of the National Academy of Sciences, 105*(39), 15070-15075.

Siegman-Igra, Y., Kulka, T., Schwartz, D., & Konforti, N. (1994). Polymicrobial and monomicrobial bacteraemic urinary tract infection. *Journal of Hospital Infection, 28*(1), 49-56.

Sifri, C. D., Mylonakis, E., Singh, K. V., Qin, X., Garsin, D. A., Murray, B. E., . . . Calderwood, S. B. (2002). Virulence effect of *Enterococcus faecalis* protease genes and the quorum-sensing locus *fsr* in *Caenorhabditis elegans* and mice. *Infection and Immunity, 70*(10), 5647-5650.

Sillanpää, J., Xu, Y., Nallapareddy, S. R., Murray, B. E., & Höök, M. (2004). A family of putative MSCRAMMs from *Enterococcus faecalis*. *Microbiology, 150*(7), 2069-2078.

Singh, K. V., Nallapareddy, S. R., & Murray, B. E. (2007). Importance of the *ebp* (endocarditisand biofilm-associated pilus) locus in the pathogenesis of *Enterococcus faecalis* ascending urinary tract infection. *The Journal of Infectious Diseases, 195*(11), 1671-1677.

Singh, K. V., Nallapareddy, S. R., Sillanpää, J., & Murray, B. E. (2010). Importance of the collagen adhesin *ace* in pathogenesis and protection against *Enterococcus faecalis* experimental endocarditis. *PLoS Pathogens, 6*(1).

Singh, K. V., Qin, X., Weinstock, G. M., & Murray, B. E. (1998). Generation and testing of mutants of *Enterococcus faecalis* in a mouse peritonitis model. *The Journal of Infectious Diseases, 178*(5), 1416-1420.

Skvortsov, T., Ignatov, D., Majorov, K., Apt, A., & Azhikina, T. (2013). *Mycobacterium tuberculosis* transcriptome profiling in mice with genetically different susceptibility to tuberculosis. *Acta Naturae (англоязычная версия), 5*(2 (17)), 62-69.

Smirnova, I. A., Hägerhäll, C., Konstantinov, A. A., & Hederstedt, L. (1995). HOQNO interaction with cytochrome b in succinate:menaquinone oxidoreductase from *Bacillus subtilis*. *FEBS Letters, 359*(1), 23-26.

Soto, S. M. (2014). Importance of biofilms in urinary tract infections: new therapeutic approaches. *Advances in Biology, 2014*.

Sprencel, C., Cao, Z., Qi, Z., Scott, D. C., Montague, M. A., Ivanoff, N., . . . Klebba, P. E. (2000). Binding of ferric enterobactin by the *Escherichia coli* periplasmic protein FepB. *Journal of Bacteriology, 182*(19), 5359-5364.

Stacy, A., McNally, L., Darch, S. E., Brown, S. P., & Whiteley, M. (2016). The biogeography of polymicrobial infection. *Nature Reviews Microbiology, 14*(2), 93-105.

Süßmuth, S. D., Muscholl-Silberhorn, A., Wirth, R., Susa, M., Marre, R., & Rozdzinski, E. (2000). Aggregation substance promotes adherence, phagocytosis, and intracellular survival of *Enterococcus faecalis* within human macrophages and suppresses respiratory burst. *Infection and Immunity, 68*(9), 4900-4906.

Suzuki, T., Wada, T., Kozai, S., Ike, Y., Gilmore, M. S., & Ohashi, Y. (2008). Contribution of secreted proteases to the pathogenesis of postoperative *Enterococcus faecalis* endophthalmitis. *Journal of Cataract & Refractive Surgery, 34*(10), 1776-1784.

Tanner, R. S., & James, S. A. (1992). Rapid bactericidal effect of low pH against *Pseudomonas aeruginosa*. *Journal of Industrial Microbiology, 10*(3-4), 229-232.

Thomas, V. C., Thurlow, L. R., Boyle, D., & Hancock, L. E. (2008). Regulation of autolysis-dependent extracellular DNA release by *Enterococcus faecalis* extracellular proteases influences biofilm development. *Journal of Bacteriology, 190*(16), 5690-5698.

Thornton, R. B., Rigby, P. J., Wiertsema, S. P., Filion, P., Langlands, J., Coates, H. L., . . . Richmond, P. C. (2011). Multi-species bacterial biofilm and intracellular infection in otitis media. *BMC Pediatrics, 11*(1), 1-10.

Thurlow, L. R., Thomas, V. C., Narayanan, S., Olson, S., Fleming, S. D., & Hancock, L. E. (2010). Gelatinase contributes to the pathogenesis of endocarditis caused by *Enterococcus faecalis*. *Infection and Immunity, 78*(11), 4936-4943.

Toledo-Arana, A., Valle, J., Solano, C., Arrizubieta, M. a. J., Cucarella, C., Lamata, M., . . . Lasa, I. (2001). The enterococcal surface protein, Esp, is involved in *Enterococcus faecalis* biofilm formation. *Appl. Environ. Microbiol., 67*(10), 4538-4545.

Tolker‐Nielsen, T. (2014). *Pseudomonas aeruginosa* biofilm infections: from molecular biofilm biology to new treatment possibilities. *Apmis, 122*, 1-51.

Trengove, N., Stacey, M., McGechie, D., Stingemore, N., & Mata, S. (1996). Qualitative bacteriology and leg ulcer healing. *Journal of Wound Care, 5*(6), 277-280.

Tropini, C., Earle, K. A., Huang, K. C., & Sonnenburg, J. L. (2017). The gut microbiome: connecting spatial organization to function. *Cell Host & Microbe, 21*(4), 433-442.

Tsuchimori, N., Hayashi, R., Shino, A., Yamazaki, T., & Okonogi, K. (1994). *Enterococcus faecalis* aggravates pyelonephritis caused by *Pseudomonas aeruginosa* in experimental ascending mixed urinary tract infection in mice. *Infection and Immunity, 62*(10), 4534-4541.

Turner, K. H., Everett, J., Trivedi, U., Rumbaugh, K. P., & Whiteley, M. (2014). Requirements for *Pseudomonas aeruginosa* acute burn and chronic surgical wound infection. *PLoS Genetics, 10*(7).

Valentino, M. D., Foulston, L., Sadaka, A., Kos, V. N., Villet, R. A., Santa Maria Jr, J., . . . Hooper, D. C. (2014). Genes contributing to *Staphylococcus aureus* fitness in abscess-and infection-related ecologies. *MBio, 5*(5), e01729-01714.

Vasileva, D., Janssen, H., Hönicke, D., Ehrenreich, A., & Bahl, H. (2012). Effect of iron limitation and *fur* gene inactivation on the transcriptional profile of the strict anaerobe *Clostridium acetobutylicum*. *Microbiology, 158*(7), 1918-1929.

Vebø, H. C., Solheim, M., Snipen, L., Nes, I. F., & Brede, D. A. (2010). Comparative genomic analysis of pathogenic and probiotic *Enterococcus faecalis* isolates, and their transcriptional responses to growth in human urine. *PloS One, 5*(8), e12489.

Vert, M., Doi, Y., Hellwich, K.-H., Hess, M., Hodge, P., Kubisa, P., . . . Schué, F. (2012). Terminology for biorelated polymers and applications (IUPAC Recommendations 2012). *Pure and Applied Chemistry, 84*(2), 377-410.

Vidal, S., Tremblay, M. L., Govoni, G., Gauthier, S., Sebastiani, G., Malo, D., . . . Gros, P. (1995). The Ity/Lsh/Bcg locus: natural resistance to infection with intracellular parasites is abrogated by disruption of the Nramp1 gene. *The Journal of Experimental Medicine, 182*(3), 655-666.

Visca, P., Imperi, F., & Lamont, I. L. (2007). Pyoverdine siderophores: from biogenesis to biosignificance. *Trends in Microbiology, 15*(1), 22-30.

Waar, K., van der Mei, H. C., Harmsen, H. J., Degener, J. E., & Busscher, H. J. (2002). Adhesion to bile drain materials and physicochemical surface properties of *Enterococcus faecalis* strains grown in the presence of bile. *Appl. Environ. Microbiol., 68*(8), 3855-3858.

Wakeman, C. A., Moore, J. L., Noto, M. J., Zhang, Y., Singleton, M. D., Prentice, B. M., . . . Chazin, W. J. (2016). The innate immune protein calprotectin promotes *Pseudomonas aeruginosa* and *Staphylococcus aureus* interaction. *Nature Communications, 7*(1), 1-12.

Warren, J. W., Tenney, J. H., Hoopes, J. M., Muncie, H. L., & Anthony, W. C. (1982). A prospective microbiologic study of bacteriuria in patients with chronic indwelling urethral catheters. *The Journal of Infectious Diseases, 146*(6), 719-723.

Weng, M., Nagy, P. L., & Zalkin, H. (1995). Identification of the *Bacillus subtilis* pur operon repressor. *Proceedings of the National Academy of Sciences, 92*(16), 7455-7459.

WHO. (2016). *Global guidelines for the prevention of surgical site infection*: World Health Organization.

Wu, T., Hu, E., Xu, S., Chen, M., Guo, P., Dai, Z., . . . Yu, G. (2021). clusterProfiler 4.0: A universal enrichment tool for interpreting omics data. *Innovation (N Y), 2*(3), 100141. doi:10.1016/j.xinn.2021.100141

Yu, C., & Genco, C. A. (2012). Fur-mediated global regulatory circuits in pathogenic *Neisseria* species. *Journal of Bacteriology, 194*(23), 6372-6381.

Yu, G., Wang, L. G., Han, Y., & He, Q. Y. (2012). clusterProfiler: an R package for comparing biological themes among gene clusters. *OMICS, 16*(5), 284-287. doi:10.1089/omi.2011.0118

Zawadzka, A. M., Kim, Y., Maltseva, N., Nichiporuk, R., Fan, Y., Joachimiak, A., & Raymond, K. N. (2009). Characterization of a *Bacillus subtilis* transporter for petrobactin, an anthrax stealth siderophore. *Proceedings of the National Academy of Sciences, 106*(51), 21854-21859.

Zhang, X., de Maat, V., Guzmán Prieto, A. M., Prajsnar, T. K., Bayjanov, J. R., de Been, M., . . . Willems, R. J. (2017). RNA-seq and Tn-seq reveal fitness determinants of vancomycin-resistant *Enterococcus faecium* during growth in human serum. *BMC Genomics, 18*(1), 1-12.

Zhang, X., Top, J., de Been, M., Bierschenk, D., Rogers, M., Leendertse, M., . . . van Schaik, W. (2013). Identification of a genetic determinant in clinical *Enterococcus faecium* strains that contributes to intestinal colonization during antibiotic treatment. *The Journal of Infectious Diseases, 207*(11), 1780-1786.

Zheng, J.-x., Bai, B., Lin, Z.-w., Pu, Z.-y., Yao, W.-m., Chen, Z., . . . Yu, Z.-j. (2018). Characterization of biofilm formation by *Enterococcus faecalis* isolates derived from urinary tract infections in China. *Journal of Medical Microbiology, 67*(1), 60.

Appendix figures and tables

This section contains the appendix figures and tables for this dissertation. Figures and tables shown in the appendix are directly referenced in **Chapters 2** and **3**. The appendix is separated into 2 sub-sections with their respective labels for each chapter.

Chapter 2 appendix

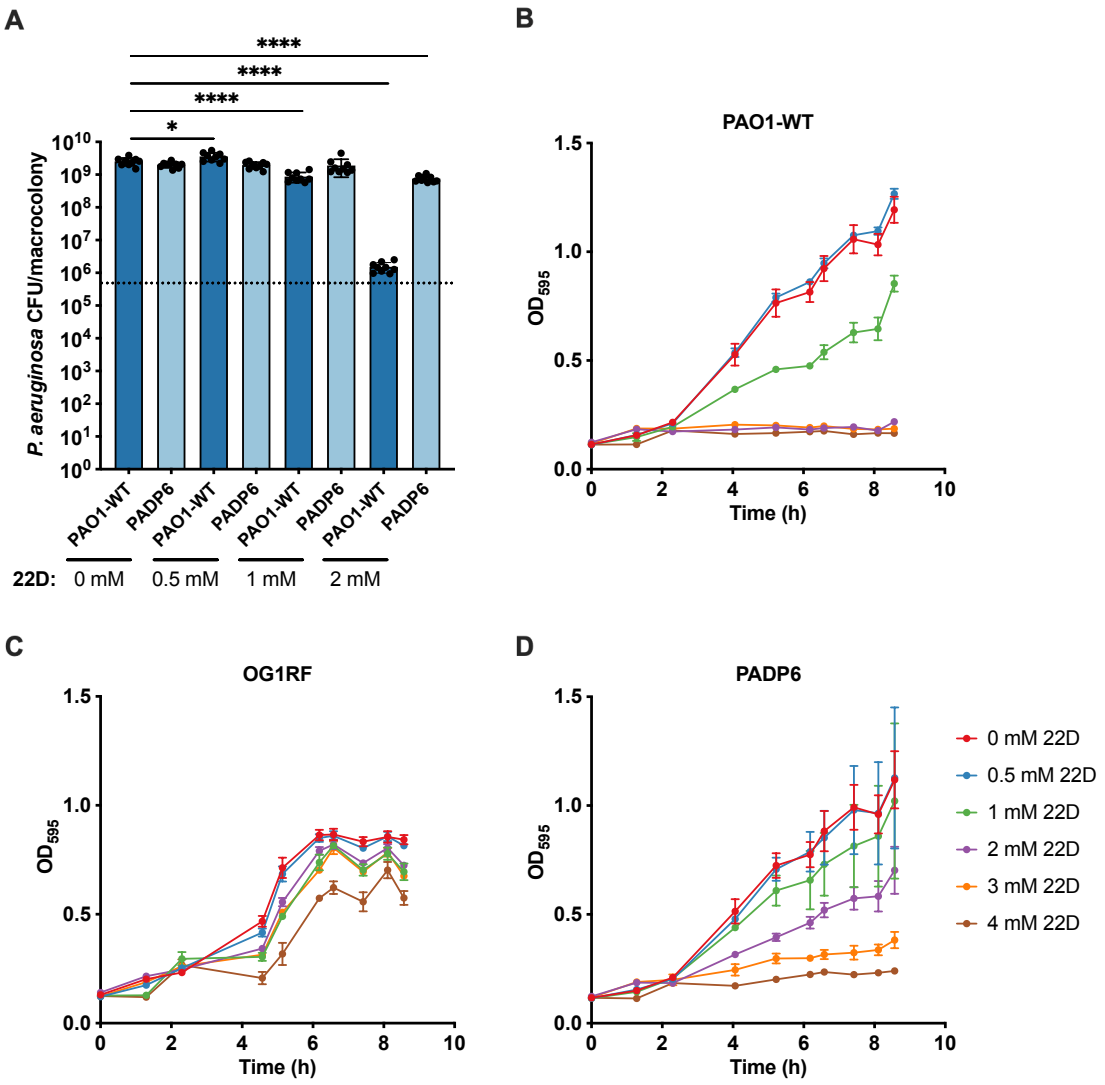

Appendix Figure 2.1 *P. aeruginosa* growth responses to iron restriction. **(A)** Enumeration of PAO1-WT and PADP6 from 24 h single-species macrocolonies grown in TSBG media supplemented without and with increasing 22D concentrations (0.5, 1 and 2 mM). Dotted lines represent inoculum of bacteria spotted. N = 3 with 3 technical replicates; error bars represent SD from the mean. Statistical analysis was performed using Mann-Whitney U test, *p < 0.05, **p < 0.01, ***p < 0.001, ****p < 0.0001. Planktonic growth of **(B)** PAO1-WT, **(C)** OG1RF and **(D)** PADP6 in TSBG media supplemented without and with increasing 22D concentrations (0.5, 1, 2, 3 and 4 mM). N = 3 with 3 technical replicates; error bars represent SD from the mean.

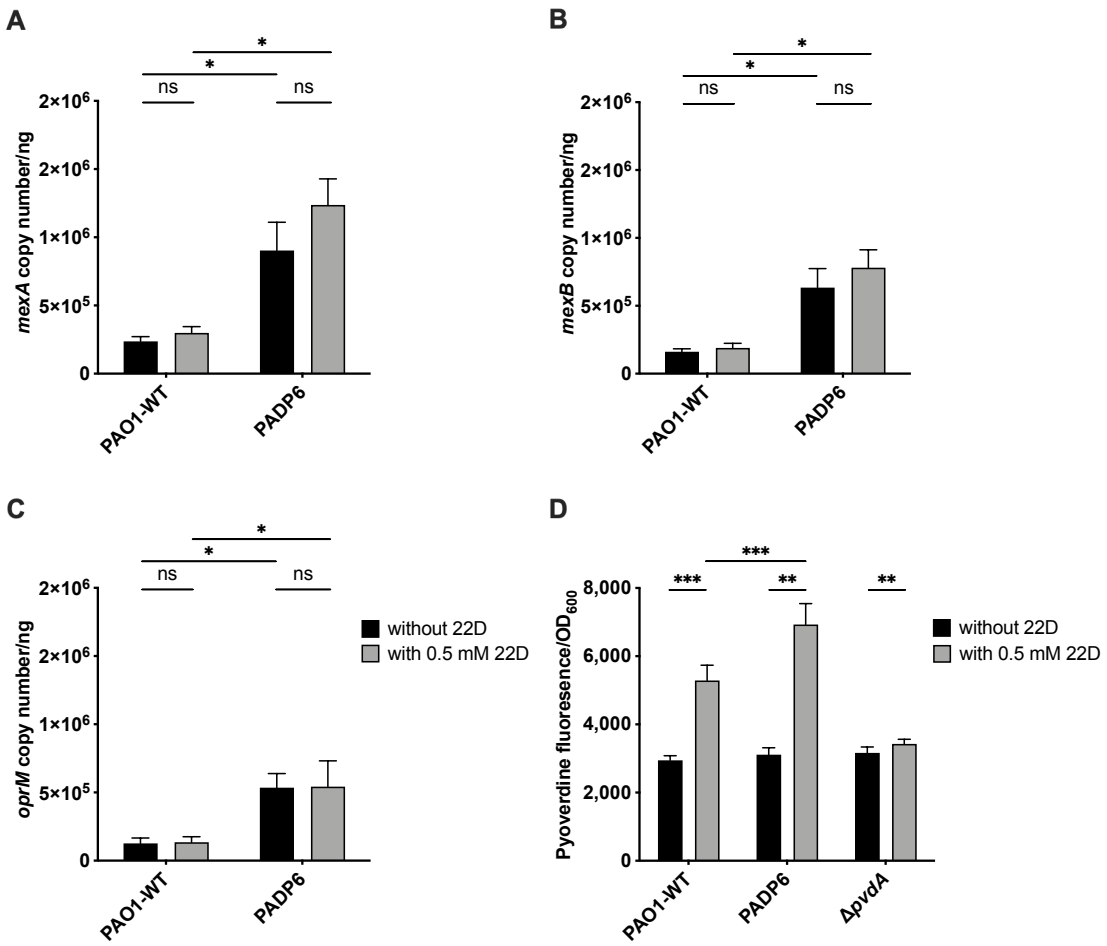

Appendix Figure 2.2 *P. aeruginosa* PADP6 confers tolerance to iron starvation by increasing pyoverdine secretion during growth under iron-restricted conditions.

Copy number of **(A)** *mexA*, **(B)** *mexB* and **(C)** *oprM* from planktonic cultures of PAO1-WT and PADP6 grown in unchelated and 0.5 mM 22D-chelated TSBG media. N = 4 with 2 technical replicates; error bars represent SD from the mean. Statistical analysis was performed using Mann-Whitney U test, *p < 0.05, **p < 0.01, ***p < 0.001, ****p < 0.0001. **(D)** Pyoverdine secretion measured from planktonic cultures of PAO1-WT, PADP6 and Δ*pvdA* (pyoverdine biosynthesis mutant) grown in unchelated and 0.5 mM 22D-chelated TSBG media. N = 4 with 2 technical replicates; error bars represent SD from the mean. Statistical analysis was performed using Mann-Whitney U test, *p < 0.05, **p < 0.01, ***p < 0.001, ****p < 0.0001.

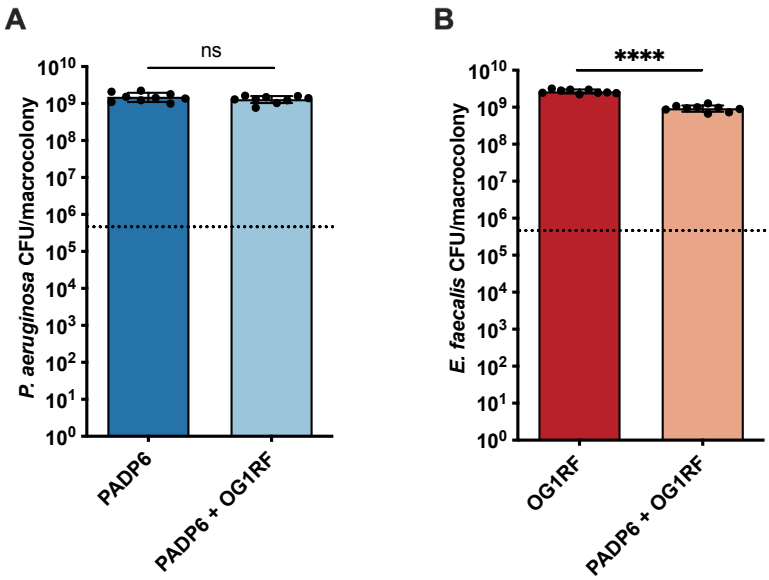

Appendix Figure 2.3 *P. aeruginosa* growth inhibition by *E. faecalis* is abolished in TSB media.
Enumeration of **(A)** PADP6 and **(B)** OG1RF from 48 h macrocolonies with single or mixed inoculums grown in TSB media supplemented with 2 mM 22D. Bacterial species were mixed at a 1:1 ratio for mixed-species macrocolonies. Dotted lines represent inoculum of bacteria spotted. N = 3 with 3 technical replicates; error bars represent SD from the mean. Statistical analysis was performed using Mann-Whitney U test, *p < 0.05, **p < 0.01, ***p < 0.001, ****p < 0.0001.

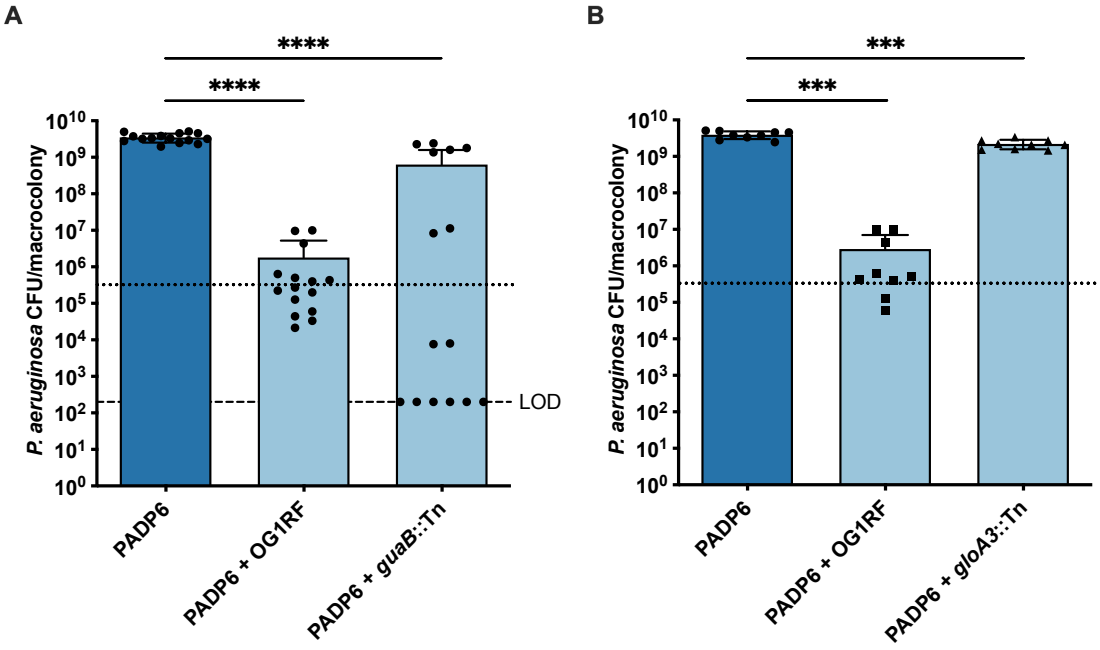

Appendix Figure 2.4 *P. aeruginosa* growth responses when grown with *E. faecalis guaB*::Tn and *gloA3*::Tn under iron-restricted conditions.
Enumeration of PADP6 from 48 h macrocolonies with single or mixed inoculums of **(A)** *guaB*::Tn and **(B)** *gloA3*::Tn grown in 2 mM 22D-chelated TSBG media.

Bacterial species were mixed at a 1:1 ratio for mixed-species macrocolonies. Dotted lines represent inoculum of bacteria spotted. N ≥ 3 with 3 technical replicates; error bars represent SD from the mean. Dashed line represents limit of detection (LOD). Statistical analysis was performed using Mann-Whitney U test, ***p < 0.001, ****p < 0.0001.

Appendix Table 2.1 *E. faecalis* transposon mutants identified from transposon library screen with PADP6 under iron-restricted conditions.

Locus tag	Name	Description
OG1RF_10199	*ldh1*	L-lactate dehydrogenase
OG1RF_10480	*gloA3*	Lactoylglutathione lyase
OG1RF_12538	*guaB*	IMP dehydrogenase

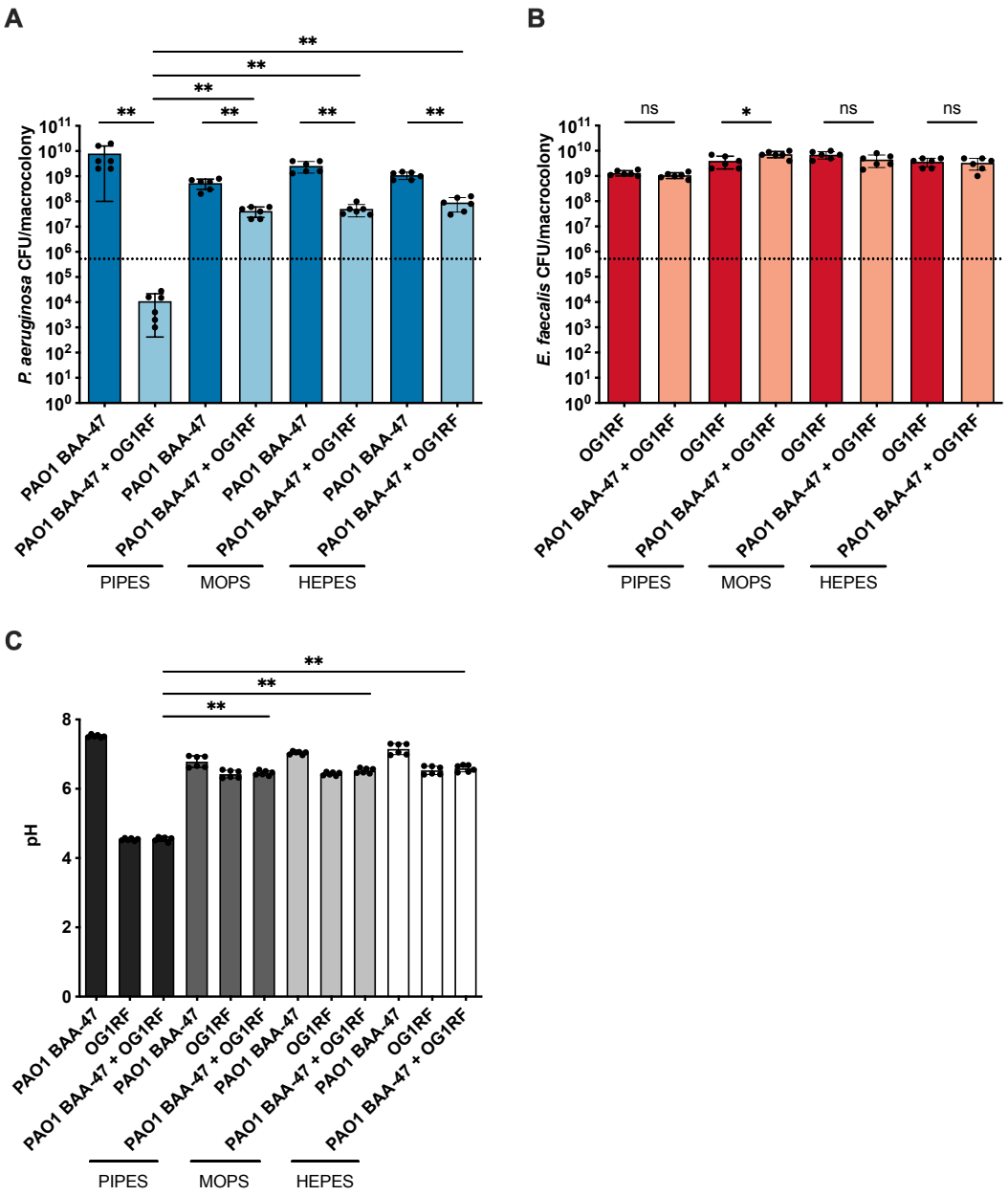

Appendix Figure 2.5 Alleviating pH acidification using buffered media partially rescues *P. aeruginosa* growth inhibition under iron-restricted conditions.

Enumeration of **(A)** PAO1 BAA-47 and **(B)** OG1RF from single- and mixed-species macrocolonies grown for 24 h in TSBG media supplemented with 1 mM 22D and either 200 mM PIPES, MOPS or HEPES buffer. Bacterial species were mixed at a 1:1 ratio for mixed-species macrocolonies. Dotted lines represent inoculum of bacteria spotted. N = 2 with 3 technical replicates; error bars represent SD from the mean. Statistical analysis was performed using Mann-Whitney U test, *p < 0.05, **p < 0.01, ***p < 0.001, ****p < 0.0001. **(C)** The corresponding pH quantification of single- and mixed-species macrocolonies in **(A)** and **(B)**. Error bars represent SD from the mean. Statistical analysis was performed using Mann-Whitney U test, *p < 0.05, **p < 0.01, ***p < 0.001, ****p < 0.0001.

Chapter 3 appendix

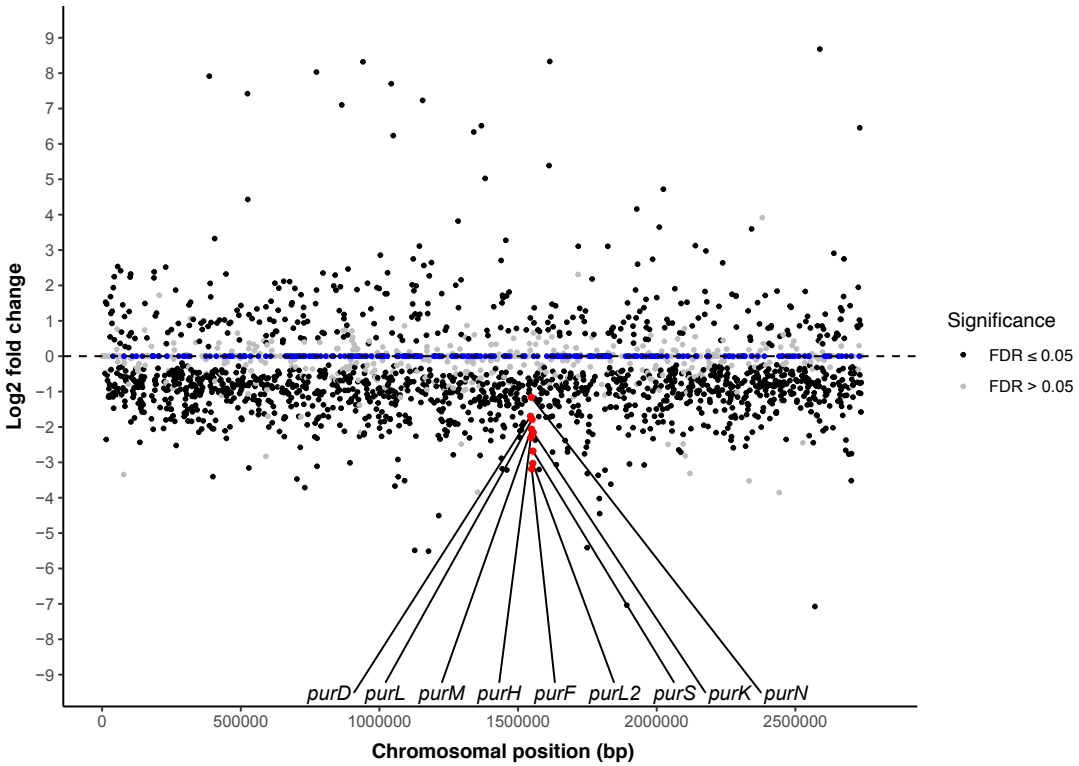

Appendix Figure 3.1 Transposon insertions in *E. faecalis de novo* purine biosynthesis genes are among the significantly underrepresented genes at 8 hpi.

Distribution of *E. faecalis* transposon mutant abundance profiled by Tn-seq from 8 hpi wounds. Significant mutants from Tn-seq analysis are colored black ($p \leq 0.05$ and FDR ≤ 0.05). *E. faecalis* genes with no transposon mutant found in the transposon library are colored in blue.

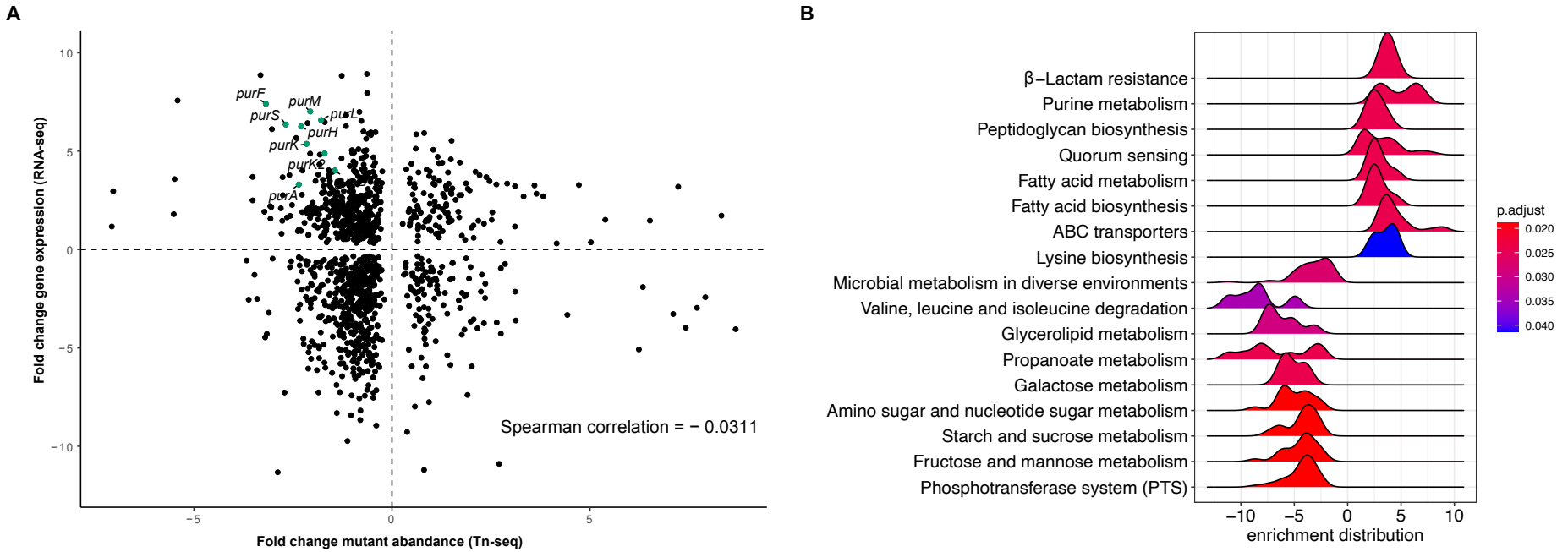

Appendix Figure 3.2 *E. faecalis* pathways that are significantly enriched in 8 hpi wounds.
(A) Correlation plot of statistically significant genes from Tn-seq and RNA-seq. **(B)** Ridge plot shows the distribution of fold-change for genes in significantly enriched pathways from 8 hpi wounds identified from the RNA-seq analysis. Color gradient represents false discovery rate (p.adjust values).

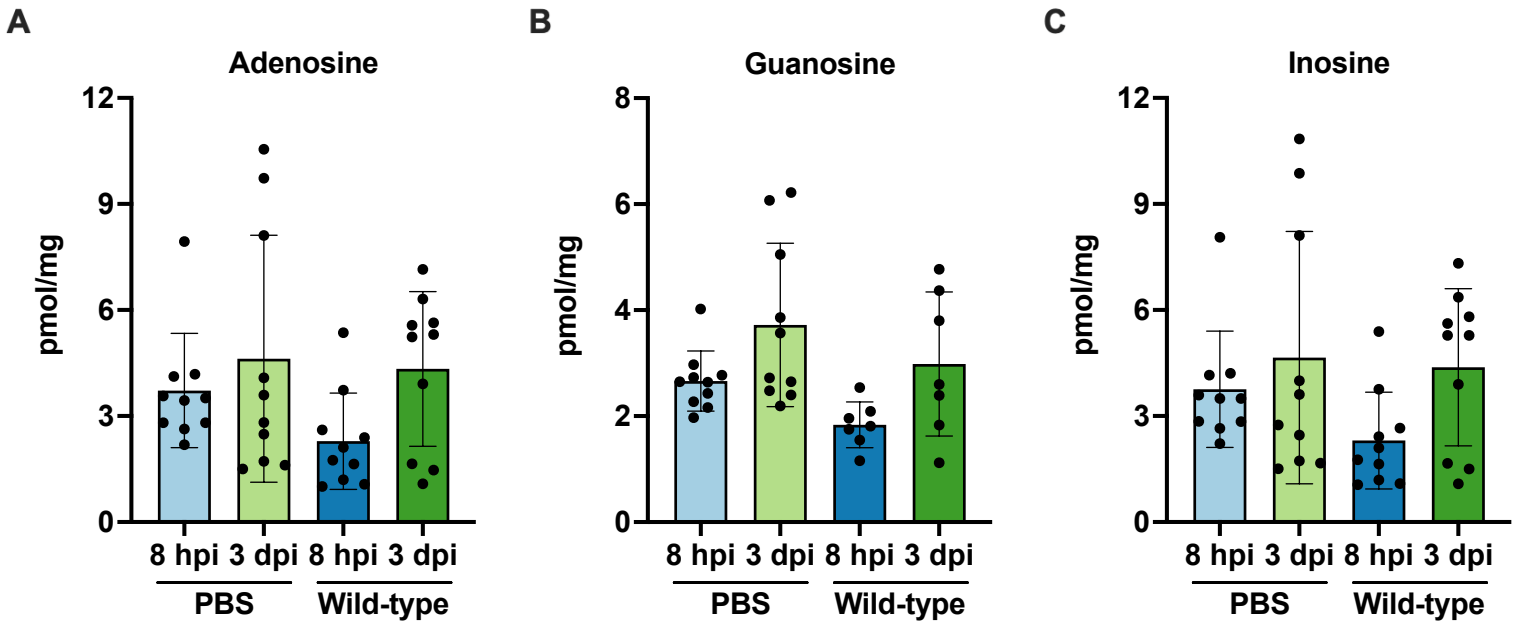

Appendix Figure 3.3 No significant differences between adenosine, guanosine, and inosine metabolites during *E. faecalis* wound infection.

Male C57BL/6 mice were wounded and inoculated with PBS or 2 – 4 × 10^6 CFU of wild-type OG1RF. Wounds were harvested at 8 hpi and 3 dpi for quantification of **(A)** adenosine, **(B)** guanosine, and **(C)** inosine using LC-MS. Each data point represents one mouse and error bars represent SD from the mean; N = 2, n = 5 mice per group per experiment. Statistical analysis was performed using the Mann-Whitney U test, *p < 0.05, **p < 0.01, ***p < 0.001.

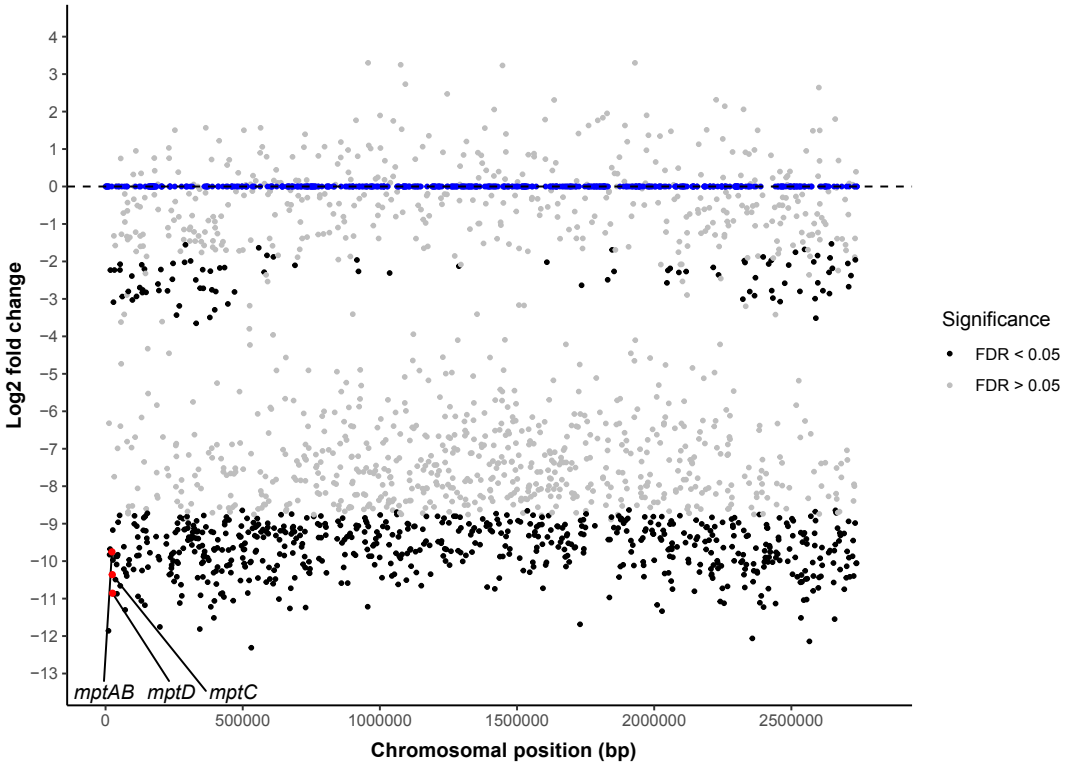

Appendix Figure 3.4 Transposon insertions in *mptABCD* are among the most significantly underrepresented genes at 3 dpi.
Distribution of *E. faecalis* transposon mutant abundance profiled by Tn-seq from 3 dpi wounds. Significant mutants from Tn-seq analysis are colored black ($p \leq 0.05$ and FDR ≤ 0.05). *E. faecalis* genes with no transposon mutant found in the transposon library are colored in blue.

Appendix Table 3.1 Complete table for carbohydrate fermentation test (API CH50) of wild-type OG1RF pMPSP3535::P*nisA*-Empty, OG1RF Δ*mptD* pMSP3535::P*nisA*-Empty, and OG1RF Δ*mptD* pMSP3535::P*nisA*-*mptD*.